Profiling of key nitrogen converting organisms in wastewater treatment plants with diffused aeration

This work is submitted in complete fulfillment of the academic requirements for the degree of Masters of Applied Sciences in the Department of Biotechnology and Food Sciences, Faculty of Applied Sciences at the Durban University of Technology, Durban, South Africa

Puseletso Constance Kumalo

2022

SUPERVISOR: Professor Faizal Bux

CO-SUPERVISOR: Professor Sheena Kumari Kuttan Pillai

CO-SUPERVISOR: Dr Oluyemi Olatunji Awolusi

APPROVAL

I hereby approve the final submission of the following thesis.

Prof. Faizal Bux

Supervisor

DTech: Biotechnology

Prof. Sheena Kumari Kuttan Pillai

Co-supervisor

Ph.D: Biosciences

Dr. Oluyemi Olatunji Awolusi

Co-supervisor

Ph.D: Biotechnology

DECLARATION

I hereby declare that this thesis entitled "**Profiling of key nitrogen converting organisms in wastewater treatment plants with diffused aeration**" submitted for the degree of Master's in Applied Sciences (Biotechnology) at the Durban University of Technology:

1. Is my original work and has not been submitted for a degree at any other university.
2. I further declare that a detailed reference list has been provided on all the sources cited or quoted

21/06/2022

Puseletso C Kumalo Msc (DUT) Date

21/06/2022

Prof. F. Bux D. Tech. (DUT) Date

21/06/2022

Prof. S.K.K Pillai Ph.D. (Mangalore University) Date

21 06 2022

Dr. O.O Awolusi Ph.D. (DUT) Date

ABSTRACT

Maintaining stable nitrification rates in biological nutrient removal (BNR) systems is difficult due to the slow growth rates of nitrifying bacteria and their sensitivity to environmental and operational conditions. Dissolved oxygen (DO) concentration in the aeration tank significantly affects nitrification and nitrifying bacterial growth. Currently, diffused aeration systems are gaining popularity over conventional surface aeration systems due to their advantages like process stability, better control, and lower cost of operation. However, studies regarding the impact of this aeration type on the selection of functional microbial communities in wastewater treatment plants are still lacking. This study focused on investigating the community structure and activity of key nitrogen converting organisms within two different municipal full-scale wastewater treatment plants (WWTP A and WWTP B) operated with fine bubble diffused aeration. WWTP A was relatively a large plant with a flow rate of 71 ML/day and consisted of three parallel BNR systems (reactor 1, 2, and 3), operated using a similar mode whereas WWTP B was relatively a small plant (0.5 ML/day) with a single BNR system.

Composite sludge samples from aeration tanks, as well as influent and effluent water samples, were collected monthly from August 2019 to February 2020 and from June 2020 to August 2020. The nutrient removal performance of the plant was estimated from the influent and effluent chemical analysis. Floc structure analysis and sludge volume index were calculated to assess the settling characteristics. In addition, nitrifying bacterial population dynamics and their activities were assessed using quantitative real-time and reverse transcriptase PCR, respectively in relation to selected plant operational (DO, temperature, substrate concentration) conditions. The average ammonia removal at WWTP A was 95±5.6% which correlated with DO concentration in the aeration tank and the nitrification rate of the plant, whereas the WWTP B recorded 98±02% average ammonia removal efficiency with a more stable DO level in this plant. The sludge volume index (SVI) values were below 150mL/g in both plants, indicating good sludge settling under fine bubble diffused aeration. However, the floc structure varied across the reactors during the study period and ranged from small to medium, open to compact, and irregular with occasional filaments branching mainly in WWTP A.

The microbial analysis of sludge samples showed that ammonia oxidising bacteria (AOB) 16S rRNA gene abundance was high in all the three reactors in WWTP A as compared with nitrite

oxidising bacteria (NOB). In WWTP B, the average 16S rRNA gene copies for NOB were observed to be higher than AOB. In addition, in WWTP A, a negative correlation was found between the AOB 16S rRNA population and DO concentration in reactor 1 (r = -0.40), while a positive correlation was found in reactor 3 (r = 0.47) with no clear correlation in reactor 2 as well as in WWTP B. In both plants, *Nitrobacter spp.* was the dominant NOB, while the relative abundance of *Nitrospira spp.* was generally consistent throughout the study. The *nxrB* copy number was observed to be higher than that of *nxr*A (encoding for *Nitrobacter spp.*). The highest *amo*A copy number was observed when the temperatures were high (22 ºC -26.1 ºC), implying that increasing temperatures possibly benefited AOB growth.

In terms of functional gene expression, a rapid decrease in expression levels of *amoA* was observed in both plants while the expression levels of *nxrB* were observed to increase rapidly as the temperature increased. In contrast, expression levels of the *nxrA* were relatively more consistent throughout the study period in both plants. At WWTP A, there was a positive correlation between AOB expression (*amoA*) and DO concentration in all reactors (reactor 1: r = 0.49; reactor 2: r = 0.78 and reactor 3: r = 0.32; p = 0.05). However, no clear correlation was found between NOB expression (*nxrA* and *nxrB*) and DO concentration. At WWTP B, a negative correlation was observed between *nxrA* expression levels and DO concentration (r = - 0.34, p = 0.05). However, DO concentration showed no clear correlation with *amoA* and *nxrB* expression levels.

The phylogenetic analysis of *nxrB* populations in both the plants also revealed similarities that are closely related to uncultured *Nitrospira spp*., nitrite oxidoreductase subunit B, which has been implicated in complete nitrification (COMAMMOX). These observations indicate a need for more research effort using next-generation sequencing to identify and quantify novel nitrifying bacterial including COMAMMOX and ANAMMOX in WWTPs that were previously unachievable using conventional molecular techniques. In conclusion, this study revealed that the fine bubble diffused aeration operated at relatively high DO concentration was able to effectively remove ammonia in both plants resulting in stable and high nitrification rates even at different seasons and loading rates. It also promoted compact flocs with good settleability as well as facilitated optimal and diverse functional nitrifying bacterial community structure and activity.

DEDICATION

This thesis is dedicated to everyone who has contributed positively to my building in life and most importantly, to my grandparents Sello and Dineo Mofokeng, for their constant support and encouragement throughout my studies.

ACKNOWLEDGEMENTS

First and foremost, I would like to give praises and thanks to God Almighty, the ever faithful, constant, and loving father, through whom all things are possible.

- My supervisor, Prof F. Bux; for the opportunity to conduct my research under his supervision. I am grateful for his time and guidance throughout my study
- My co-supervisor, Prof S.K.K Pillai; for her patient guidance, encouragement, immense knowledge, and most importantly for her time and continuous support.
- My co-supervisor, Dr. O.O Awolusi; for his mentorship, and willingness to help during the study especially when the protocols were not working out. Thank you for always believing in me and for your constructive criticism and input throughout the project.
- My sister, Mamotsheare, my brothers, Dikotsi and Mpho, my uncle, Tsietsi, and my whole family for their consistent love, prayers, and support. Thank you for believing in me and always being there for me.
- My friends for their constant support, advice, and dependable friendship. Special thanks to Precios Mthetwa, Thobela Conco, and Kriveshin Pillay, for your friendship and assistance during the sampling period and running analysis.
- To my Institute for Water and Wastewater Technology family (staff and students), thank you for your support and friendliness.
- Special thanks to Umgeni Water management and their staff for their assistance during sampling at their treatment plants.
- The National Research Foundation for funding this project

TABLE OF CONTENTS

LIST OF FIGURES

LIST OF TABLES

ABBREVIATIONS

ADWF	: Average dry weather flows
ALR	: Ammonia loading rate (kg COD/m3.d)
AmoA	: Ammonia monooxygenase
ANAMMOX	: Anaerobic ammonium oxidation
AOA	: Ammonia oxidizing archaea
AOB	: Ammonia oxidizing bacteria
BLAST	: Basic Local Alignment Search Tool
BOD	: Biological oxygen demand
BNR	: Biological nutrient removal
CAS	: Conventional activated sludge
COD	: Chemical oxygen demand
COMOMMAX	: Complete ammonia oxidation bacteria
DNA	: Deoxyribonucleic acid
DO	: Dissolved oxygen
FBDA	: Fine bubble diffused air
FISH	: Fluorescent in situ hybridization
F/M	: Food to microorganism ratio
HAO	: Hydroxylamine oxidoreductase
HRT	: Hydraulic retention time
mRNA	: Messenger ribonucleic acid
MLSS	: Mixed liquor suspended solids
MLVSS	: Mixed liquor volatile suspended solids
NCBI	: Centre for the Biotechnology Information

Ng	: Nanogram
NH_3	: Ammonia
NO_2^-	: Nitrite
NO_3^-	: Nitrate
NOB	: Nitrite oxidizing bacteria
NXR	: Nitrite oxidoreductase
PCR	: Polymerase chain reaction
q-PCR	: Quantitative real-time
RT-PCR	: Reverse transcription PCR
$Rnitrification$	: Rate of plant's nitrification
rRNA	: Ribosomal ribonucleic acid
SBR	: Sequencing batch reactor
SRT	: Sludge retention time
SVI	: Sludge volume index
WWTP	: Wastewater treatment plant

PREFACE

Kumalo PC, Awolusi OO, Kumari SK, Bux F. 2021. Profiling of key nitrogen converting organisms in the diffused aerated wastewater treatment plant. Paper presented at the South African society of microbiology 2021 conference, digital, May 4-6, 2021. (Oral presentation).

Kumalo PC, Awolusi OO, Kumari SK, Bux F. 2022. Evaluation of nitrification dynamics within the fine bubble diffused aerated wastewater treatment system using advanced molecular techniques. *Applied and Environmental Microbiology* (in preparation)

CHAPTER 1: INTRODUCTION

Nitrification is a common process of nitrogen conversion in biological nutrient removal (BNR) systems. The process is carried out aerobically by two distinct classes of chemolithoautotrophic bacteria/: (a) ammonia-oxidizing bacteria (AOB) which oxidize ammonia to nitrite and (b) nitrite-oxidizing bacteria (NOB). Recently, a single bacterial group known as complete ammonia oxidizers (COMAMMOX) with the capacity to oxidize ammonia directly to nitrate has also been discovered (Bae *et al.*, 2015, Daims *et al.*, 2015, Ge *et al.*, 2015). The predominant AOB in BNR systems belongs to one of three genera; *Nitrosomonas, Nitrosococcus,* or *Nitrosospira* while the predominant NOB belong to; *Nitrobacter, Nitrospira,* or *Nitrospina* (Speirs *et al.*, 2019). Nitrifying bacteria are generally slow-growing microorganisms and require a longer sludge age, which results in the proliferation of slow-growing filamentous bacteria leading to settling problems in wastewater treatment plants. Therefore, although the nitrification process has been widely studied, sustaining an efficient nitrification rate in wastewater systems is still challenging.

In BNR systems, the nitrification process is commonly hindered by the nitrifiers' physiological activities and their high susceptibility to environmental changes including pH, temperature, dissolved oxygen, as well as aeration rate (Soliman and Eldyasti, 2018). Monitoring nitrifying bacterial growth in the wastewater treatment plant is significant to prevent nitrification failure (Pan *et al.*, 2018). Since nitrification depends on aeration, dissolved oxygen has been noted as an important operational factor that affects nitrification, depending on the oxygen diffusion rate into the bulk liquid and the flocs. Aeration, therefore, plays an important role in the distribution and activity of nitrifying community structures in wastewater treatment systems (Yin *et al.*, 2018).

Surface aeration using agitators is the most commonly used aeration method in BNR systems, which are carried out with horizontal or vertical shaft aerators, and air pump systems that transport air into the wastewater. However, this mode of aeration has been associated with high energy consumption, coupled with insufficient oxygen transfer within the reactor due to limited mixing, which could impact the performance of the functional microbes, including nitrifiers (Roman and Mureşan, 2014). Diffused aeration systems are currently becoming increasingly popular as a choice of technology in the municipal wastewater treatment industry due to their high oxygen transfer efficiency and cost savings (Odize, 2018). These systems supply air in the form of fine bubbles to transfer oxygen in biological wastewater treatment processes, thus resulting in a better aeration efficiency and reduction of energy consumption (Qin, 2018).

This type of diffuser does not cause mechanical disruption of the flocs as the air bubbles circulate evenly in the aeration tank and allow the plant to develop ideal compact flocs with good settling properties (Drewnowski *et al.*, 2019). However, their impact on the functional microbial community is not yet fully understood due to a lack of studies. According to a report by Cydzik-Kwiatkowska and Zielińska (2016), to design functionally reliable wastewater treatment systems, it is important to understand how operating conditions affect the functional microbial community. Up till now, there is little or no information on the impact of fine bubble diffused aeration mode on nitrifiers' community structure and nitrification process in the full-scale WWTPs (Brotto, 2016, Drewnowski *et al.*, 2019). This study, therefore, focuses on understanding the structure and activity of nitrifiers in a full-scale wastewater treatment system operated with diffused fine bubble aeration.

The introduction of culture-independent molecular techniques for the identification and quantification of functional microbes in WWTPs has brought a better understating of microbial

community structure and their activities (Ferrera and Sanchez, 2016, Kim *et al.*, 2013, Awolusi *et al.*, 2015a). These molecular techniques based on DNA and RNA such as fluorescent in situ hybridization (FISH) (Jin *et al.*, 2011), polymerase chain reaction (PCR) (Fukushima and Bond, 2010), quantitative real-time PCR (qPCR) (Cho *et al.*, 2014), and droplet digital PCR (ddPCR) (Suryavanshi *et al.*, 2019) are more sensitive and accurate than culture-based methods. The reverse-transcription PCR (RT-PCR) is usually the method of choice for rapid and sensitive quantitative measurements of mRNA copy numbers analyzing gene expression levels (Zhang and Liu, 2019). The study of gene expression, which is based on RNA, will give more useful information on microbial function compared to DNA-based studies.

The majority of the existing studies on the microbial community structure of full-scale wastewater treatment systems are DNA-based, which does not directly relate to the microbial function (Zhang and Liu, 2019). However, RNA extracted from the activated sludge provides more valuable data than from DNA in revealing 'active' microbial communities versus 'dormant' microbial populations as mRNA is considered an indicator of functionally active microbial populations (Taylor *et al.*, 2017b). In addition, little is known about the impact of the fine bubble diffused aeration systems on the community structure and activity of different nitrifiers within wastewater treatment plants. This study, therefore, seeks to investigate the community structure and activity of key nitrogen converting organisms within a municipal full-scale wastewater treatment plant operated with fine bubble diffused aeration mode using molecular techniques.

1.1 AIMS AND OBJECTIVES OF THE STUDY

1.1.1 Aim

- To investigate the community structure and activities of nitrifying bacteria in WWTPs with fine bubble diffused aeration technology using advanced molecular techniques

1.1.2 Objectives

- To assess the nitrogen removal performance of two diffused aerated WWTPs in relation to their operating and environmental parameters
- To quantify key nitrifying bacterial community by targeting species-specific primers using the qPCR method
- To analyze the functional gene expression profiles of the key nitrifiers using reverse transcriptase PCR

CHAPTER 2: LITERATURE REVIEW

2.1 NITROGEN CYCLE

Nitrogen is one of the primary nutrients required for the survival of all living organisms as a building material for DNA, proteins, and amino acids (Cao *et al.,* 2020, Abdollahbeigi and Asgari Bajgirani, 2020). Therefore, during the nitrogen cycle process, nitrogen undergoes different transformations and is converted into multiple chemical forms as it circulates through the atmosphere, the soil, and microorganisms. The traditional nitrogen cycle includes steps such as nitrogen fixation, nitrification; denitrification, and ammonification (Stein and Klotz, 2016) (Fig. 2.1). During the process of nitrogen fixation, the atmospheric N_2 gas is reduced by the enzyme nitrogenase to produce ammonia and subsequently assimilated into the cell material of nitrogen-fixing bacteria (Vu *et al.*, 2018). Ammonia is also produced during the decomposition of organic substances in a process known as ammonification or mineralization (van Hullebusch *et al.*, 2019). Some of this released ammonium is recycled and converted to amino acids, whilst the remaining ammonia/ammonium may be catabolized either aerobically or anaerobically through two distinct microbial key processes in the nitrogen cycle.

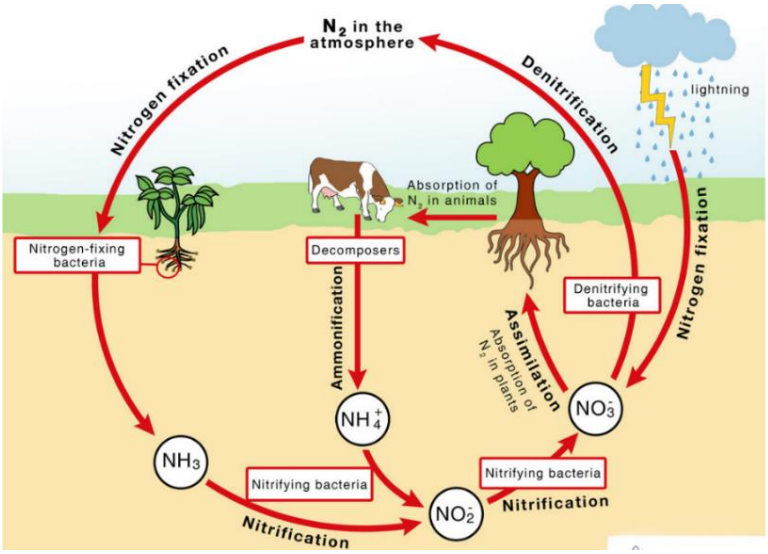

Figure 2.1: Microbial nitrogen cycle (Stein and Klotz, 2016).

Nitrification is an important process of the global biochemical nitrogen cycle, carried out via a two-step aerobic process (Bae *et al.*, 2015). The process is mediated by two groups of microorganisms: AOB and AOB. The AOB is responsible for the conversion of ammonia to nitrite (ammonia oxidation, Eq. 1) using ammonia monooxygenase (amoA) and hydroxylamine oxidoreductase (Amoo and Babalola, 2017). The NOB further oxidizes nitrite to nitrate (nitrite oxidation, Eq. 2 and Eq. 3) using the nitrite oxidoreductase (Ushiki *et al.*, 2017).

$$NH_4^+ + 1.5\ O_2 \rightarrow NO_2^- + 2H^+ + H_2O \qquad \text{(Eq. 1)}$$

$$NO_2^- + 0.5\ O_2 \rightarrow NO_3^- \qquad \text{(Eq. 2)}$$

$$NH_4^+ + 2\ O_2 \rightarrow NO_3^- + 2H^+ + H_2O \qquad \text{(Eq. 3)}$$

A novel group of bacteria known as COMAMMOX can oxidise ammonia to nitrate (Eq. 4-6) in a single-step process (Bae *et al.*, 2015, Daims *et al.*, 2015, Ge *et al.*, 2015). The discovery of the COMAMMOX process has redefined key components of the traditional nitrogen cycle (Fig. 2.2).

$NH_4^+ + 1.5\ O_2 \rightarrow NO_2^- + H_2O + 2\ H^+$ ($\Delta G°' = -274.7$ kJ/mol) (Eq. 4)

$NO_2^- + 0.5\ O_2 \rightarrow NO_3^-$ ($\Delta G°' = -74.1$ kJ/mol) (Eq. 5)

$NH_4^+ + 2\ O_2 \rightarrow NO_3^- + H_2O + 2\ H^+$ ($\Delta G°' = -348.9$ kJ/mol) (Eq. 6)

Denitrification is the process in which nitrogen compounds are returned to the atmosphere by converting nitrate (NO_3^-) to nitrogen gas (N) (Eq.7-8) under anoxic conditions using organic electron donors, thus completing the nitrogen cycle (Holmes *et al.*, 2019). Traditionally, denitrification was thought to be carried out by a group of denitrifying heterotrophic bacteria under anaerobic conditions using organic materials as electron donors (Du *et al.*, 2017).

$NO_3 + 2H + 2e \rightarrow NO_2 + H_2O$ (Nitrate reductase) (Eq. 7)

$NO_2 + 2H + e \rightarrow NO + H_2O$ (Nitrite reductase) (Eq. 8)

A specific group of autotrophic microorganisms, known as anaerobic ammonia oxidation (ANAMMOX) bacteria, are capable of oxidising ammonia directly to nitrogen gas under anaerobic conditions (Ma *et al.*, 2017a, Wu *et al.*, 2019, Mulder *et al.*, 1995). The process is mediated by specific ANAMMOX bacterial groups within the planctomycetes phylum and presents an alternative process that converts ammonia to nitrogen gas in a single step (Eq. 9), using nitrite as an electron acceptor and ammonium as electron donor (Kartal *et al.*, 2012).

$NH_4^+ + 1.32NO_2^- + 0.066HCO_3^- + 0.13H^+ \rightarrow 1.02N_2 + 0.26NO_3^- + 0.066CH_2\ O_{0.5}N_{0\ 15}N_{0.15} + 2.03H_2O$ (Eq. 9)

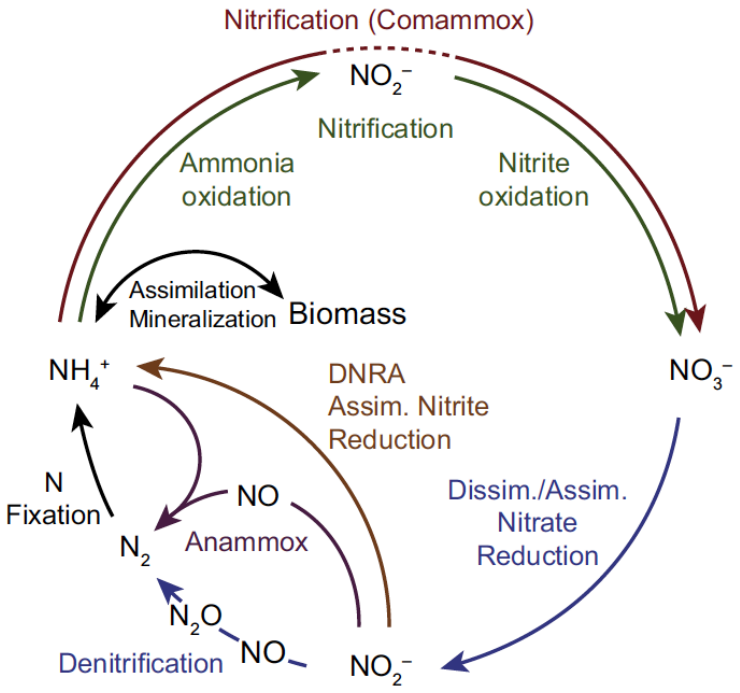

Figure 2.2: Modified microbial nitrogen cycle, which includes COMAMMOX (Daims *et al.*, 2016)**.**

2.2 NITRIFYING MICROBIAL COMMUNITY STRUCTURE

2.2.1 Ammonia oxidizing bacteria (AOB)

Ammonia oxidizing bacteria are aerobic chemolithotrophic bacteria currently found in two taxonomic groups *Betaproteobacteria* and *Gammaproteobacteria*. The genera *Nitrosomonas*, *Nitrosospira*, and *Nitrosovibrio* belong to *Betaproteobacteria* AOB except for the *Nitrosococcus*, which belongs to a *Gammaproteobacteria* AOB (Zou *et al.*, 2019) (Fig. 2.3) (Table 2.1). According to the previous reports, *Nitrosomonas* and *Nitrosospira* are found to be the most common AOB in WWTPs (Lukumbuzya *et al.*, 2020, Aalto *et al.*, 2018, Zorz *et al.*, 2018). The community structure and activity of AOB are also influenced by several environmental and operational factors, such as temperature, dissolved oxygen (DO), pH, and nutrient analysis in WWTPs (Bani *et al.*, 2020). Previously, AOB was considered the only dominant microorganism in the ammonia oxidation process. However, with the extensive

molecular biology development in recent years, it was found that ammonia oxidising archeas (AOA) have similar ammonia-monooxygenase (Amo) enzymatic pathways as that of AOB, and *amoA* can be used as a useful marker to evaluate the distribution of AOB and AOA in WWTPs (Fig. 2.4) (Ferrera and Sanchez, 2016).

2.2.2 Nitrite oxidizing bacteria (NOB)

Nitrite oxidation is the second step of the nitrification process carried out by the nitrite-oxidizing bacteria (NOB) whereby NO_2^- is oxidized to NO_3^- by the nitrite oxidoreductase (NXR) (Eq 8). This NXR consists of two or three subunits which include the α-subunit (*nxrA*) and the β-subunit (*nxrB*) (Smeulders *et al.*, 2020). All known NOB belongs to the genera *Nitrobacter, Nitrospira, Nitrosococcus,* and *Nitrospina.* They are classified within alpha and delta-subclasses of *Proteobacteria* except for the *Nitrospira* (Duan *et al.*, 2013), which has its distinct phylum, and *Nitrospina*, which belongs to the beta-subclass of *Proteobacteria (Zeng et al., 2012)* (Fig. 2.3). *Nitrobacter* and *Nitrospira* are considered to be the key and most dominant NOB in BNR plants. The genus *Nitrobacter* consists of *Nitrobacter winogradskyi, Nitrobacter hamburgensis, Nitrobacter vulgaris,* and *Nitrobacter alkalicus* while the genus *Nitrospira* consists of the most diverse group, *Nitrospira marina* and *Nitrospira moscoviensis* (Table 2.1) (Ngugi *et al.*, 2016).

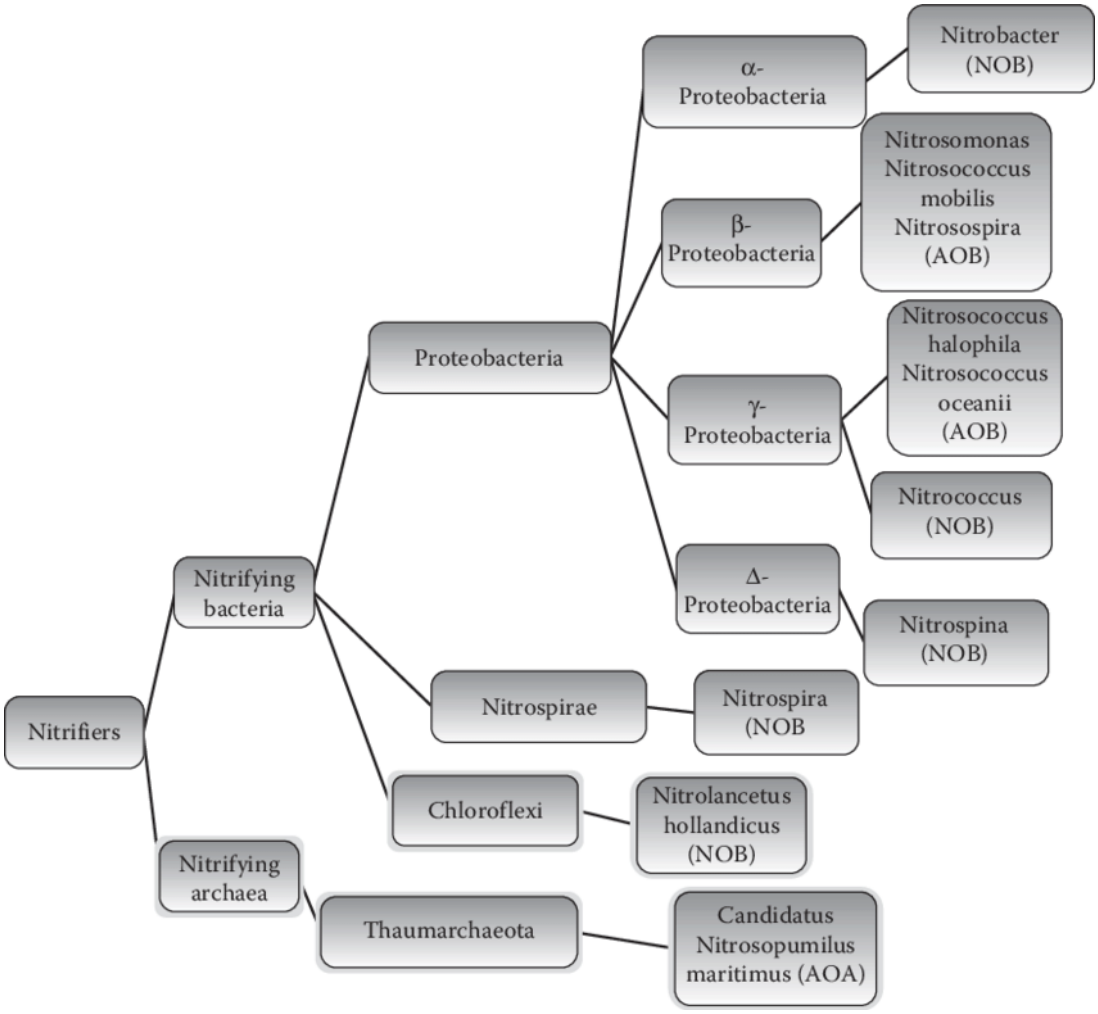

Figure 2.3: Schematic representation of conventional AOB, NOB, and AOA in wastewater (Awolusi *et al.*, 2015a)

2.2.3 Complete ammonia oxidation bacteria (COMOMMAX)

For over 100 years, it was thought that the consecutive nitrification process was a two-step process carried out by AOB and NOB (Daims *et al.*, 2015, Zhao *et al.*, 2019). However, COMAMMOX, a single organism within the genus Nitrospira (NOB), is capable of complete ammonia oxidation to nitrate in a single step (Daims *et al.*, 2015). The discovery of COMAMMOX has redefined key components of the traditional nitrogen cycle (Wang *et al.*, 2017c, Daims *et al.*, 2016). It has been reported that the ammonia monooxygenase (amoA) of COMAMMOX is unique and is different from the *amoA* sequences of AOB and AOA. The

degenerate COMAMMOX *amoA*-targeted primers, therefore, offer a straightforward, fast, and robust approach for the detection and identification of COMAMMOX and *Nitrospira* from wastewater samples (Pjevac *et al.*, 2017). Thus far, three candidate COMAMMOX species have been described in the literature, namely, Ca. *N. nitrosa, Ca. N. inopinata,* and Ca. *N. nitrificans* (Table 2.1) (Fowler *et al.,* 2018). Sensitive and reliable identification methods for COMAMMOX bacteria are needed to assess their role in biological nitrogen removal processes. Due to the morphological similarity of *Nitrospira* members to other NOB, only DNA-based methods are able to identify COMAMMOX (Nowka *et al.*, 2015).

Currently, the next-generation sequencing (NGS) approach is the most useful and powerful method used to identify COMAMMOX bacteria. Metagenomic analysis has been used for the identification of COMAMMOX bacteria by Pinto *et al.* (2016), Chao *et al.* (2016), Palomo *et al.* (2016), and Sobotka *et al.* (2018). However, the metagenomics analysis does not provide information about the activity of the bacteria. Hence, the metagenomic approach could be integrated with metatranscriptomics, which analysis mRNA extracted from the living cells of microbial communities. Thus far, this procedure has not been applied to COMAMMOX bacteria.

Table 2.1: List of nitrifying bacteria reported from activated sludge (Wang *et al.*, 2016a, Sorokin *et al.*, 2012, Nowka *et al.*, 2015, Ushiki *et al.*, 2013).

Ammonia-oxidising Bacteria	**Beta-proteobacteria**	*Nitrosomonas nitrosa* *Nitrosomonas communis* *Nitrosomonas eutropha* *Nitrosomonas europaea* *Nitrosomonas aestuarii* *Nitrosomonas marina* *Nitrosomonas oligotropha* *Nitrosomonas halophila* *Nitrosomonas stercoris* *Nitrosomonas ureae*
	Gamma-proteobacteria	*Nitrosococcus halophilus* *Nitrosococcus mobilis* *Nitrosococcus nitrosus* *Nitrosococcus oceani* *Nitrosococcus watsonii* *Nitrosococcus wardiae*
Nitrite-oxidising Bacteria	**Alpha-proteobacteria**	*Nitrobacter winogradskyi* *Nitrobacter vulgaris* *Nitrobacter alkalicus* *Nitrobacter hamburgensis*
	Beta-proteobacteria	*Nitrococcus mobilis* *Nitrotoga*
	Delta-proteobacteria	*Nitrospina gracilis* *Nitrospina watsonii* *Phylum Nitrospirae* *Nitrospira defluvii* *Nitrospira moscoviensis* *Nitrospira marina* *Nitrospira moscoviensis* *Nitrospira calida* *Nitrospira lenta* *Nitrospira japonica*
COMAMMOX		*Ca. Nitrospira nitrosa*, *Ca. Nitrospira inopinata*, *Ca. Nitrospira nitrificans*

2.3 BIOLOGICAL NITROGEN REMOVAL IN WASTEWATER

Nitrogen removal in wastewater is achieved by complete sequential oxidation of ammonia to nitrate (nitrification) and reduction of nitrate to nitrogen gas (denitrification) (Stein and Klotz, 2016). To achieve this, the BNR systems are designed with a combination of aerobic (nitrification) and anaerobic/anoxic (denitrification) treatment processes with internal recycles (Fig. 2.4) to allow for complete nitrogen removal (Zhang *et al.*, 2018). Various BNR configuration processes to conventional activated sludge processes have been developed over the years to achieve optimum nutrient removal from plants. A few examples of BNR configuration processes are listed below (Table 2.2).

Table 2.2: Examples of BNR configuration processes and their advantages

Configuration Process	Advantages	References
Ludzack-Ettinger (MLE)	The MLE process is highly effective in removing nitrogen and phosphorus compounds, with a removal efficiency of 76% and 56%, respectively. In this process, nitrification occurs in the aeration zone, and the sludge-containing nitrate generated in the aeration tank is denitrified in the anoxic zone.	(Liu and Wang, 2017)
Five-stage Bardenpho Process	The Bardenpho Process was developed for the removal of both nitrogen and phosphate. This process has an additional anaerobic zone for efficient nitrogen removal and good phosphorus removal.	(Barnard *et al.*, 2017)
The 3-stage Phoredox Process	The 3-stage Phoredox Process is capable of both nitrogen and phosphorus removal. This process was designed (anaerobic, aerobic, and clarifier with sludge recycling only from the clarifier to the anaerobic tank) to prevent NO_3^- from entering the anaerobic tank.	(Barnard *et al.*, 2017)

Modified University of Cape Town (UCT) Process	The Modified UCT process was designed to minimize the effect of nitrate-oxygen in the anaerobic zone and to achieve internal nitrate recycling. This process provides good nitrogen and phosphate removal.	(Ge *et al.*, 2011)
Johannesburg (JHB) Process	This process was designed to overcome the detrimental effects of nitrate, by introducing a sludge denitrification vessel in the RAS line. This results in the return flow to the anaerobic zone being very low in oxygen and nitrogen and near-optimal use of the anaerobic reactor is achieved.	(Barnard *et al.*, 2017)
Sequencing Batch Reactor (SBR) Process	The anaerobic/anoxic/aerobic progression in this process is essential for the removal of phosphorus and total nitrogen. Due to the fill-and-draw nature of SBRs, it is vital to remove the remaining nitrates after the aerobic cycle before anaerobic conditions can be established.	(Song *et al.*, 2017)

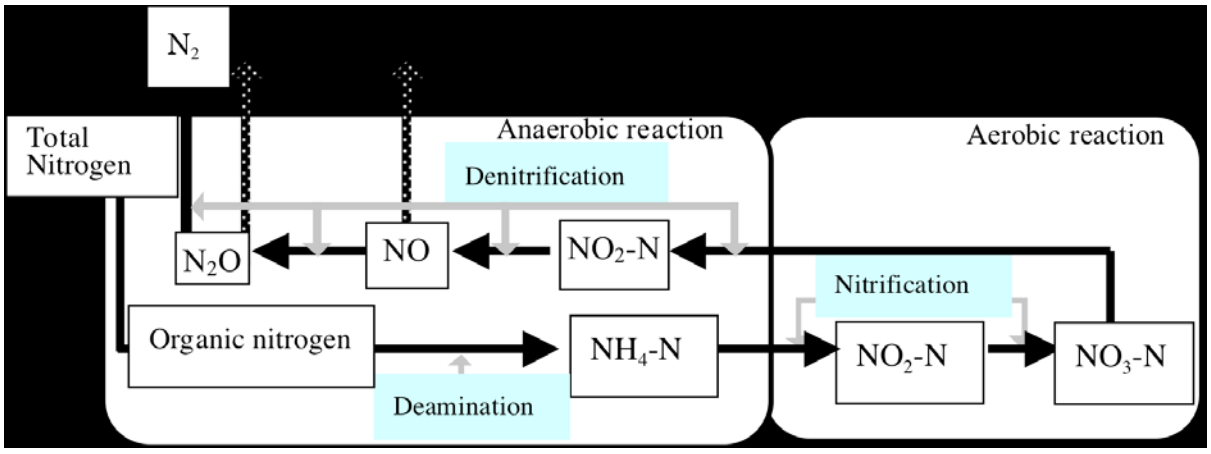

Figure 2.4: Conventional activated sludge process (Lares *et al.*, 2018)

Although the nitrification process has been extensively studied, it is still difficult to achieve stable nitrogen removal in WWTPs. This is principally due to the slow growth rates of nitrifying bacteria and their sensitivity to toxic shocks, pH, substrate, and temperature fluctuations (Zhang *et al.*, 2019). Factors such as the sludge age and the temperature are

essential for the adequate growth of nitrifying bacteria. Dissolved oxygen concentration has been widely reported as a critical factor for the distribution and performance of nitrifiers during wastewater treatment due to their higher affinities towards oxygen (Khatri *et al.*, 2020, Wang *et al.*, 2018). Even though all nitrifiers are known to be slow-growing organisms, their specific growth rate under different operational conditions varies which might impact the overall nitrogen removal process (Bassin *et al.*, 2012, Reboleiro-Rivas *et al.*, 2015). Therefore, quantification and monitoring the physiological activity with a balance in the linked activities of these different nitrifying bacterial groups involved is essential (Kumwimba and Meng, 2019). All known AOB belong to genera *Nitrosomonas*, *Nitrosovibrio*, *Nitrosospira*, and *Nitrosolobus* while *Nitrobacter*, *Nitrospira*, *Nitrosococcus* and *Nitrospina* belong to NOB (Table 2.2). *Nitrosomonas spp*. and *Nitrobacter spp*. are usually regarded as the typical dominating AOB and NOB in wastewater, respectively (Daims *et al.*, 2016).

Besides the conventional nitrogen removal process, novel and economically feasible biological nitrogen removal processes have been developed. This includes COMAMMOX with the capacity to oxidize ammonia directly to nitrate (Koch *et al.*, 2019) and simultaneous nitrification and denitrification, anaerobic ammonium oxidation (ANAMMOX), with the capacity to convert ammonia to nitrogen gas in a single step (Ahmad *et al.*, 2020, Wang *et al.*, 2017c). These COMAMMOX bacteria are expected to have a competitive advantage in biofilms and other microbial aggregates with low substrate concentrations (Daims *et al.*, 2016, Annavajhala *et al.*, 2018, Yu *et al.*, 2018). All COMAMMOX organisms identified to date belong to "Candidatus *Nitrospira nitrosa*", "Candidatus *Nitrospira nitrificans*", "Candidatus *Nitrospira inopinata*", and *Nitrospira sp*. strain Ga0074138 (Van Kessel *et al.*, 2015, Sobotka *et al.*, 2018). However, understanding COMAMMOX metabolic activity and interactions with other bacterial groups is still limited in BNR processes. Therefore, there is a need for more

research effort toward understanding the abundance of COMAMMOX and their contribution to BNR process configurations which will guide process design and operation.

On the other hand, the denitrification process is the reduction of nitrite, nitric oxide, and nitrous oxide to dinitrogen gas under anoxic using organic carbon as the electron donor. Denitrification is carried out by a diverse group of prokaryotes, which includes species in the genera *Bacillus, Paracoccus*, *Pseudomonas, Hyphomicrobium*, and *Methylobacterium* (Ferrera and Sanchez, 2016). In contrast, ANAMMOX-based BNR processes are more sustainable for nitrogen removal due to their ability to remove both NH_4 and NO_2 simultaneously without producing the greenhouse gas, N_2O (Liu *et al.*, 2017). Compared to conventional BNR systems, ANAMMOX systems can save up to 63% oxygen supply (aeration), 100% organic carbon requirement, and 35% lower sludge production, which results in less sludge treatment cost (Dan *et al.*, 2021, Qiu *et al.*, 2021). So far, ANAMMOX-based BNR has been successful in both lab-scale and full-scale applications, especially with wastewater that has high ammonia concentrations or low C/N ratios (Ronan *et al.*, 2021, Wen *et al.*, 2020).

The sequencing batch reactor (SBR) was the most commonly used and successfully applied system for ANAMMOX enrichment studies (Wang *et al.*, 2012a, De Lille *et al.*, 2015). However, this system could not provide an ideal condition for long-term ANAMMOX cultivation as the ANAMMOX bacteria are often inhibited by their substrates (Puyol *et al.*, 2014). The continuous stirred-tank reactor (CSTR) system offers a longer hydraulic retention time and a continuous source of the fresh substrate, with the simultaneous removal of toxic metabolic by-products, however, it has been criticized for its inefficient biomass retention (Carvajal-Arroyo *et al.*, 2014). In contrast, membrane-based bioreactor systems (MBRs) have an efficient biomass retention time. Nevertheless, bulk mixing and substrate mass transfer in

this system were suboptimal. Thus, moving bed biofilm reactors (MBBRs) were developed, which maximizes the advantages of both the MBR and CSTR systems.

2.4 FACTORS INFLUENCING NITRIFICATION AND NITRIFYING BACTERIA

The nitrification process especially in BNR systems is commonly hindered by the nitrifiers' physiological activities and their highly susceptible nature to environmental and operational changes including pH, alkalinity, temperature (Li *et al.*, 2018), DO, sludge retention time (SRT), and hydraulic retention time (HRT) (Soliman and Eldyasti, 2018).

2.4.1 Environmental factors

2.4.1.1 pH and alkalinity

The pH of the WWTP system strongly affects nitrification. The optimal pH for nitrification ranges from 7.5 to 8.5 (Wang *et al.*, 2020). However, reported complete nitrification to nitrate at pH ranging from 6.45 to 8.95. Furthermore, a pH lower than 6.45 or higher than 8.95 may completely inhibit nitrification. Rakocy *et al.* (2016) reported a higher pH of 8 – 9 favored the elevation of nitrite accumulation, thereby affecting the optimal nitrification process.

2.4.1.2 Temperature

The temperature has a significant effect on the specific growth rates of both AOB and NOB in wastewater (Collings *et al.*, 2020). According to Duan *et al.* (2019), the specific growth rate of NOB was higher than that of AOB at low temperatures (10 – 20^{o}C), while at a higher temperature of 20 – 25°C, the growth of NOB was reduced with activation of AOB. Furthermore, at temperatures above 25°C, the activity of AOB was higher than that of NOB

due to their high activation energy which is between 72 and 60 $kJmol^{-1}$ for AOB, whereas it is from 43 to 47 $kJ\ mol^{-1}$ for NOB (Guillén, 2017). These discoveries, therefore, indicate that the influence of temperature on the AOB and NOB populations differs.

2.4.2 Plant operational factors

2.4.2.1 Dissolved oxygen

Oxygen plays an important role in the nitrification process and nitrifying bacteria require a high amount of oxygen for nitrification to occur. DO concentration provides significant information regarding the biological activity of the biomass, which is often used to control the aeration rate (Biechele *et al.*, 2015). However, DO concentrations have been proven as a key limiting factor that can result in the inhibition of the AOB and NOB populations. For 1 mol of ammonia, AOB uses 1.5 mol of oxygen while NOB converts nitrite to nitrate using 0.5 mol of oxygen. The optimal DO concentration for the growth of AOB and NOB ranges between 1.5–2.0 mg/L (Guillén, 2017). However, according to Wen *et al.* (2020), higher nitrogen removal efficiency may be observed at low DO concentrations (1.5 mg/L).

2.4.2.2 Sludge retention time (SRT) and Hydraulic retention time (HRT)

The sludge retention time (SRT) and hydraulic retention time (HRT) are regarded as one of the most important designs and operating parameters affecting the performance of nutrient removal and the microbial community of WWTPs (Wang *et al.*, 2017a). Due to the slow growth of nitrifying bacteria, nitrification may not occur at low SRT (<5-10 days). Therefore, to ensure effective nitrification, a longer SRT is needed. However, Li and Wu (2014) report that a longer SRT may reduce the efficiency of phosphorus removal because of the low sludge wasting rate which may lead to the possible phosphorus release in the clarifier. Metcalf *et al.* (2014) and Tchobanoglous (2014) studied the BNR system in sequencing batch reactors (SBRs) at SRTs

of 5–30 days and it was observed that simultaneous nitrogen and phosphorus removal could be achieved effectively under SRTs of 10 and 15 days. However, at SRT above 15 days, the ammonium removal efficiency was reduced due to the high endogenous decay of microorganisms at high SRTs. Hence, currently, many WWTPs are operated at long SRTs (>20-30 days) to obtain full nitrogen and phosphate removal and reduce excess sludge production (Van den Broeck *et al.*, 2012). However, previous studies report that longer SRT (>30 days) may impact the phosphate removal efficiency negatively due to the low sludge-wasting rate (Wang *et al.*, 2017a).

Previous studies have reported the impact of HRT on nitrification efficiency in WWTPs. Li *et al.* (2013) studied the effect of HRT on nitrification efficiency and microbial community structure in conventional activated sludge systems. The study showed that specific ammonium-oxidizing and nitrate-forming rates increase with the decrease in HRT, which strengthens the dominance of NOB especially fast-growing *Nitrobacter spp*., whereas the AOB population reduced. Hu *et al.* (2019) report the reduction of COD and total nitrogen efficiency in SBR treating soak liquor from 95 to 92% and 96 to 54 % respectively with a decrease in HRT from 5 to 3.3 days. Similar results were reported by Li *et al.* (2013) who studied the effect of HRT on the performance of SBR treating tannery wastewater and found that the reduction of COD efficiency was observed with a decrease in HRT from 3 to 2 days.

2.5 AERATION IN BNR SYSTEMS

Aeration in BNR systems plays an important role in solid-liquid separation and distribution of the nitrifying community. Activated sludge aeration tanks such as mechanical surface agitators or submerged diffusers are used to supply oxygen for the biological conversion of soluble organic compounds into settleable solids. According to a report by Cydzik-Kwiatkowska and

Zielińska (2016), to design functionally reliable wastewater treatment systems, it is important to understand how operating conditions affect the reactor's microbial community flocs' structural properties. However, there is little or no information on the impact of fine bubble diffused aeration mode on nitrifiers' community structure and nitrification process in the full-scale WWTPs. Therefore, evaluating the nitrifying community structure and nitrification process of BNR systems with fine bubble diffused aeration will be valuable for WWTP operators in making an informed decision (Brotto, 2016).

2.5.1 Surface aeration

Surface aerations are the most widely used technology in biological wastewater systems which are carried out with horizontal or vertical shaft aerators, and air pump systems that transport air into the wastewater (Fig. 2.5) (Drewnowski *et al.*, 2019). The use of these aeration systems has become very important to overcome numerous difficulties in the aeration processes due to their simplicity, lower maintenance, and ease of operation (Turunen *et al.*, 2018). The surface aerators are designed to promote the growth of aerobic microorganisms which in turn reduce the biological demand oxygen (BOD) in the wastewater by increasing dissolved oxygen in the aeration tank (Drewnowski *et al.*, 2019). These systems supply atmospheric air in the water by creating small droplets propelled to create the necessary liquid/gas contact area. However, this mode of aeration has been associated with high energy consumption, coupled with inefficient oxygen transfer within the reactor due to limited mixing, which could impact the performance of the functional microbes including nitrifiers (Roman and Mureşan, 2014).

Figure 2.5: Illustration of surface aeration system (Liai *et al.*, 2017).

2.5.2 Diffused aeration

Diffused aeration systems are gradually becoming a popular choice for municipal WWTPs due to their high oxygen mass transfer efficiency and reduced energy consumption. These systems supply air in the form of fine bubbles for oxygen transfer in biological wastewater treatment processes (Fig. 2.6). The commonly used diffusers are fine-pore diffused aeration due to their high oxygen transfer efficiency when compared to coarse bubbles aeration and surface aerators (Brotto, 2016, Drewnowski *et al.*, 2019). This type of diffuser does not cause mechanical disruption of the flocs as the air bubbles circulate evenly in the aeration tank and allow the plant to develop ideal compact flocs with good settling properties (Odize, 2018). However, their impact on the functional microbial community structure and nitrification process in full-scale WWTP has not been fully understood due to the lack of studies on it (Brotto, 2016).

Figure 2.6: Illustration of diffused aeration system.

2.6 ACTIVATED SLUDGE FLOC STRUCTURE

The activated sludge is an important process that has been successfully used to treat municipal WWTPs. The effectiveness of this process depends on solid-liquid separation, which is determined by its settling properties (Asensi *et al.*, 2019a). Sequentially, the settling properties of activated sludge depend on the flocs' structural properties and microbial population (Asensi *et al.*, 2019b). Additionally, the properties of activated sludge flocs formed in the aeration tank depend on plant operation conditions such as organic loading, DO, and solids retention time (Campbell *et al.*, 2021, Shao *et al.*, 2021). Therefore, poorly formed flocs may result in excessive growth of filamentous bacteria, a phenomenon known as bulking sludge, which may slow down settling and nitrification performance. The bulking sludge usually occurs when oxygen levels are low or when the microbial community is too young or too old (Wang *et al.*, 2016b).

Aeration also gives rise to different turbulence conditions in the aeration tank thus influencing the activated sludge flocs. According to literature reports, small, robust, and compact flocs are produced at high homogenous flow regimes such as in diffused reactors whereas large, irregular, and open flocs are produced at less high homogenous flow regimes such as surface

reactors (Li *et al.*, 2020, Wang *et al.*, 2020, He *et al.*, 2018). Compact, round and firm flocs (Fig 2.7A) have been reported to have good settling properties resulting in low suspended solids produced in the effluent (Campbell *et al.*, 2019, Han *et al.*, 2021), while large, irregular, and weak flocs (Fig 2.7B) have poor settling properties, due to their large surface area (Nethaji *et al.*, 2021). The settling properties of sludge in the aeration tank are measured using Sludge Volume Index (SVI) (Giokas *et al.*, 2003). The sludge settling is based on the volume (in mL) that sludge occupies (1 gram) after 30 minutes of settling, with the optimum range of 50 - 150 mL/g.

Diffused aeration systems have been reported to produce significantly higher DO concentrations than surface aeration systems which were previously reported to have a positive influence on floc formation (Drewnowski *et al.*, 2019, Nethaji *et al.*, 2021). Adonadaga (2015) reported that at high DO concentrations, flocs have higher compactness (Fig 2.7A) than at low DO concentrations, while low DO levels could disrupt the biological processes and result in the production of irregular floc (Fig 2.7B) with poor sludge settleability due to excessive growth of filamentous bacteria. In addition, fine-bubble diffused aeration has advantages over surface aeration due to its high oxygen transfer efficiency and evenly mixing in the aeration tank which allows the plant to develop ideal compact flocs with good settling properties (Wanner and Torregrossa, 2017). Furthermore, fine bubble aeration systems have been reported to minimize floc rupture (Pechaud *et al.*, 2021, De Temmerman *et al.*, 2015). Nevertheless, there is little information in the literature regarding the efficiency of floc structure under varying operational conditions in diffused aerated full-scale WWTP.

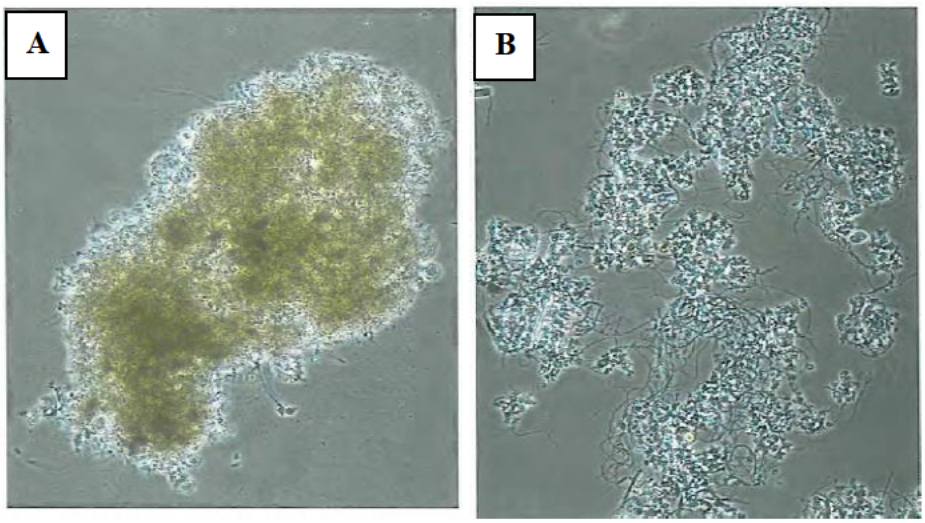

Figure 2.7: Illustration of sludge floc structure showing (A) rounded, compact floc and (B) irregularly shaped, open floc (Eikelboom, 2000).

2.7 DETECTION AND QUANTIFICATION OF NITRIFIERS FROM WWTP

Previously, culture-dependent methods were solely dependent on studying the microorganisms present in the environment, including WWTPs. However, these culture-dependent methods have limitations in characterizing the microbial structure and functional diversity of microorganisms in the environment because most microorganisms involved are non-culturable. Thus, the introduction of culture-independent molecular techniques for the identification and quantification of nitrifying bacteria in WWPTs has brought a better understating of microbial community structure (Awolusi *et al.*, 2015b). These culture-independent molecular techniques based on DNA and RNA include the analysis of whole genomes of selected marker genes such as 16S ribosomal RNA (16S rRNA) and functional genes (De Vrieze *et al.*, 2018).

The culture-independent molecular techniques are divided into two major approaches depending on their capability of revealing the microbial diversity structure and function: (1) partial community analysis and (2) whole community analysis (Fig. 2.8). These techniques

include PCR (Fukushima and Bond, 2010), qPCR (Suryavanshi *et al.*, 2019), RT-PCR, and gene expression, which is more sensitive and accurate than culture-based methods (Tsotetsi *et al.*, 2018). However, these molecular techniques have their shortcomings, hence a combinatory approach has been recommended, whereby two or more techniques are usually combined (Taylor *et al.*, 2017b).

Nevertheless, these techniques require known sequence alignments to design oligonucleotide primers to target specific microorganisms of interest. On the other hand, the NGS allows for a deeper, speedy, and relatively inexpensive alternative to investigating deeper layers of microbial communities and their functional activities in the environment (Sanz and Köchling, 2019). Due to the ability of the NGS technique to generate millions of reads, applications such as metagenomics (16S rRNA gene amplicon- and whole-genome sequencing) and metatranscriptomics (RNA sequencing) have been used to generate data of collective microbial genomes in wastewater without prior knowledge of the microbial communities and allows for interpreting transcriptional activity (Metch *et al.*, 2018). Some of the commonly used techniques are highlighted below.

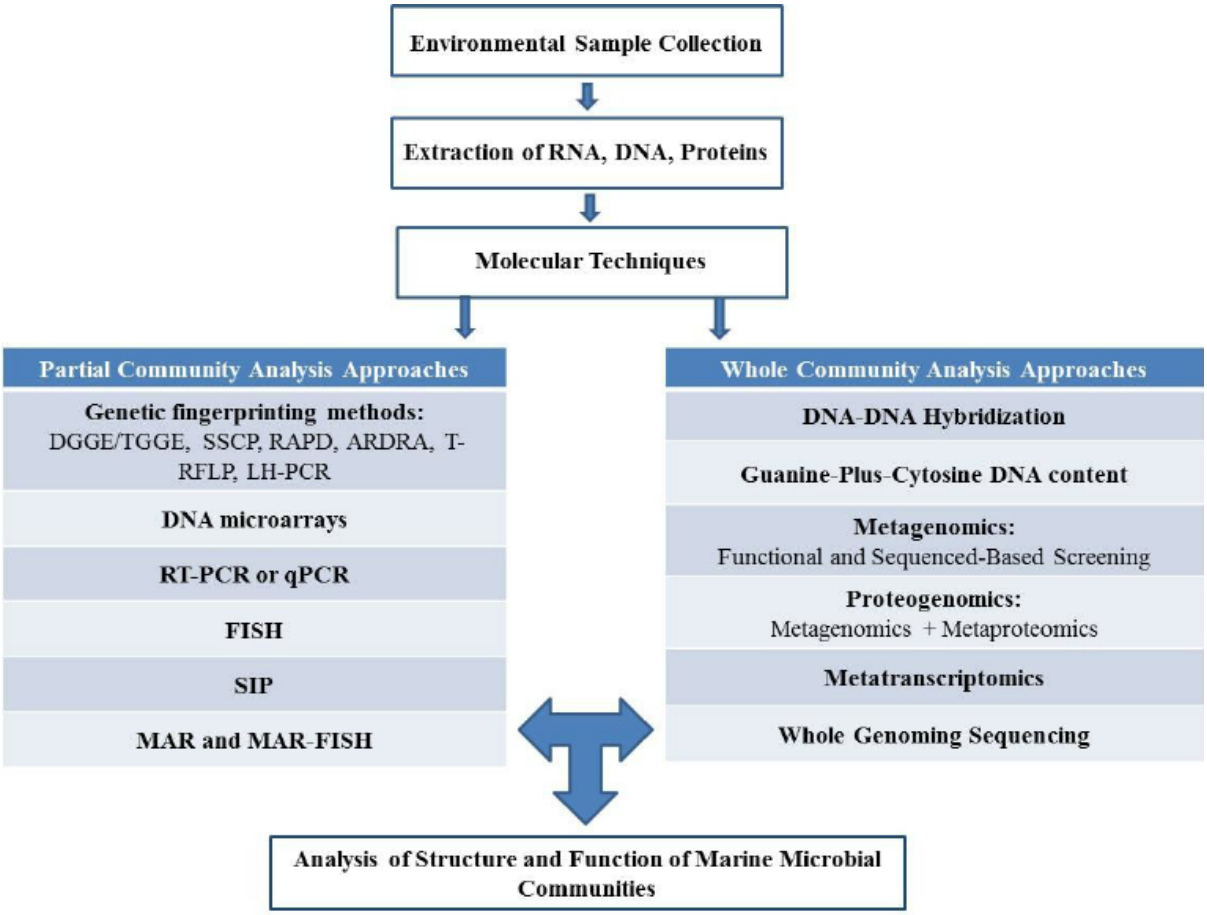

Figure 2.8: Culture-independent molecular techniques to characterize the structural and functional diversity of microorganisms in the environment (Taylor *et al.*, 2017b).

2.7.1 Polymerase chain reaction (PCR)

PCR is a fundamental and regularly used culture-independent molecular technique for the analysis of activated sludge community structures and their functional gene. The overall microbial diversity in activated sludge communities is determined by targeting the the16S rRNA gene while the genes such as ammonia monooxygenase (*amoA*) (Jin *et al.*, 2011), nitrite oxidoreductase (*nxrA* and *nxrB*) (Poly *et al.*, 2008, Pester *et al.*, 2014), nitrite reductase (*nirK* and *nirS*) (Braker *et al.*, 2000), and nitrate reductase (*narG*) (Philippot *et al.*, 2002) have been designed to targets the functional population present in WWTPs (Table 2.3). PCR-based methods are limited as they do not provide quantitatively valid information. Hence, PCR-based

techniques have been developed to overcome some of these limitations by increasing amplification specificity and amplicon yield. qPCR methods were developed to allow targeted rRNA genes and appropriate functional genes copy numbers to be quantified (Ramdhani, 2013).

Table 2.3: PCR primers for the detection of nitrifying functional genes in activated sludge

PRIMER	TARGET GENE	SEQUENCE (5'-3')	REFERENCE
nirK1F	nitrite reductase (*nir*K)	GGMATGGTKCCSTGGCA	(Braker *et al.*, 2000)
nirK4R	nitrite reductase (*nir*K)	GGRATRARCCAGGTTTCC	(Braker *et al.*, 2000)
nirS1F	nitrite reductase (*nir*S)	CCTAYTGGCCGCCRCART	(Braker *et al.*, 2000)
nirS5R	nitrite reductase (*nirS*)	CTTGTTGWACTCGSSCTGCAC	(Braker *et al.*, 2000)
narG 1960 F	nitrate reductase (*narG*)	TAYGTSGGCCARGARAA	(Philippot *et al.*, 2002)
narG 2659 R	nitrate reductase (*narG*)	TTYTCRTACCABGTBGC	(Philippot *et al.*, 2002)
amoA-1F	ammonia monooxygenase (*amoA*)	GGGGTTTCTACTGGTGGT	(Jin *et al.*, 2011)
amoA-2R	ammonia monooxygenase (*amoA*)	CCCCTCKGSAAAGCCTTCTTC	(Jin *et al.*, 2011)
nxrA f1	nitrite oxidoreductase (*nxrA*)	CAGACCGACGTGTGCGAAAG	(Poly *et al.*, 2008)
nxrA r2	nitrite oxidoreductase (*nxrA*)	TCCACAAGGAACGGAAGGTC	(Poly *et al.*, 2008)
nxrB169f	nitrite oxidoreductase (*nxrB*)	TACATGTGGTGGAACA	(Pester *et al.*, 2014)
nxrB638r	nitrite oxidoreductase (*nxrB*)	CGGTTCTGGTCRATCA	(Pester *et al.*, 2014)

2.7.2 Quantitative real-time PCR (qPCR)

qPCR is the most commonly used technique to quantify the abundance and diversity of microbial community structure and profile functional gene expression profile activated sludge. This technique has been applied in activated sludge systems to quantify gene copies targeting *amoA* and *nxrA*/*nxrB* and the 16S rRNA gene using species-specific primers (Pester *et al.*, 2014). These qPCR techniques are more commonly applied due to their robust, highly reproducible, and sensitive traits than culture-based methods. However, Kumar *et al.* (2017) reported that the application of either AOB 16S rDNA or *amoA* has their different limitations of false positives and false negatives, respectively. Therefore, the combination of the two or more techniques is used to overcome the disadvantages of AOB detection and quantification (Cho *et al.*, 2014). A combination of qPCR and reverse transcription reaction is usually used to quantify functional genes, fully understand the microbial diversity of nitrifiers, and characterize their gene expression profile.

2.7.3 Reverse transcription PCR (RT-PCR)

RT-PCR is usually the method of choice for rapid and sensitive quantitative measurements of mRNA copy numbers analysing gene expression levels (Tsotetsi *et al.*, 2018). The study of gene expression which is based on RNA will give more useful information on the microbial function compared to DNA-based studies. Most of the existing studies on the microbial community structure of full-scale wastewater treatment systems are DNA-based, which does little to inform the understanding of functional microbial status. However, RNA extracted from the activated sludge provides more valuable data than from DNA in revealing 'active' microbial communities versus 'dormant' microbial populations as mRNA is considered an indicator of functionally active microbial populations (Taylor *et al.*, 2017b). However, little is known about the impact of the diffused aeration systems on the gene expression profiles

regarding the performance of different nitrifying community groups within wastewater treatment plants.

CHAPTER 3: NITROGEN REMOVAL PERFORMANCE AND FLOC STRUCTURE ANALYSIS OF SELECTED WASTEWATER TREATMENT PLANTS WITH DIFFUSED AERATION

3.1 INTRODUCTION

In activated sludge systems, both mechanical surface agitators and submerged diffusers have been designed and developed to supply sufficient DO for microbial activities such as nitrification and to keep the biomass in a compact structure with good settling properties (Rosso *et al.*, 2020, Smarzewska and Morawska, 2021). Among the two, diffused aeration systems are currently gaining ground due to their energy efficiency and improved plant performance (Pittoors *et al.*, 2014). In addition, the fine-pore diffusers do not cause mechanical disruption of the flocs as the air bubbles circulate evenly in the aeration tank and allow the plant to develop ideal compact flocs (Odize, 2018). According to previous reports, diffused aeration systems have been reported to produce significantly higher DO concentrations than surface aeration systems (Nethaji *et al.*, 2021, Drewnowski *et al.*, 2019).

Conventionally, DO concentration in the diffused aerated plants should be sufficiently high (≥2 mg/L) to ensure good effluent quality, which was reported to have a positive influence on floc formation (Drewnowski *et al.*, 2019). Therefore, an insufficient amount of DO concentration in the aeration tank could disrupt the biological processes resulting in the production of irregular floc with poor sludge settleability. Additionally, filamentous bacteria may compete with floc-forming organisms under low DO concentrations (<1.5 mg/L) due to slow-growing filaments, which affects sludge settleability (Nethaji *et al.*, 2021). However, more research is still required to understand the efficiency of floc structure under varying operational conditions in diffused aerated full-scale WWTP.

Due to the slow growth of nitrifying bacteria and their high susceptibility to environmental and operational parameters, maintaining an efficient nitrification process in BNR systems is usually a challenge (Cao *et al.*, 2020). Apart from DO, plant performance and nitrification efficiency in WWTP can be affected by several other factors such as toxic shocks, pH, substrate concentrations, and temperature fluctuations which often lead to failure of the system (Liu *et al.*, 2019). According to the report by Mbakwe *et al.* (2013) factors such as high ammonia concentrations and low DO levels may disrupt the two-step nitrification process which may lead to toxic nitrite build-up and a subsequent nitrification failure. However, studies regarding the impact of plant operational parameters such as DO on nitrogen removal performance and nitrification efficiency under fine bubble diffused aeration mode at the full-scale level are still lacking. Thus, this chapter aimed to investigate the nitrogen removal performance and sludge settling properties of two full-scale WWTPs operating using a fine bubble diffused aeration system.

3.2 MATERIALS AND METHODS

3.2.1 Plant description

This study focused on two full-scale WWTPs (WWTP A and WWTP B) located in the Pietermaritzburg region of KwaZulu Natal, South Africa (Table 3.1). WWTP A is operated using the modified Johannesburg process (Fig 3.1) and has a calculated treatment capacity of 71 ML/day average dry weather flows (ADWF). Briefly, after the initial screening, the raw wastewater is directed to a primary settling tank with an average HRT of 24 h (Fig. 3.1). Thereafter the primary influent is divided into three equal portions and flows into three identical biological reactors consisting of pre-anoxic/anoxic/anaerobic zones followed by the aeration basin. Air is supplied to the system by four duty and one standby blower fine bubble diffused aerator. The treated effluent from all three parallel reactors is thereafter combined and flows into the secondary settling tank. Thereafter, chlorinated and final effluent is discharged into the river. The second plant, WWTP B, is a small system operated using an SBR and was designed to treat 0.5 ML/day (ADWF) of screened and degritted raw sewage. In this plant, the raw wastewater is directed into the primary settling tank with an average HRT of 24 h (Fig. 3.2). The primary influent flows into the aeration basin, and then the treated effluent flows into the secondary settling tank. Thereafter, chlorinated and final effluent is discharged into the river. Aeration in the aerobic zone of the biological reactor of both plants is achieved with fine bubble diffused air (FBDA) aeration type. The wastewater characteristics and operational parameters of the selected plants are shown in Table 3.2.

Table 3.1: List of BNR plants

WWTP	WWTP A	WWTP B
Plant configuration	Modified Johannesburg process	Sequence batch reactor (SBR)
Influent composition	Municipal (90% Domestic + 10% industrial)	Domestic
Aerators	Fine bubble diffused air aeration	Fine bubble diffused air aeration

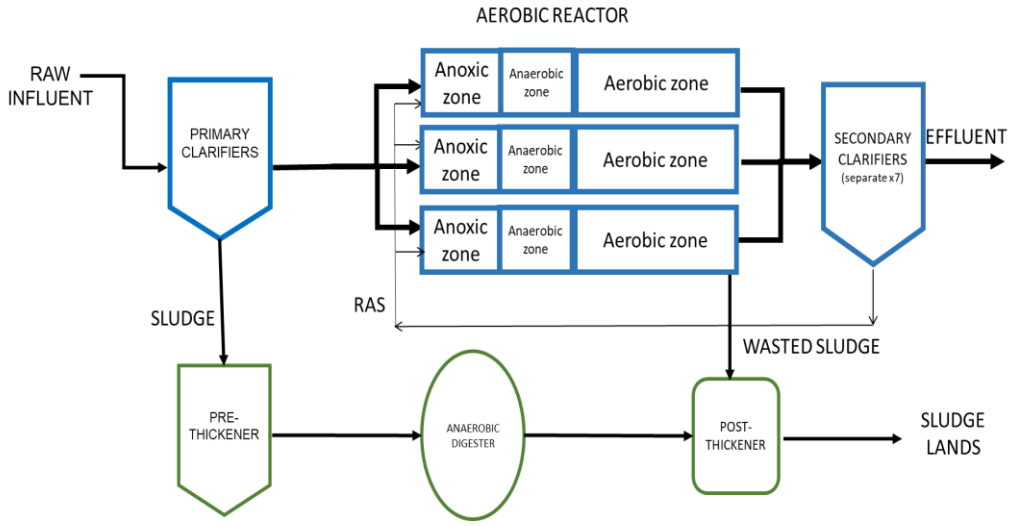

Figure 3.1: Schematic diagram of the WWTP A full-scale wastewater treatment plant.

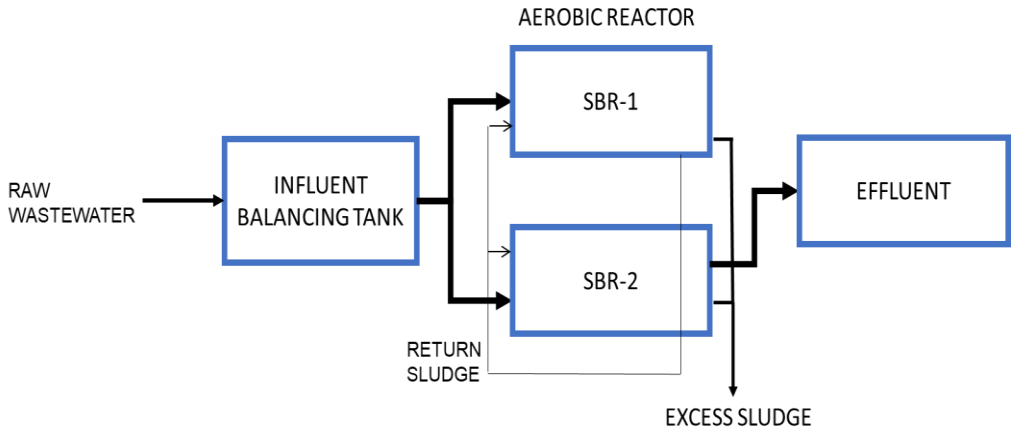

Figure 3.2: Schematic diagram of the WWTP B full-scale wastewater treatment plant

Table 3.2: Average wastewater influent and aeration sample characteristics and operational parameters of the selected plant as observed during the study period.

Parameters	WWTP A			WWTP B
	Reactor 1	Reactor 2	Reactor 3	
Temperature (ºC) (Aeration sample)	22.10±2.70	22.10±2.70	21.90±2.50	20.73±2.52
pH (Aeration sample)	6.40±0.20	6.40±0.30	6.60±0.30	7.04±0.34
DO (mg/L) (Aeration sample)	4.00±1.60	3.80±1.10	2.90±.1.6	4.65±1.86
COD (mg/L) (influent)	740.90±185.23	740.90±185.23	740.90±185.23	305.58±95.21
Ammonia (mg/L) (influent)	26.05±4.05	26.05±4.05	26.05±4.05	23.43±4.89
COD removal (%) (influent)	88.58±6.16	88.58±6.16	88.58±6.16	82.55±10.58
Ammonia removal (%) (influent)	95.26±5.60	95.26±5.60	95.26±5.60	98.02±1.20
Nitrification rate (Aeration sample)	0.03±0.01	0.02±0.01	0.04±0.00	0.001±0.00
MLSS (mg/L) (Aeration sample)	6811.90±1242.80	7228.40±1231.10	5059.6±1045.59	53375.33±1773.57
MLVSS (mg/L) (Aeration sample)	5582.50±1364.87	5536.40±929.13	3847.60±839.72	3685.33±1344.41
SVI (mL/g)	103.51±16.10	104.25±11.59	102.50±18.29	51.73±15.20
Flow rate (ML/Day) (influent)	71	71	71	0.50
HRT (h) (influent)	24	24	24	24
SRT (days) (influent)	7	7	7	7
F/M (g-COD/g-MLSS.d) (Aeration sample)	0.80±0.51	0.09±0.05	0.10±0.02	0.18±0.05
ALR (g-NH4/m3. d) (influent)	142.10±22.09	142.10±22.09	142.10±22.09	2.79±0.58

3.2.2 Sample collection

Composite sludge samples from aeration tanks, as well as influent and effluent water samples, were collected monthly from August 2019 to February 2020 and from June 2020 to August 2020. In total 10 samples were collected from each plant. The sampling period however was disrupted from March 2020 to May 2020 due to the onset of the Covid-19 pandemic and subsequent implementation of lockdown regulations. Sterile sampling bottles were used for collecting the samples, and the samples were transported at 4°C to the laboratory until further use. Temperature, DO concentrations, and pH measurements were taken on-site using a portable YSI meter (YSI 556 Multiprobe System).

3.2.3 Plant operational parameters

3.2.3.1 Nutrient analysis

Nitrogen in the forms of ammonia (NH_3–N), nitrate (NO_3–N), and nitrite (NO_2^-–N) were measured spectrophotometrically using the Gallery Autoanalyser (ThermoScientific, USA) according to the protocols outlined in Standard Methods (APHA, 2012).

3.2.3.2 Chemical oxygen demand (COD)

The COD concentration in wastewater (influent and effluent) was determined according to the standard method 5220D - closed reflux colorimetric method using microwave digestion (Apha, 1998). About 1.5 mL of digestion solution and 3.5 mL of sulphuric acid were carefully added to the 2.5 mL sample, carefully mixed, tightly capped, and digested at 150^{o}C for 2 h in COD vials using the microwave digester (Milestone Start D, Sorisole, Italy). Standards and blank reagents were prepared and digested with the samples as controls. After cooling, the COD concentration was measured using a spectrophotometer at 600 nm and results were recorded in mg/L.

3.2.4 Calculation of nitrification rate

Nitrification rates were calculated based on the parameters monitored in the plant and the information supplied by the plant operators in this study. The nitrification rate was calculated according to the equation below:

$$Rnitrification = \frac{Qin\ ([NH_4^+ - N] - [NH_4^+ - N])}{Vreactors[MLSS]reactors}$$

Where:

$Rnitrification$ = rate of plant's nitrification

Qin = influent flowrate (L^3/ T)

$[MLSS]reactors$ = Mixed liquor suspended solid of the reactor (M/L^3) and

$Vreactors$ = reactor working volume (L^3).

3.2.5 The mixed liquor suspended solids (MLSS) and the mixed liquor volatile suspended solids (MLVSS)

The mixed liquor suspended solids (MLSS) and mixed liquor volatile suspended solids were measured according to the standard methods with slight modifications (APHA, 2012). For the MLSS measurement, 25 mL of the mixed samples were added to a clean, pre-weighed ceramic crucible. The crucibles were heated at 105°C for 2 h after which they were cooled in a desiccator containing silica gel. The crucibles were then weighed using a Mettler-Toledo ME204 analytical balance (Mettler-Toledo International Inc., USA) to gravimetrically determine the dry biomass. To determine the MLVSS, the crucibles were subsequently incinerated at 550°C for 30 min. The crucibles were then cooled in a desiccator containing silica gel and weighed. The MLSS and MLVSS were calculated using the equations below:

$$MLSS\ (\text{mg/L}) = \frac{(\text{Crucible+Biomass}) - \text{Mass (Crucible)}}{\text{Sample volumes (mL)}} \times 1000$$

$$\text{MLVSS (mg/L)} = \frac{(\text{Crucible+Biomass}) - \text{Mass(Crucible after incineration at 550°C)}}{\text{Sample volume(mL)}} \times 1000$$

3.2.6 Sludge volume index (SVI)

The SVI was determined according to the method of Jenkins *et al.* (1993). About 1 L of sludge was poured into an Imhoff Settling Cone and was allowed to settle for 30 min. The volume occupied by the sludge was read from the Imhoff Settling Cone. The SVI was calculated using the equation below

$$\text{SVI (mg/L)} = \frac{settled\ volume\ of\ sludge\ (mL/L) \times 1000\ (mg/g)}{\text{MLSS (mg/L)}}$$

3.2.7 Analysis of floc structure using conventional staining and microscopic methods.

Floc structure analysis was done by assessing the morphological characteristics of the activated sludge floc samples obtained from the aeration tank following protocols by Jenkins *et al.* (1993) and Eikelboom (2000). A wet mount preparation was made using activated sludge samples to evaluate floc shape (rounded or irregular), structure (compact or open), strength (firm or weak), and size (diameter). A wet mount slide was prepared using a well-mixed sample, placing it on a clean slide and carefully covering it with a coverslip, and examined immediately using bright-field light microscopy (Carl Zeiss, Germany). The Gram staining was done to assess the filamentous growth (low, moderate, and high filaments) by placing the sample onto the

microscope slides which were then air-dried and heat-fixed. About 1 mL of crystal violet was added onto the slide for 60 seconds and then rinsed with water, followed by 1 mL of Gram's Iodine for 60 seconds then rinsed well with water. The smeared sample was decolorized with 95% ethanol for 30 seconds then rinse well with water. Safranin was added for 60 seconds then rinsed well and blot dried. The slide was examined immediately using a bright-field light microscope (Carl Zeiss, Germany).

3.2.8 Statistical analysis

GraphPad Prism version 5.00 for Windows (GraphPad Software, San Diego California USA) was used to carry out statistical analysis including Pearson correlation. Microsoft Excel 2010 was used to calculate the standard deviation.

3.3. RESULTS

3.3.1 Process performance and operational conditions

3.3.1.1 Effect of DO concentration on nutrient removal and nitrogen removal performance at WWTP A

A full-scale WWTP A was monitored over a period of 10 months (August 2019 - February 2020 and June 2020 – August 2020). A significant seasonal variation in temperature (17.5°C to 26.1°C) was observed in the reactors (Fig S1.1). The ammonia concentration in the influent and effluent during the sampling period ranged from 20.4 to 35.35 mg/L and 0.27 to 3.81 mg/L, respectively. The influent and effluent nitrite concentrations were always lower than 1 mg/L throughout the study period, while nitrate concentration was higher than 1 mg/L (Fig. 3.4). However, effluent nitrite concentration was observed to increase from November to February whereas the effluent nitrate concentration decreased. The system showed an efficient performance in ammonia removal efficiency with an average of 95±5.6% throughout the study period (Fig. 3.3).

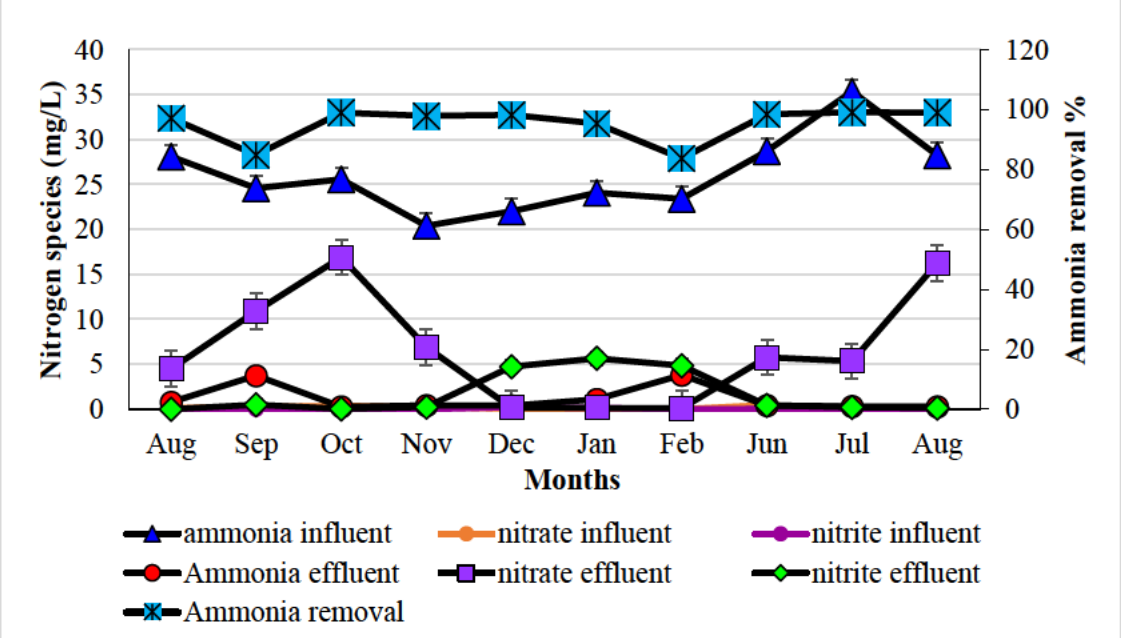

Figure 3.3: Measured nitrogen species concentrations in the reactor during the study and ammonia removal efficiency at WWTP A.

The influent COD concentration showed varying results throughout the sampling period with an overall average of 740.92±185.2 mg/L (Fig. 3.4). The plant recorded a COD removal rate of 88.6±6.16% throughout the study period (Fig. 3.4). The lowest COD removal and ammonia removal efficiency of 75.09 % and 83.71 % respectively, was recorded when the COD/N ratio was low (17.4) in Feb 2020. The COD/N ratio was observed to decrease with the increasing nitrite effluent between Nov 2019 to Feb 2020. The COD/N ratio showed positive correlation with COD removal rate (r = 0.54; p = 0.05). However, COD/N showed no clear correlation with ammonia removal efficiency.

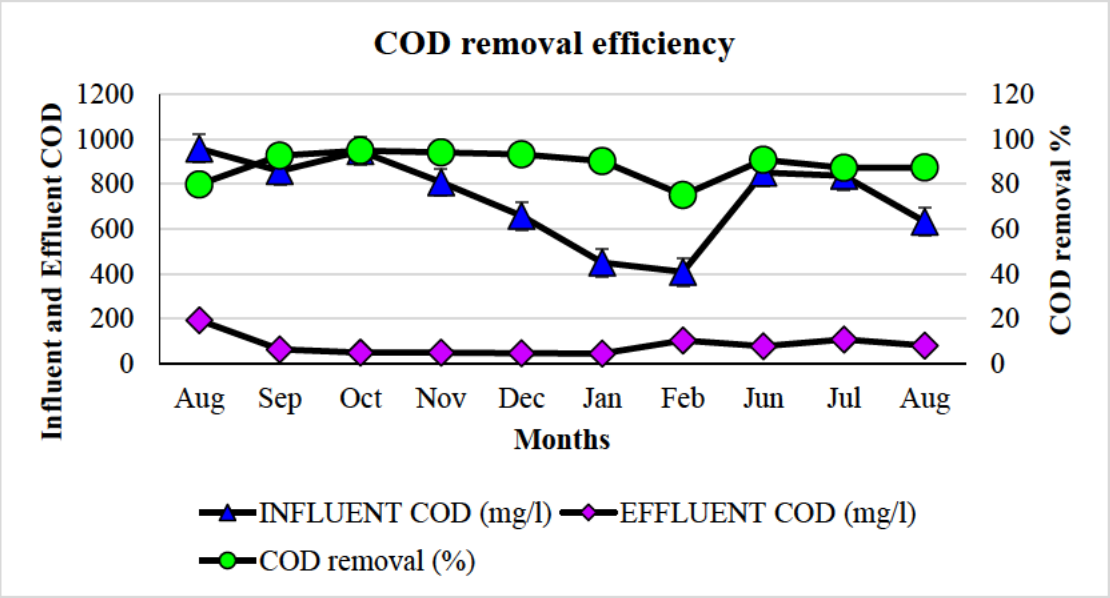

Figure 3.4: Wastewater quality indicating COD concentrations in the influent and effluent at WWTP A.

Dissolved oxygen has been implicated as one of the operating parameters affecting nitrogen removal and overall process performance in WWTPs. A high DO concentration was recorded

in two of the systems (reactor 1 and reactor 2) with an average of 4.0±1.6 mg/L and 3.8±1.1 mg/L, respectively, while the third system (reactor 3) recorded a relatively low DO concentration with an average of 2.9±1.6 mg/L. The decrease in DO concentration in September was observed in all 3 reactors which may be due to an increase in temperature. Previous reports have stated that temperature can affect the DO concentration in WWTP. The DO levels in all the three parallel reactors, however, were within the optimum range for the nitrification process (1.5 to 3 mg/L) (Fig. 3.5). The DO concentration was observed to be more consistent from Feb 2020 to Aug 2020 during cold temperatures (Fig S1.1) in all 3 reactors. However, no clear correlation was observed between DO and temperature. When the DO concentration was below 1.4 mg/L and 2.1 mg/L in reactor 1 and reactor 3, the effluent nitrite was observed to increase to 5.6 mg/L in Jan 2020 (Figs. 3.5 & 3.3). A negative correlation was found between effluent nitrite and DO concentration (reactor 1, r = -0.58; reactor 2, r = -0.47 and reactor 3, r = -0.39; p = 0.05). Statistically ammonia removal showed positive correlation with DO concentration (reactor 1: r = 0.40; reactor 2: r = 0.52; reactor 3: r = 0.53; p = 0.05) and nitrification rate (reactor 1: r = 0.43; reactor 2: r = 0.40; reactor 3: r = 0.51; p = 0.05) in all 3 reactors. Furthermore, the effluent nitrite was observed to have a significantly strong positive correlation with temperature and pH in the reactors (reactor 1: rs = 0.71, 0.71; reactor 2: rs = 0.70, 0.78 and reactor 3: rs = 0.67. 0.76; p = 0.05). However, no clear correlation was found between ammonia removal efficiency and temperature in all 3 reactors.

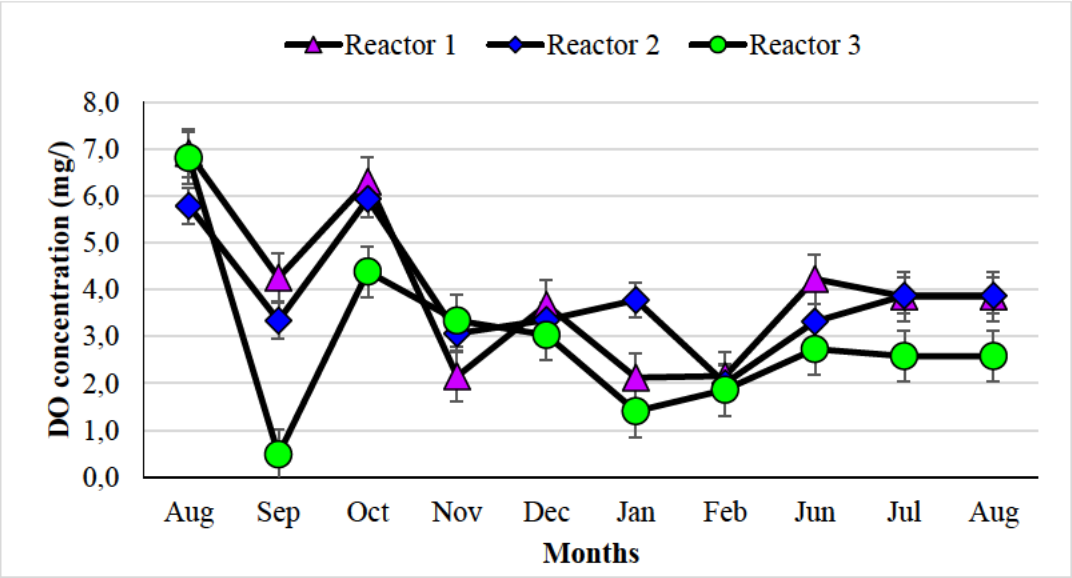

Figure 3.5: The DO concentration within the reactor during the study at WWTP A.

Reactor 1 and reactor 3 showed a higher average nitrification rate of 0.026±0.007 g $N\text{-}NH_4^+$ g $MLVSS^{-1}$ d^{-1}, and 0.036± 0.005 g $N\text{-}NH_4^+$ g $MLVSS^{-1}$ d^{-1} respectively compared with reactor 2 (0.025±0.007 g $N\text{-}NH_4^+$ g $MLVSS^{-1}$ d^{-1}) (Fig. 3.6). The lowest nitrification rate was observed during high temperatures in reactors 1 and 2 (Dec 2019 to Feb 2020) when the nitrite concentration was above 1mg/L, indicating incomplete nitrification. However, the effluent nitrite concentration decreased to lower than 1 mg/L during cold temperatures in all 3 reactors (Jun 2020 to Aug 2020), indicating that complete nitrification was achieved. In this plant, a significantly positive correlation was found between nitrification rate and DO concentration in reactor 1 and reactor 3 ($r = 0.43$ and $r = 0.52$, $p = 0.05$), however, no clear correlation was observed between nitrification rate and DO concentration (r = 0.2.1) in reactor 2. Similarly, no correlation was observed between the temperature and nitrification rate (reactor 1: $r = 0.46$, reactor 2: $r = 0.59$, and reactor 3: $r = 0.22$; $p = 0.18$).

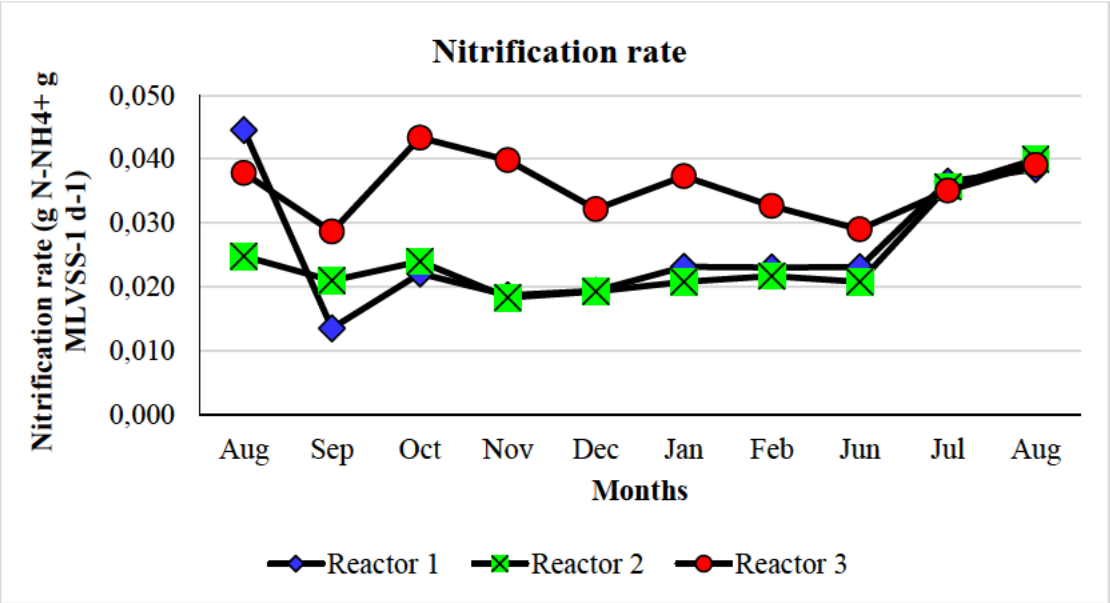

Figure 3.6: The variations in nitrification rates observed in WWTP A during the time of the investigation.

3.3.1.2 Effect of DO concentration on nutrient removal and nitrogen removal performance at WWTP B

The plant recorded an average ammonia concentration of 23.44±4.89 mg/L and 0.43±0.023 mg/L in the influent and effluent, respectively. The influent and effluent nitrite concentrations were within the range of 0 – 0.1 mg/L and 0 – 11.6 mg/L throughout the study period while the nitrate influent and effluent ranged between 0.02 - 0.47 mg/L and 0.11 – 16.26 mg/L (Fig. 3.7). Nitrite accumulation was observed in the effluent from Nov 2019 to Feb 2020 from 0.03 to 11.6 mg/L when the temperature was above 22°C, and the pH was above 7 (Fig. S1.2). Effluent nitrite concentration was observed to have strong positive correlation with temperature ($r = 0.83$; $p = 0.05$) and pH ($r = 0.064$; $p = 0.05$) while no clear correlation was found between DO concentration and nitrite accumulation. The system showed an efficient performance in ammonia removal efficiency with an average of 98.02±1.2% throughout the study period (Fig.

3.7). In this plant, ammonia removal efficiency showed no clear correlation with DO concentration, temperature, and nitrification rate.

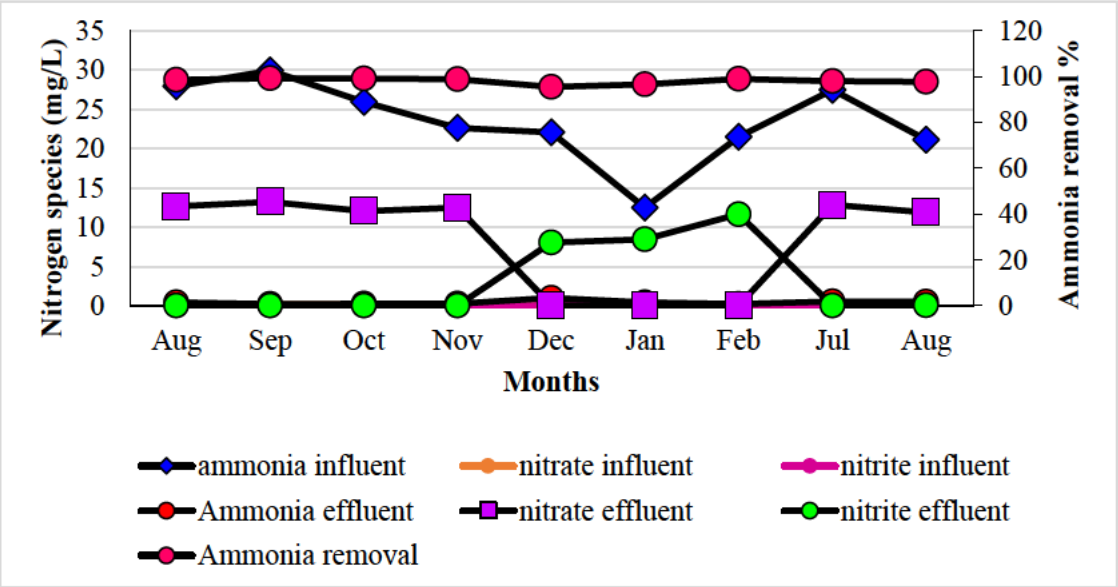

Figure 3.7: Measured nitrogen species concentrations in the reactor during the study and ammonia removal efficiency at WWTP B.

The influent COD concentration was within the range 180 – 442 mg/L with an overall average of 305.58±90.33 mg/L whilst an overall average of 55.5±3.85 mg/L COD was recorded in the effluent (Fig. 3.8). The plant showed an efficient COD removal rate of 82.5±10.04% during the study period. The plant recorded a low COD/N ratio ranging from 0.061 to 1.1, throughout the study period which was found to have no influence on nitrification rate and DO concentration. Statistically, COD/N also showed no significant correlation between COD removal and ammonia removal efficiency.

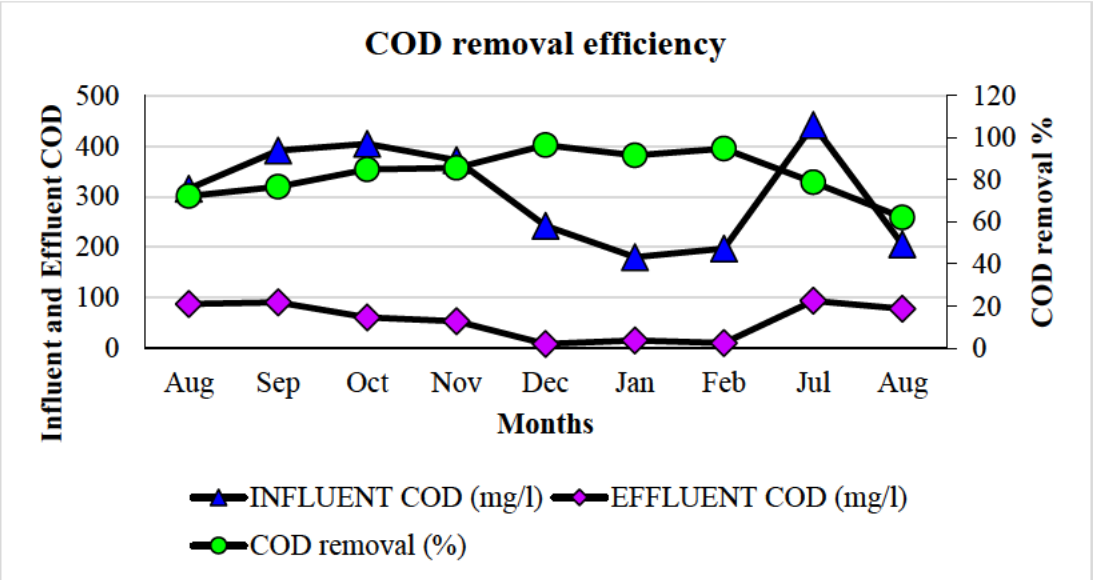

Figure 3.8: Wastewater quality indicating COD concentrations in the influent and effluent at WWTP B.

The DO concentration of the plant was in the range of 2.12 to 8.45 mg/L with an overall average of 4.32 mg/L within the reactor (Fig. 3.9). The DO concentration was noted to decrease (Sep) as the temperature decreased. However, no clear correlation between DO concentration and temperature was found. In this plant, the nitrification ranged from 0.001 to 0.0024 g $N\text{-}NH_4^+$ g $MLVSS^{-1}$ d^{-1} during the study period. The plant recorded a nitrification rate with an overall average of 0.002 ±0.0004 g $N\text{-}NH_4^+$ g $MLVSS^{-1}$ d^{-1}. No significant correlation was found between nitrification rate and DO concentration and temperature. The nitrification rates of the plant during the period investigated are shown in Fig 3.10.

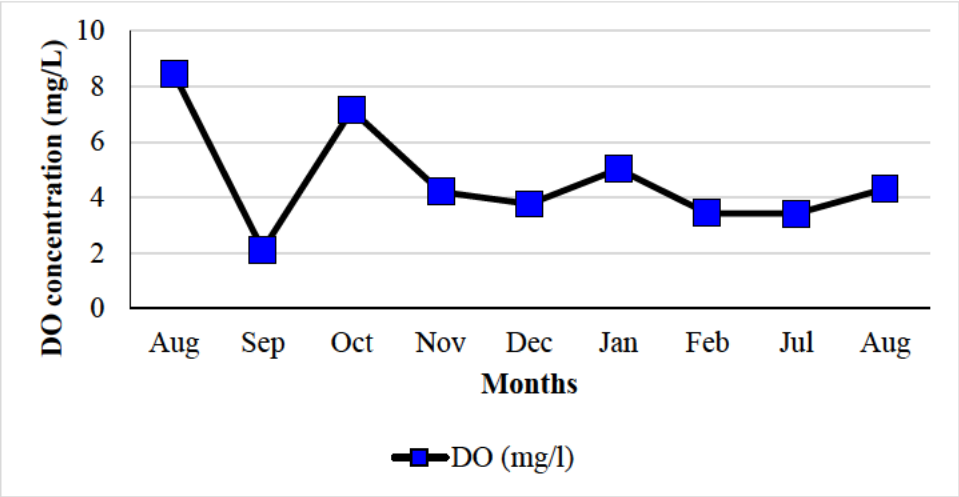

Figure 3.9: DO concentration within the reactor during the study at WWTP B

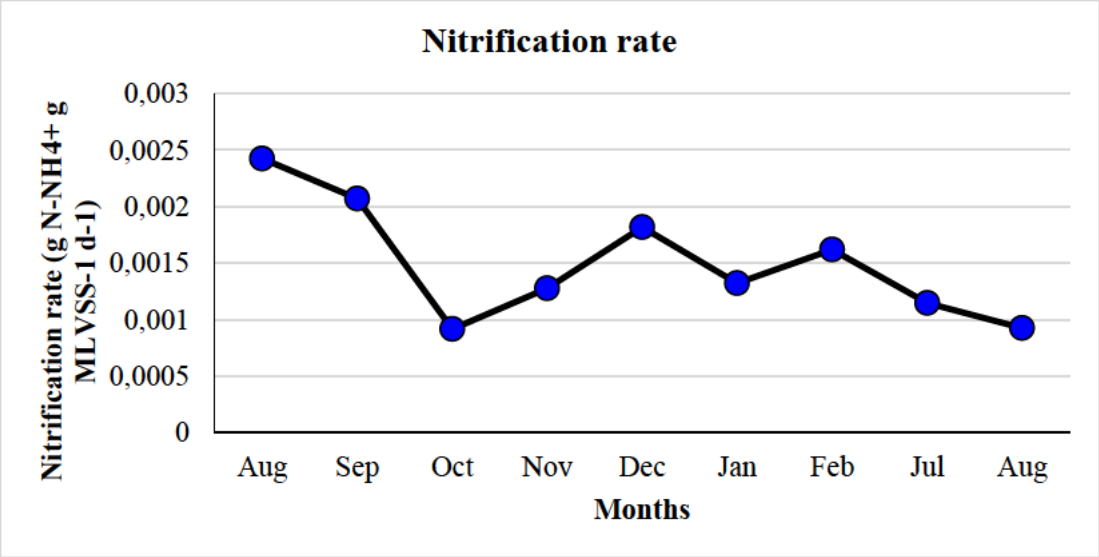

Figure 3.10: The nitrification rates measured in the aeration tanks during the period investigated.

3.3.2 Floc structure analysis

3.3.2.1 Effects of DO on floc structure analysis at WWTP A

Biomass levels (MLSS and MLVSS) in different reactors (reactor 1, 2 and 3) are represented in Figs. 3.11 A & B. Higher MLSS and MLVSS were recorded in reactors 1 and 2 compared with reactor 3 throughout the study period. Reactor 1 recorded an overall average MLSS of 6811.9±1242 mg/L and MLVSS concentration of 55582.5±1364.87 mg/L, whilst reactor 2 recorded an overall average MLSS and MLVSS concentration of 7228.4±1231.09 mg/L and 5536.4±929.12 mg/L, respectively. Reactor 3 recorded overall average MLSS and MLVSS concentration of 5059.6±1045.59 mg/L and 3847.6±839.72 mg/L, respectively (Figs. 3.11 A & B). In this study, high MLSS, MLVSS and DO concentration were observed to have a negative influence on nitrification rate. Statistically significant negative correlations between MLSS, MLVSS concentrations and nitrification rate were observed from reactors (reactor 1: rs = -0.54, -0.83; reactor 2: rs = -0.68, -0.64; reactor 3: rs = -0.53, -0.52; $p < 0.05$), while MLSS/ MLVSS showed no clear correlation with DO concentration and temperature.

The plant experienced foaming problems (Fig. S2.1) almost throughout the study period in reactor 1 and reactor 2 due to an oil spillage that occurred during the first few days of sampling. The foaming did not cause settling problems but often, an increase in MLSS and MLVSS concentration was observed. All three reactors were observed to have good sludge settleability which was within the range of 50 -150 mL/g. The SVI was observed to be consistent throughout the study period with an overall average of 103.51±16.10 mL/g (reactor 1), 104.24±11.59 mL/g (reactor 2), and 102.5±18.29 mL/g (reactor 3) (Fig. 3.11 C). The SVI was not influenced by the DO concentration, during the study period. There was no clear relation between the DO concentration and SVI values in reactor 1 and reactor 2, while reactor 3 ($r = 0.47$; $p = 0.05$)

showed a positive correlation between the DO concentration and SVI values. The microscopic investigation showed the flocs were generally relatively small to medium, open, and irregular flocs due to moderate filaments protruding out of the flocs in reactor 1 and reactor 2 while reactor 3 showed small to medium, compact, robust flocs with low to medium filaments protruding out of the flocs (Table 3.3 and Fig. 3.12). All reactors showed a good sludge settling throughout the study period.

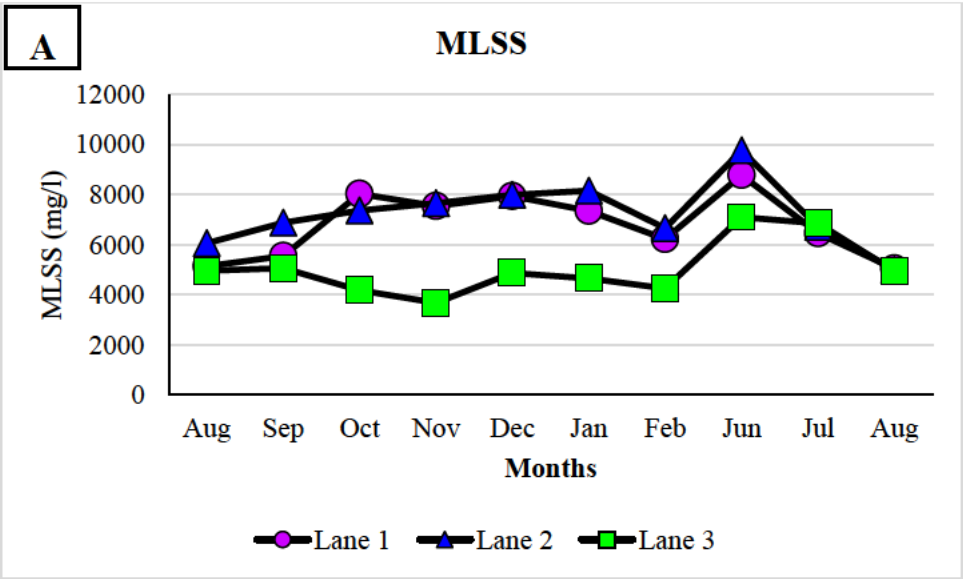

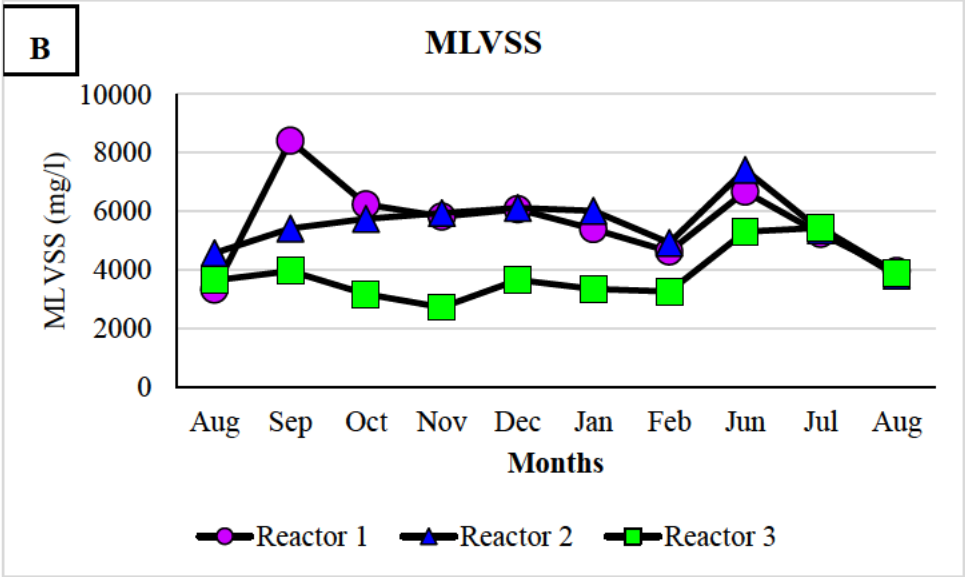

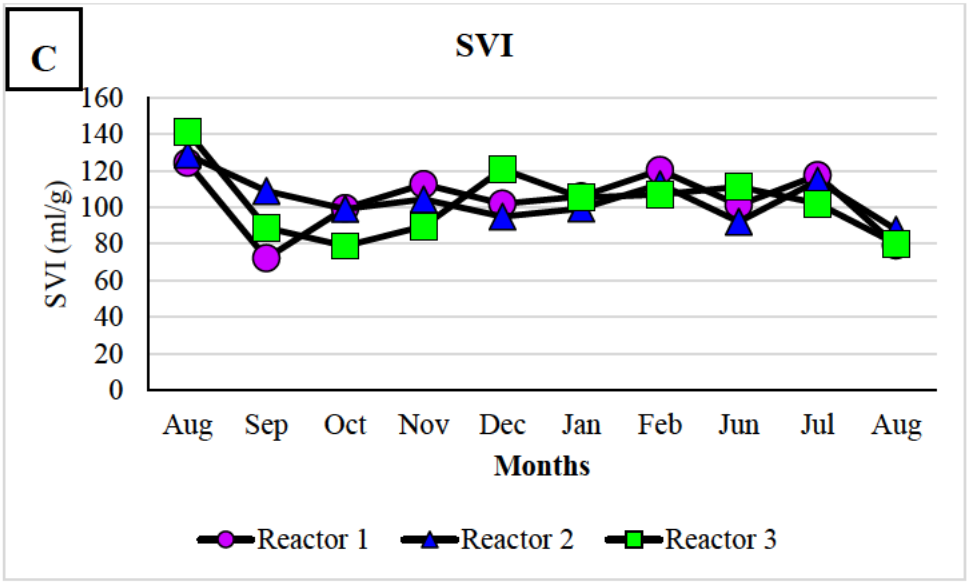

Figure 3.11: Variation in MLSS (A), MLVSS (B), and SVI concentration (C) during the study at WWTP A.

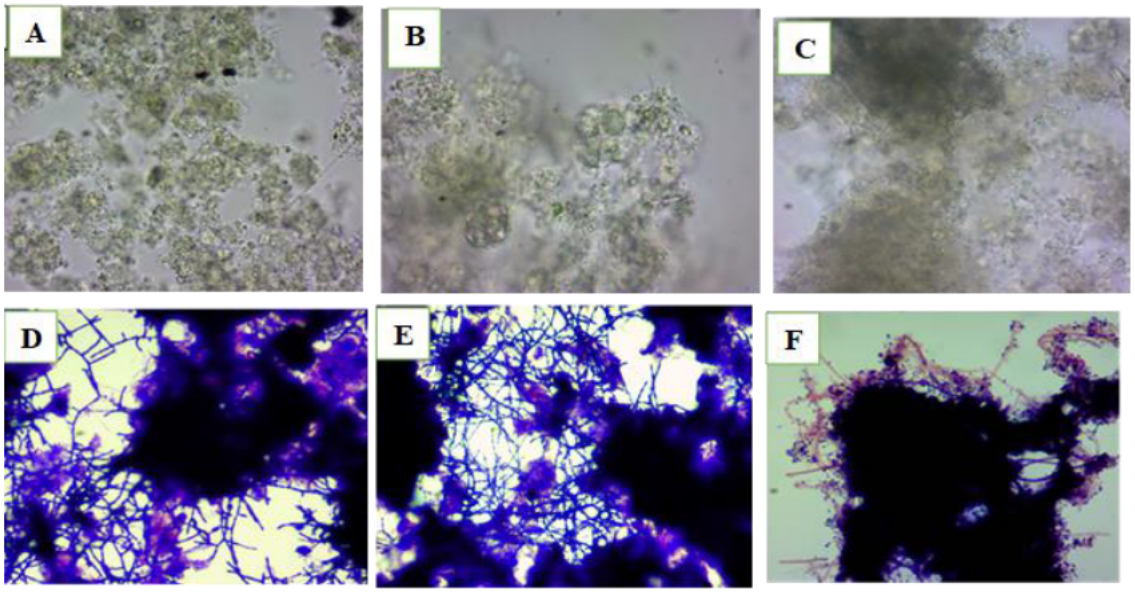

Figure 3.12: Representative of the floc structures from WWTP A aeration tanks. (A-C) denotes a wet mount and (D-F) denotes Gram-stain (1000×). Reactor 1 (A & D) & reactor 2 (B & E) showed showing irregular, open, and weak flocs with moderate to excessive while reactor 3 (C & F) showed rounded, compact, and robust flocs with few filaments.

Table 3.3: Floc structure analysis at WWTP A

Months	Sample name	Floc size [(a)]	Floc shape [(b)]	Floc strength[(C)]	Floc structure [(d)]	Filament index [(e)]	Visible Form (YES/NO)
Aug 2019	reactor 1	M	RO	R	C	3	YES
	reactor 2	M	IR	W	O	3	YES
	reactor 3	M	RO	R	C	2	NO
Sep 2019	reactor 1	M	IR	W	O	4	YES
	reactor 2	M	IR	W	O	4	YES
	reactor 3	M	RO	R	C	3	YES
Oct 2019	reactor 1	M	IR	W	O	4	YES
	reactor 2	M	IR	W	O	4	YES
	reactor 3	M	RO	R	C	2	NO
Nov 2019	reactor 1	M	IR	W	O	4	YES
	reactor 2	M	IR	W	O	4	YES
	reactor 3	M	RO	R	C	2	NO
Dec 2019	reactor 1	M	IR	R	C	4	YES
	reactor 2	M	RO	R	C	3	YES
	reactor 3	M	RO	R	C	2	NO
Jan 2020	reactor 1	M	IR	R	C	3	YES
	reactor 2	M	RO	R	C	4	YES
	reactor 3	M	RO	R	C	2	NO
Feb 2020	reactor 1	M	IR	R	C	4	YES
	reactor 2	M	IR	R	C	4	YES
	reactor 3	M	RO	R	C	2	NO
Jun 2020	reactor 1	M	IR	W	O	5	YES
	reactor 2	M	IR	W	O	5	YES
	reactor 3	M	RO	W	O	5	YES
Jul 2020	reactor 1	M	IR	W	O	5	YES
	reactor 2	M	IR	W	O	5	YES
	reactor 3	M	RO	W	O	4	YES
Aug 2020	reactor 1	M	RO	W	O	4	YES
	reactor 2	M	RO	W	O	4	YES
	reactor 3	M	RO	W	O	3	YES

a) Size = S - small (<25µm)
M – medium (25 - 250µm)
L – large (> 250µm)
b) Shape = RO – rounded
IR - irregular
c) Strength = R – robust
W – weak
d) Structure = C- compact
O - open

f) Sludge quality =

	Good	Moderate	Poor
Filament Index	< 3	3–4	4–5
Free-living cells	0–1	2–3	≥ 3
Spirils	0	1	≥ 2
Ciliates/Testate amoeba	≥ 1	< 1	0
Flagellates/Amoeba	0	1–2	≥ 3
%flocs > 25 µm	> 80 to 90	> 50 to 70	< 50
Floc structure	compact	open	—
Floc 'strength'	robust	weak	—
Floc shape	rounded	irregular	—

3.3.2.2 Effect of DO on floc structure at WWTP B

The MLSS and MLVSS concentrations were observed to be varying with an overall average of 5375±1773 mg/L and 3685±1344 mg/L, respectively (Fig 3.13). MLSS and MLVSS were found to have a strong negative correlation with nitrification rate (r = -0.70 and r = - 0.71). However, MLSS and MLVSS were found to have no clear correlation with DO concentration and temperature. The plant was revealed to have a good sludge quality that settles faster with an average SVI of 51.73±15.2 mL/g (Fig 3.13). There was no clear relation between DO concentration and SVI values in the reactor. Based on floc morphology, WWTP B was observed to have small to medium, round, compact, robust flocs with few filaments protruding from the floc (Table 3.4, Fig.3.14).

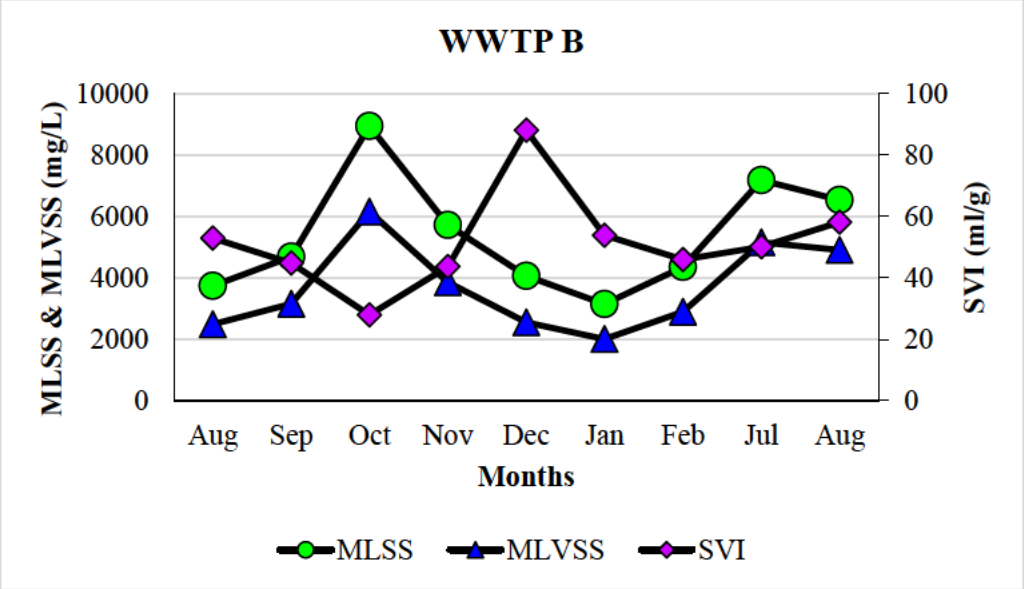

Figure 3.13: Variation in MLSS, MLVSS, and SVI concentration during the study at WWTP B.

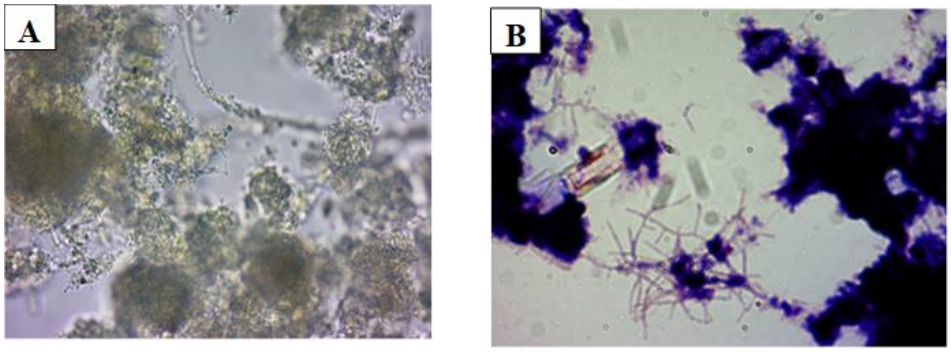

Figure 3.14: Floc structure from WWTP B aeration tanks. (A) denotes a wet mount showing rounded, compact and robust flocs while (B) denotes Gram-stain showing few filaments (1000×).

Table 3.4: Floc structure analysis at WWTP B

Months	Sample name	Floc size (a)	Floc shape (b)	Floc strength(c)	Floc structure (d)	Filament index (e)	Form (YES/NO)
Aug 2019	reactor 1	M	RO	R	C	2	NO
Sep 2019	reactor 1	M	RO	R	C	3	NO
Oct 2019	reactor 1	M	RO	R	C	2	NO
Nov 2019	reactor 1	M	RO	R	C	2	NO
Dec 2019	reactor 1	M	RO	R	C	2	NO
Jan 2020	reactor 1	M	RO	R	C	2	NO
Feb 2020	reactor 1	M	RO	R	C	2	NO
Jul 2020	reactor 1	M	RO	R	C	2	NO
Aug 2020	reactor 1	M	RO	R	C	2	NO

a) Size = S - small (<25µm)
M – medium (25 - 250µm)
L – large (> 250µm)
b) Shape = RO – rounded
IR - irregular
c) Strength = R – robust
W – weak
d) Structure = C- compact
O - open
e) Scale 0-5 = none to numerous filaments

f) Sludge quality =

	Good	Moderate	Poor
Filament Index	< 3	3–4	4–5
Free-living cells	0–1	2–3	≥ 3
Spirils	0	1	≥ 2
Ciliates/Testate amoeba	≥ 1	< 1	0
Flagellates/Amoeba	0	1–2	≥ 3
%flocs > 25 µm	> 80 to 90	> 50 to 70	< 50
Floc structure	compact	open	—
Floc 'strength'	robust	weak	—
Floc shape	rounded	irregular	—

3.4 DISCUSSION

The DO concentration is an important operational parameter for activated sludge processes with nitrification. The fine bubble diffused aeration systems in this study were found to produce significantly higher DO concentrations (Figs.3.5 & 3.9) than the recommended DO concentration (2 mg/L) for complete nitrification in both plants (Uri-Carreño *et al.*, 2021, Behnisch *et al.*, 2018). However, this increase in DO concentration may not always improve nitrification but rather leads to high energy consumption. In this study, the unlimited DO concentration suggested that the fine bubble diffused aeration was able to remove ammonia from WWTP A (average of 95±5.6%) (Fig.3.3) and WWTP B (average of 98.02%) (Fig. 3.7). Similar observations were made by (Pigue, 2013), whereby the disc diffuser was found to produce a high DO concentration resulting in higher ammonia removal.

When the DO was ≥4 mg/L, the effluent nitrite concentration was less than 1 mg/L, indicating complete nitrification in WWTP A (Fig. 3.3) and WWTP B (Fig. 3.7). When the DO was ≤3 mg/L, the nitrite effluent concentration increased to about 5 mg/L in WWTP A and 11 mg/L in WWTP B, during high temperatures (22 to 26^{o}C) (Figs. S1.1 & S1.2), indicating that nitrite oxidation was more sensitive to the change in DO concentration. Nitrite accumulation can be attributed to AOB outcompeting NOB due to free ammonia inhibition, DO, temperature, and pH concentration (Kent *et al.*, 2019, Ma *et al.*, 2017b). These observations were similar to Pigue (2013). According to a study by Jiang *et al.* (2018), AOB remained unaffected by DO fluctuations while NOB was strongly inhibited resulting in the accumulation of nitrite. Wang *et al.* (2017b) and (Kent *et al.*, 2019) also reported similar results whereby the AOB was found to endure DO fluctuations more than NOB.

A moderate increase in nitrite between Nov 2019 and Feb 2020 in WWTP A and WWTP B (Fig. 3.3 and Fig 3.7), could also be due to high temperatures (22 to 26^{o}C) during this period. In contrast to ammonia removal, DO concentration was observed to not influence COD removal in both plants. The COD removal was efficient in both the plants with WWTP A recording an average COD removal efficiency of 88.6± 6.16% (Fig. 3.4) while WWTP B recorded average COD removal of 82.5±10.04 % (Fig. 3.8) throughout the study period even under low DO levels (≤2 mg/L). It was evident that as long as enough oxygen was supplied by aeration, the ability of WWTPs to remove COD was not substantially limited by low DO concentrations in the wastewater. Hasan *et al.* (2013), also found that effective COD removal could be achieved in a system operating at DO levels as low as 0.1 mg/L.

According to Pelaz *et al.* (2018), the COD/N ratio is one of the most critical parameters in wastewater for nitrogen removal, due to its effects on ammonium oxidation and, nitrite oxidation. At WWTP A, the nitrite accumulation rate was observed to increase with the decreasing influent COD/N ratio (r = -0.61) while the nitrification rate was observed to decrease when the COD/N ratio increased in reactor 3 (r = -0.36). No clear correlation was observed between the influent COD/N ratio and nitrification rate in reactor 1 and reactor 2. Pelaz *et al.* (2018) obtained similar results, whereby low COD/N ratios were recorded as the nitrite effluent increased, which are reconfirmed in WWTP A. In contrast, the nitrite was observed to increase with an increasing COD/N ratio (r = 0.470) in WWTP B. In this study, the nitrification rate was observed to increase with high DO concentration, observed in the reactors in both WWTP A (Fig 3.6) and WWTP B (Fig 3.10), indicating complete nitrification. Similarly, Liu (2012) reported that the nitrification rate in activated sludge doubled when the DO concentration increased from 1.0 to 3.0 mg/L. However, How *et al.* (2018), found that complete nitrification could be achieved when the DO was near 0.5 mg/L.

The MLSS and MLVSS concentrations are given in Figs. 3.11 A & B and Fig 3.13. High MLSS and MLVSS concentrations were observed even under high DO concentration (≥4 mg/L) in both plants. The MLSS and MLVSS concentrations in this study were observed to be higher (>4000 mg/L) than the typical normal MLSS (2000 to 4000 mg/L) and MLVSS (70 to 80% of MLSS) concentrations for conventional activated sludge plants. An increase in bacterial yield has been reported as one factor contributing to an increase in MLSS and MLVSS concentrations (Huang *et al.,* 2020). Baek and Kim (2013) found that the nitrifier and heterotrophic yield increased when the conditions varied from excess to low DO conditions which led to an increase in MLSS and MLVSS concentration. The increasing MLSS and MLVSS in WWTP A (especially in reactor 1 and reactor 2) were due to foaming (Fig. S2.1) caused by oil spillage. However, the foaming did not cause settling problems but led to an increase in flocs with filaments.

The SVI values were below 150 mL/g in all reactors in both plants, necessary for good settling sludge as seen in Fig. 3.11C (WWTP A) and Fig 3.13 (WWTP B) (Adonadaga, 2015). All the reactors showed a good sludge settling throughout the study period in both plants with high DO concentrations which were observed to be consistent with findings by Mohammed *et al.* (2014). At WWTP A, the microscopic analysis showed that the flocs were generally relatively small to medium, open and irregular due to moderate protruding out of the flocs in reactor 1 and reactor 2, while flocs in reactor 3 were observed to be small to medium, compact, robust, and contained low to filaments protruding out of the flocs as seen in Table 3.3 & Fig. 3.12. At WWTP B the floc structure was observed to be small to medium, compact, robust, and contained low to filaments protruding out of the flocs (Table 3.4 and Fig. 3.14). Similarly, Geng *et al.* (2021) and (Wagner *et al.*, 2014) reported small, robust, and compact flocs in fine bubble diffused aeration systems, due to high evenly mixing in the diffused reactors. Kulkarni

(2012), reported that the presence of filamentous bacteria in an SBR resulted in the production of porous and irregularly shaped flocs. Additionally, high DO concentrations produced in fine bubble diffused aeration systems have been reported to have a positive influence on floc formation (Drewnowski *et al.*, 2019, Nethaji *et al.*, 2021). Although DO concentration and floc structure did not correlate properly, there was a trend toward flocs with moderate filaments at high DO concentrations, which is consistent with results by Mohammed *et al.* (2014) and (Guo *et al.*, 2012).

3.5 CONCLUSION

The fine bubble diffused aeration systems in this study were observed to produce higher DO concentrations than recommended (2 mg/L) concentration for complete nitrification in both plants. Nitrite oxidation was observed to be more sensitive to low DO and high temperature and pH, thereby resulting in nitrite accumulation. Effluent nitrite was observed to have a significantly strong positive correlation with temperature and pH in all reactors at WWTP A. However, no clear correlation was observed at WWTP B. The DO concentration had an effect on ammonia removal and nitrification rate suggesting that complete nitrification was achieved quickly in diffused aerated plants operated on high DO concentration. However, DO concentration had no impact on COD removal efficiency in excess DO in both plants. The effect of DO concentration on MLSS/MLVSS and SVI could not be properly established in diffused aerated plants operated on high DO levels, suggesting that sludge settleability was also affected by the oil spillage which resulted in foaming and flocs with moderate to high filaments. The mode of aeration however had a positive impact on floc structure since more round and compact flocs were found in both plants with diffuse aeration operated at relatively high DO concentration thus resulting in good settleability.

CHAPTER 4: THE IMPACT OF OPERATIONAL PARAMETERS ON DOMINANT NITRIFYING BACTERIAL COMMUNITIES AND THEIR FUNCTIONAL GENE EXPRESSION

4.1 INTRODUCTION

Since the introduction of the activated sludge process in the early 1900s, many different types of diffused aeration systems have been designed and developed to dissolve oxygen into wastewater (Al-Ahmady, 2006). With increasing energy consumption and insufficient oxygen transfer associated with surface aeration systems, fine bubble aeration systems are currently becoming the most frequently used systems in WWTPs due to their energy efficiency and high oxygen transfer efficiency (Åmand *et al.*, 2013). As introduced previously, the DO concentration is the most important operational parameter in the aeration tank when designing functionally stable and effective treatment systems. Insufficient DO concentration (below 2 mg/L) has been reported to inhibit the growth of nitrifying bacteria in the aeration tank, leading to incomplete nitrification (Metcalf *et al.*, 2014, Thakur and Medhi, 2019).

Traditionally, nitrification is known as a two-step process carried out via two distinct groups of bacteria: ammonia oxidized into nitrite by AOB and then nitrate by nitrite-oxidizing bacteria (NOB) (Qian *et al.*, 2017). The NOB has been reported to be more sensitive to low DO concentration than AOB. As a result, nitrite may accumulate under low DO concentration (Qian *et al.*, 2017). The activity of nitrifying bacteria in WWTPs is sensitive to shifts in the plant's temperature, DO concentration, and ammonia/nitrite concentrations, often leading to nitrification failure (Johnston *et al.*, 2019). Even though nitrifying bacteria have been well studied, maintaining efficient nitrification in BNR systems is usually a challenge, and understanding the microbial community structure has never been an easy task. However, the

introduction of culture-independent molecular techniques for the identification and quantification of nitrifying bacteria in wastewater treatment plants has brought a better understanding of microbial community structure (Awolusi *et al.*, 2015c). The culture-independent molecular techniques based on DNA and RNA, such as PCR and qPCR (Suryavanshi *et al.*, 2019), have been successfully used in identifying and quantifying the nitrifying communities in WWTPs. However, while these techniques have been successfully used in identifying and quantifying the bacterial presence, they have been criticized for their failure to accurately characterize the microbial diversity and functional status in WWTPs (Awolusi *et al.*, 2015c). Thus, a combinatory approach has been recommended, whereby two or more techniques are usually combined. The majority of the existing studies on the microbial community structure of full-scale wastewater treatment systems are DNA-based, which does not directly relate to the microbial function (Zhang and Liu, 2019).

The RNA-based approach is expected to provide more reliable data than DNA in revealing the 'active' microbial communities versus 'dormant' microbial populations as mRNA is considered an indicator of functionally active microbial populations (Taylor *et al.*, 2017a). Reverse transcription (RT) analyses are now increasingly being combined with qPCR methods in reverse-transcription PCR (RT-PCR) assays, leading to a powerful tool for quantifying gene expression and relating microbial community structure to environmental function. The RT-PCR is usually the method of choice for rapid and sensitive quantitative measurements of mRNA copy numbers analysing gene expression levels (Tsotetsi *et al.*, 2018). Thus, the introduction of a gene expression study gives more useful information on microbial function than DNA-based studies. However, little is known about the impact of the fine bubble diffused aeration systems on the gene expression profiles regarding the performance of different nitrifying community groups within wastewater treatment plants. Thus, the goal of this chapter

was to determine the abundance and diversity of dominant AOB and NOB and their gene expression profile from activated sludge plants with a fine bubble diffused aeration system in KwaZulu-Natal.

4.2. MATERIALS AND METHODS

4.2.1 Wastewater treatment plant operation and samples

Wastewater characteristics and operational parameters for the plant are shown in Table 3.2. The detailed plants' configuration and sampling for this objective are shown in sections 3.2.1 and 3.2.2, respectively.

4.2.2 DNA and RNA extraction

DNA was extracted from 0.25 g of activated sludge using the DNeasy Powersoil extraction kit (Qiagen, USA) as per the manufacturers' instructions. The quantity and quality of the DNA were determined using the IMPLEN NanoPhotometer NP 80 (Implen GmbH, Munich, Germany), as well as electrophoresis in 1% (w/v) agarose gel electrophoresis. Total RNA was extracted from a concentrated 3 mg activated sludge sample using the RNeasy PowerMicrobiome Kit, (QIAGEN) according to the manufacturer's instructions. The potential genomic DNA contamination was eliminated with the gDNase reagent (ThermoFisher Scientific, USA). The first strand of cDNA was synthesized with reverse transcriptase using the QuantiTect Reverse Transcriptase kit (Qiagen, Valencia, CA). RNA purity was confirmed using the Implen NanoPhotometer® NP80 UV/Vis spectrophotometer (ThermoFisher Scientific, USA).

4.2.3 Polymerase Chain Reaction

The PCR was carried out using the AOB and NOB 16S rRNA primers sets and optimized protocols as described in Table 4.1 and Table 4.2. The DNA was amplified using a thermocycler (Bio-Rad T100). Thermocycling conditions are shown in Table 2. Each PCR reaction consisted of a total reaction volume of 25 µL containing 20 ng of DNA template (2 µL), PCR Master Mix (2×) (12.5 2 µL) (Thermo Scientific™), and 0.5 µM of each primer (Table 4.1) in a final volume of 25 µL (Avrahami *et al.*, 2011). To confirm the positive amplification, the amplicons were run on 1.2 % (w/v) agarose gel (pre-stained with ethidium bromide) electrophoresis, and the products were visualized using a gel documentation unit. The purified PCR amplicons were submitted to Inqaba Biotechnical Industries (Pty), South Africa, for further confirmation using sequencing and analysis.

Table 4.1: Primers used for PCR amplification of nitrifiers and their functional genes.

Gene target	Primer name	Primer sequence (5′→3′)	Base pair
AOB 16S rRNA	CTO 189fA/B	GGAGRAAAGCAGGGGATCG	467
	CTO 189fC	GGAGGAAAGTAGGGGATCG	
	RT1r	CGTCCTCTCAGACCARCTACTG	
***Nitrospira* 16S rRNA**	NSR1113F	CCTGCTTTCAGTTGCTACCG	151
	NSR1264R	GTTTGCAGCGCTTTGTACCG	
***Nitrobacter* 16S rRNA**	Nitro 1198f	ACCCCTAGCAAATCTCAAAAAACCG	229
	Nitro 1423r	CTTCACCCCAGTCGCTGACC	
AOB *amoA* gene	*amoA*-1f	GGGGTTTCTACTGGTGGT	491
	amoA-2r	CCCCTCKGSAAAGCCTTCTTC	
NOB *nxrA* gene (*Nitrobacter spp*.)	*nxrA* f1	CAGACCGACGTGTGCGAAAG	322
	nxrA r2	TCCACAAGGAACGGAAGGTC	
***Nitrospira nxrB* uwm-2**	NitrospiraG2-a-F	5′-ACG TCA AAA TCA CGCAGC TG-3′	123
	NitrospiraG2-a-R	5′-CGG CAT CGA AAA TGGTCA TCC-3′	

Table 4.2: Primers and the amplification conditions

Primer	Initial Denaturation		Cycles	Denaturation		Annealing		Elongation		Final elongation		Reference
	ºC	Min		ºC	S	ºC	S	ºC	S	ºC	Min	
CTO 189fA/B CTO 189fC RT1r	95	3	45	95	15	61	30	72	60	72	7	(Hermansson and Lindgren, 2001)
NSR1113F NSR1264R	94	5	40	94	30	65	30	72	30	72	15	(Wang *et al.*, 2011)
Nitro 1198f Nitro 1423r	95	10	40	94	60	58	60	72	60	72	7	(Graham *et al.*, 2007)
***amoA*-1f *amoA*-2r**	95	10	40	94	60	57	60	72	60	72	7	(Jin *et al.*, 2011)
***nxrA* f1 *nxrA* r2**	94	3	30	94	30	55	45	72	45	72	5	(Poly *et al.*, 2008)
NitrospiraG2-a-F NitrospiraG2-a-R	95	2	40	95	05	65	45	72	30	72	10	(Bartelme *et al.*, 2017)

4.2.4 Sequencing and verifying the presence of COMAMMOX

The obtained sequences were edited using Finch TV software (version 1.4.0). The partial sequences that were 97% similar were grouped into the same operational taxonomic unit (OTU), with their representative nucleotide sequences used for further analysis. The sequences obtained were compared to the National Centre for Biotechnology Information (NCBI) GenBank database using the Basic Local Alignment Search Tool (BLAST) to determine the phylogenetic affiliations. CLUSTALX implemented in BioEdit (Hall, 1999) was used to align the nucleotide sequences from this study and those obtained from the NCBI database. Thereafter, the aligned sequences were exported into MEGA6 (version 10.2.5) where matrices of evolutionary distances were computed (Tamura *et al.*, 2013). Phylogenetic trees were then constructed and checked by bootstrap analysis (based on 1000 replicates) (Tamura *et al.*, 2011).

4.2.5 Quantitative real-time PCR (qPCR) analysis of nitrifiers

The RT-PCR quantification was carried out with the primer sets targeting different nitrifying bacteria and their functional genes (Table 4.1) according to the modified method described by Awolusi *et al.* (2018). A Bio-Rad C1000 Touch Thermal Cycler-CFX96 Real-Time System (BIO-RAD, USA) was employed for the qPCR. The qPCR reaction mixture was made up of 4 µL of PowerUp SYBR Green PCR Master Mix (Applied Biosystems), 0.4 µL of each primer (final concentration of 0.4 µM), 2 µL of template DNA (final concentration of 1 ng), and molecular grade water to a final volume of 10 µL. For each experimental setup, appropriate negative controls containing no genomic DNA were subjected to the same amplification condition. The specificity of each qPCR assay was confirmed by using both melting curve analysis and agarose gel electrophoresis.

4.2.6 Functional gene expression

Functional gene expression encoding for ammonia oxidation (*amoA*) and nitrite oxidation (*nxrA* and *nxrB*) in AOB, and NOB respectively (Table 3.1) were quantified using the RT-qPCR to understand the activity of nitrifiers in a given condition. The mRNA concentrations of the selected functional genes were normalized using 16S rRNA as a reference gene. The RT-qPCR was performed with SYBR Green PCR Master Mix (Applied Biosystems), using qPCR as described in section 4.2.6.

4.2.7 Statistical analysis

GraphPad Prism version 5.00 for Windows (GraphPad Software, San Diego California USA) was used in carrying out Pearson correlation. Microsoft Excel 2010 was used in calculating the standard deviation.

4.3. RESULTS

4.3.1 Detection of the dominant nitrifiers and their functional genes using PCR

Successful amplification of *Nitrospira spp*. (a), *Nitrobacter spp*. (b), and AOB 16S rRNA (c) gene was confirmed with amplicons yielding the expected product sizes of 151 bp, 229 bp, and 189 bp, respectively (Fig 4.1). Similarly, successful amplification of functional genes viz., *nxrA* (a), *nxrB*. (b), and *amoA* (e) were obtained with amplicons yielding the expected band sizes of 322 bp, 104 bp, and 491 bp, respectively (Fig. 4.2).

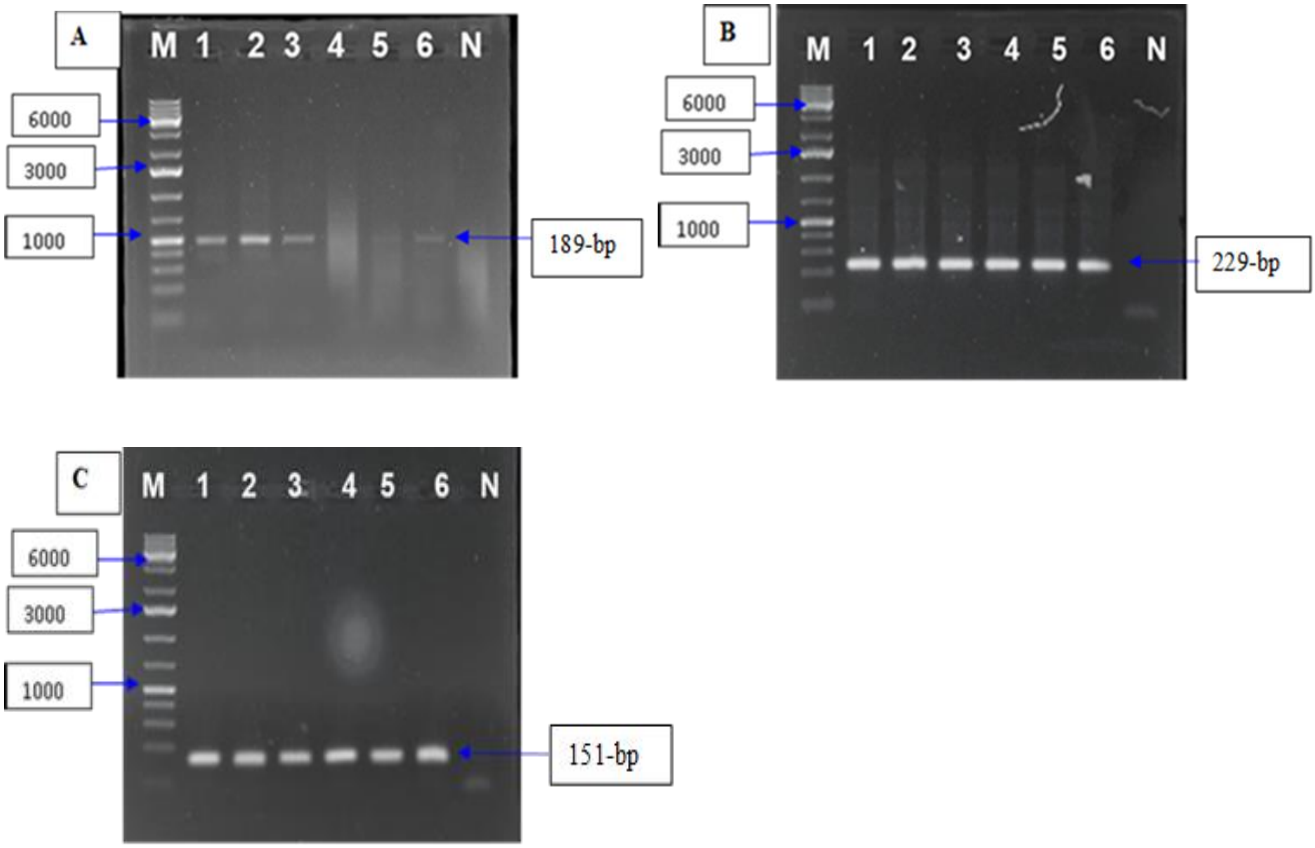

Figure 4.1: Agarose gel showing PCR products for (a) AOB 16S rRNA at 189-bp, (b) *Nitrobacter spp*. at 229-bp and (c) *Nitrospira spp*. at 151 bp. Lane M denotes the GeneRuler^{TM} 1kb DNA ladder, whilst lanes 1–6 indicate resulting bands from using (a) CTO 189fA/B/ CTO 189fC/RT1r, (b) Nitro 1198F/Nitro, and (c) NSR 1113F/NSR 1264R, and lanes N depicting negative control.

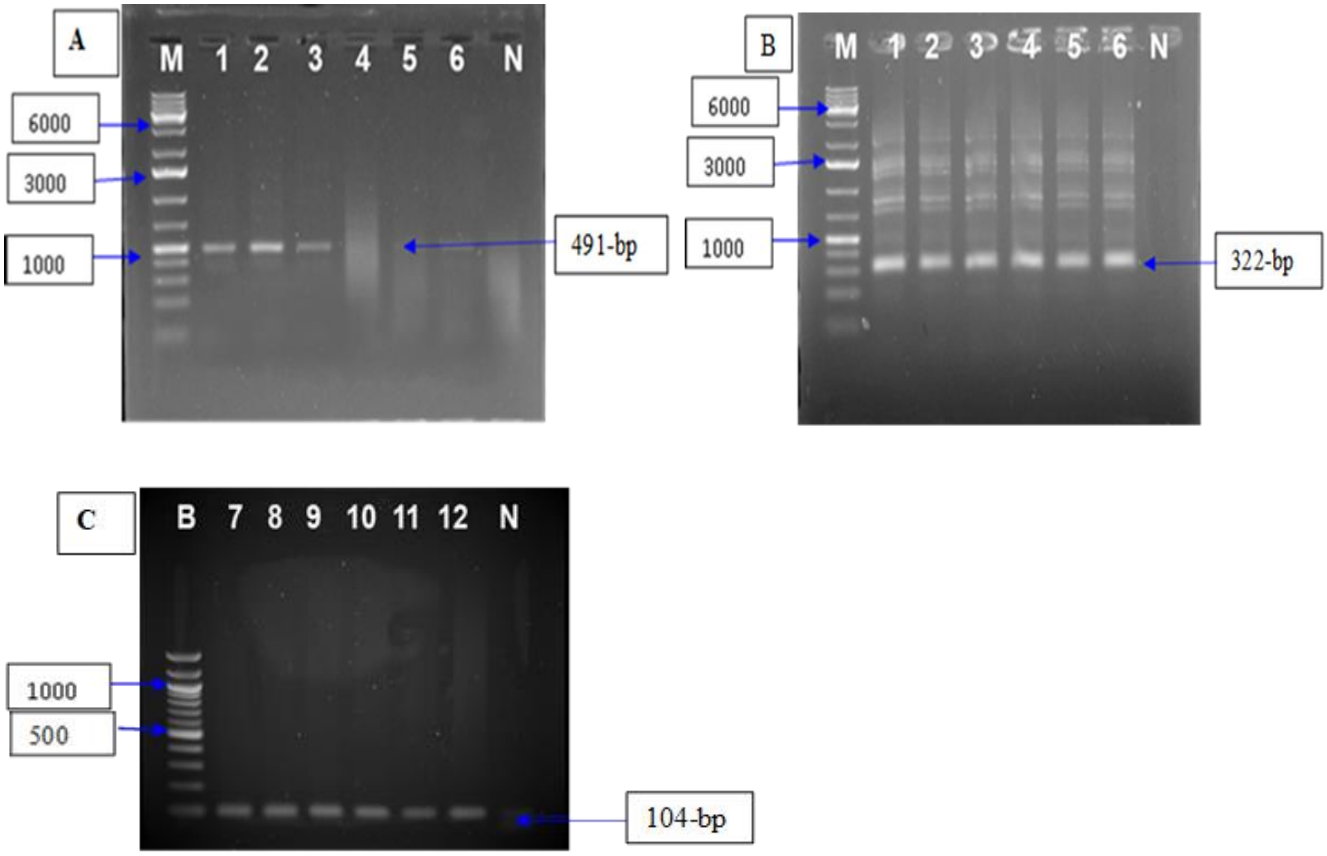

Figure 4.2: Agarose gel showing PCR products for (a) AOB (amoA) at 491 bp and NOB (*nxrA* and *nxrB*) at (b) 322 bp and (c)104 bp, respectively. Lane M denotes the GeneRuler^{TM} 1kb DNA ladder, whilst lanes 1–6 indicate resulting bands from using (a) amoA1F/ amoA2R and (c) *nxrA* F1/*nxrA* R2. Lane B denotes 100 bp DNA ladder while lanes 7–12 depict resultant bands from using (c) *nxrB* NitrospiraG1-a-F/ *nxrB* NitrospiraG1-a-R and lanes N depicting negative control.

4.3.2 Verification of the presence of COMAMMOX

The amplification of *nxrB* (encoding for *Nitrospira spp.*) was confirmed using sequencing since COMAMMOX is closely related to the canonical *Nitrospira* (Daims *et al.*, 2015). All the partial sequences obtained from the *nxrB* in both plants were closely related to uncultured *Nitrospira spp.*, nitrite oxidoreductase subunit B which has been implicated in COMAMMOX (Daims et al., 2015, Wang et al., 2017b) with 97 – 100% similarity (Fig. 4.3).

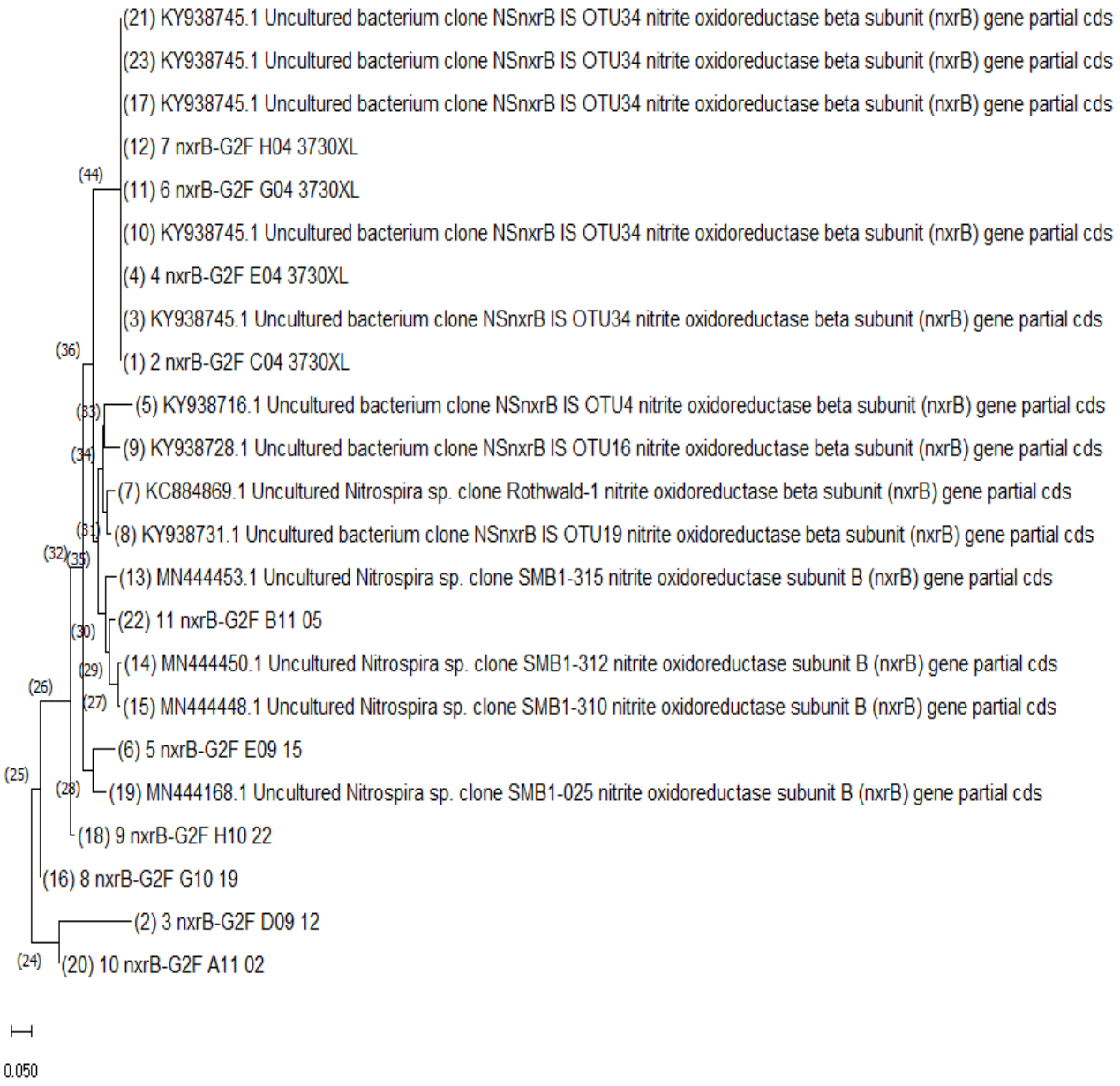

Figure 4.3: Phylogenetic tree of the bacterial *nxrB* sequences recovered from municipal activated sludge was used to construct a neighbor-joining tree from the resulting alignment with MEGA 7.

4.3.3 Dominant nitrifying bacterial communities

4.3.3.1 Influence of DO concentration on dominant nitrifying bacterial communities and their functional genes in WWTP A

The AOB and NOB populations were quantified using the primer sets targeting the nitrifying bacteria and their functional gene within reactors with fine bubble diffused aeration (Table 4.1). The qPCR efficiencies for all the primers tested were between 90 and 110% and the standard curves were linear over six orders of magnitude (R2>0.99) (Table 4, Fig. 4.4). From Fig. 4.5 it was evident that the AOB16S rRNA population was high in all 3 systems (reactor 1, 2, and 3) compared with the NOB population (*Nitrospira* and *Nitrobacter spp*.) throughout the study. When the DO was ≥ 3 mg/L in reactor 1 and reactor 2, AOB ranged from 3.57×10^2 – 7.78×10^4 copies/L and 3.57×10^2 – 1.02×10^5 copies/L, respectively. When the DO was ≤ 3 mg/L, or less in aerator 3, the number of AOB was in the range of 3.57×10^2 – 1.35×10^5 copies/L.

Table 4.3: Description of qPCR standard curve parameters optimized for the analysis during this study.

Parameter	**Target**					
	nxrA	*nxrB*	*amoA*	*Nitrobacter spp.*	*Nitrospira spp.*	AOB (CTO)
Efficiency (%)	90.3	90.1	110.5	98.4	95.0	100.2
Slope	0.997	0.983	0.993	0.990	0.993	0.995
R^2 of Slope	-3.578	-3586	-3.095	-3.361	-3.448	-3.318
Intercept	41.751	40.058	32.376	37.587	37.398	39.521

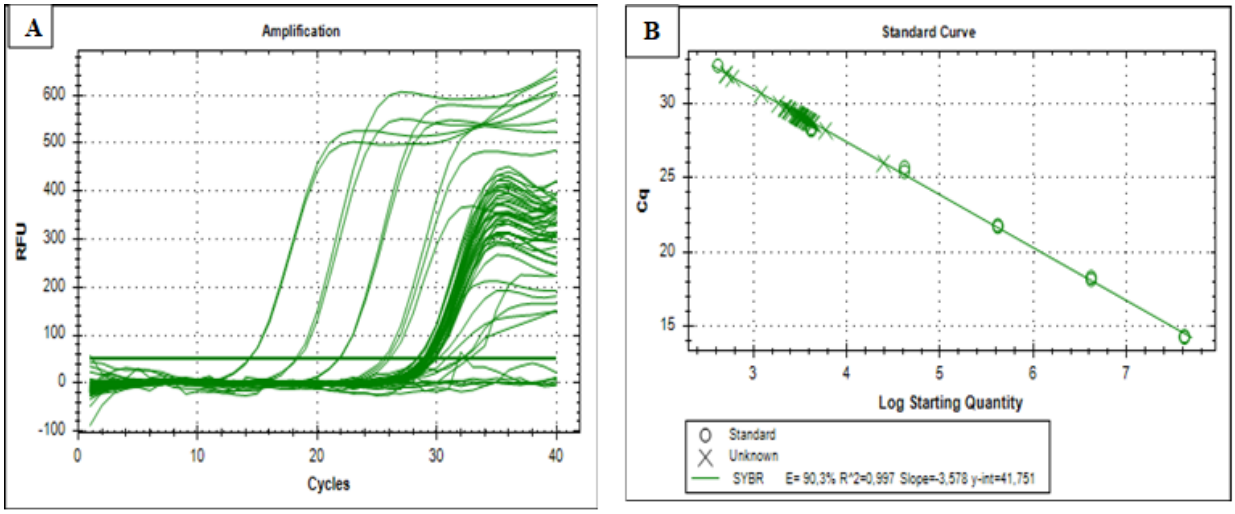

Figure 4. 4: Real-time PCR data for the purified DNA (*nxrA*) used in generating standard curve indicating linearity over six orders of magnitude (R2>0.99) (a) The qPCR amplification curve (b) Standard curve.

Between the reactors, statistically, a negative correlation was found between the AOB16S rRNA copies and DO concentration in reactor 1 (r = -0.40) while a positive correlation was found in reactor 3 (r = 0.47). However, no clear correlation was observed between AOB16S rRNA copies and DO concentration in reactor 2. It was also noted that the change in temperature and COD/N ratio could be one of the contributing factors to the abundance of the AOB16S rRNA population in the reactors along with the DO. The AOB 16S rRNA copies showed a positive correlation with temperature and COD/N ratio in reactor 1 (rs = 0.43 and 0.47) and reactor 3 (rs = 0.43 and 0.63) while no clear correlation was observed for reactor 2.

The *Nitrobacter spp.* was the dominant NOB while the relative abundance of *Nitrospira spp.* was generally low and consistent throughout this study in all three reactors (Fig. 4.5). There was no clear correlation observed between DO concentration and *Nitrobacter spp.* However, there was a trend toward a higher population of *Nitrobacter spp.* at higher DO concentrations.

For instance, the *Nitrobacter spp.* was found to be high in reactor 3 ($2.18\times 10^1 - 3.73\times10^3$ copies/L) with a high DO level compared to reactor 1 ($2.18\times 10^1 - 2.19\times10^3$ copies/L) and reactor 2 ($3.27\times 10^2 - 2.62\times10^3$ copies/L). These results demonstrate that higher DO concentrations supported the growth of *Nitrobacter spp*. The increase in *Nitrobacter spp.* at high DO concentration and the high temperature was probably due to the elevated nitrite concentration (0.01 - 5.6 mg/L) from Nov 2019 and Feb 2020 (Fig. 3.4). *Nitrobacter spp.* was found to have a positive correlation with temperature and nitrite concentration in all 3 reactors (reactor 1: rs = 0.50, and 0.41; reactor 2: rs = 0.71 and 0.43; reactor 3: rs = 0.63 and 0.31; p = 0.05). A positive correlation was found between *Nitrospira spp.* and DO concentration in reactor 1 (r = 0.33) and reactor 3 (0.44) while reactor 2 showed no clear correlation. The changes in AOB 16S rRNA (CTO), *Nitrospira spp*., and *Nitrobacter spp*. abundance across the study period is shown in Fig. 4.5.

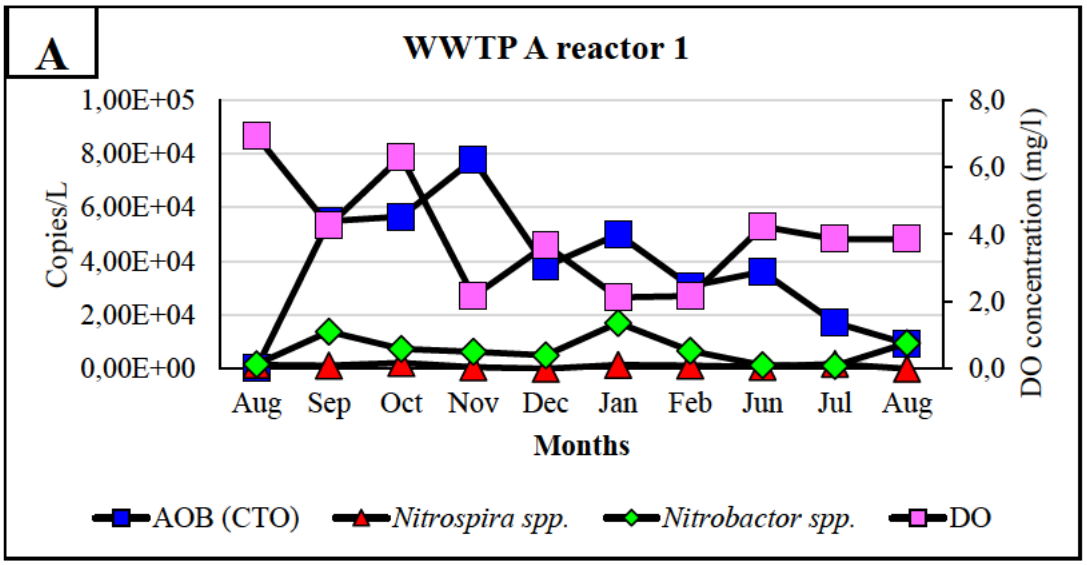

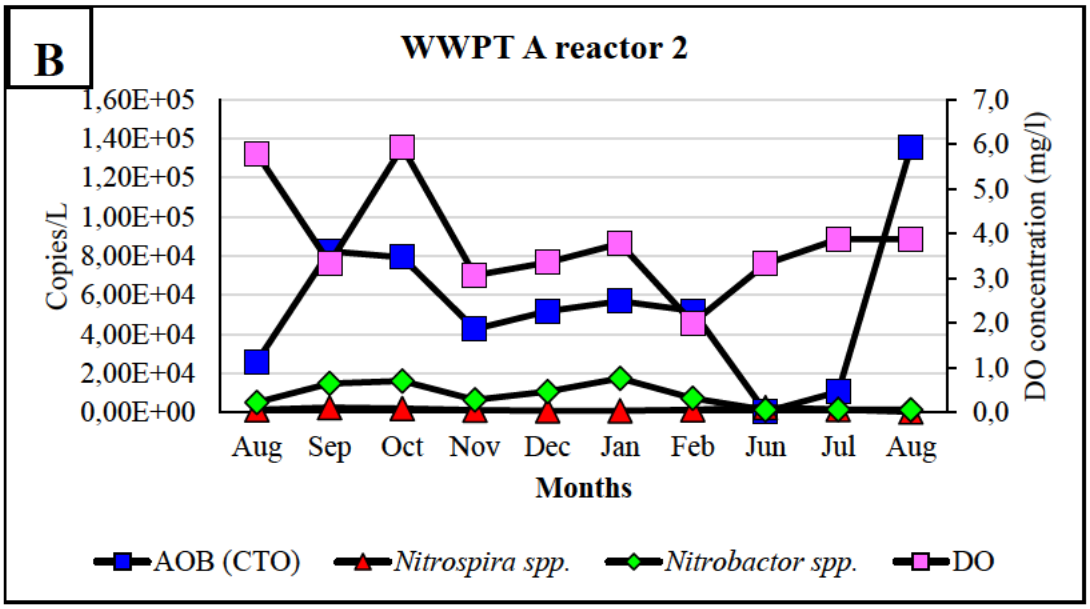

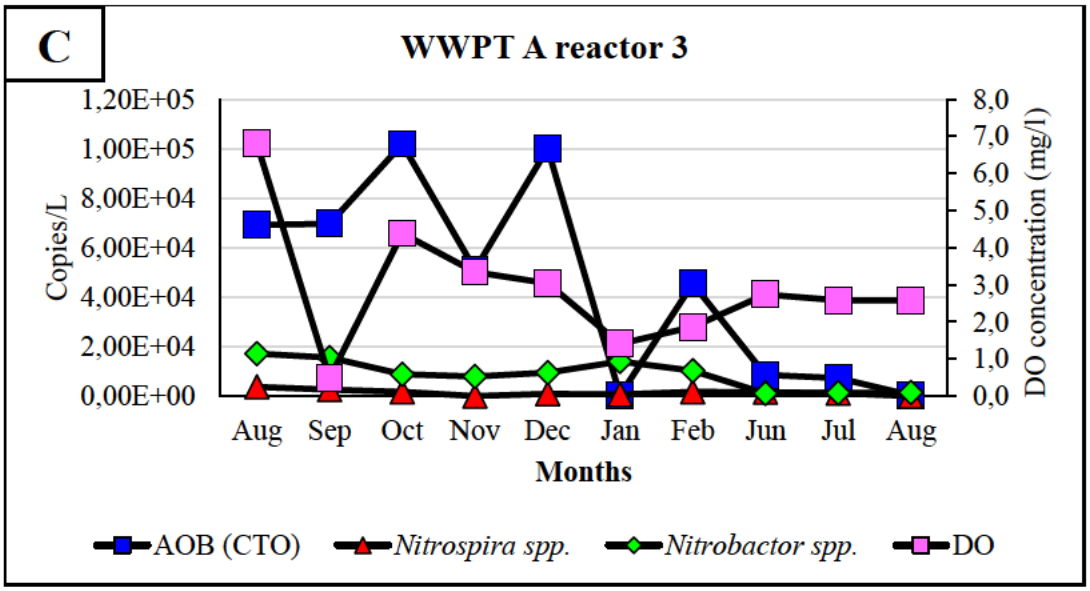

Figure 4.5: qPCR temporal changes in AOB (CTO), *Nitrospira spp*., and *Nitrobacter spp*, (a) reactor 1, (b) reactor 2, and (c) reactor 3 during this study and ammonia removal rate of WWTP A.

The AOB functional gene was quantified using the primer set targeting the ammonia monooxygenase (*amoA*) and the NOB functional genes were quantified using the primer sets nitrite oxidoreductase (*nxrA* - coding for nitrite oxidation of *Nitrobacter spp.* and *nxrB* - coding for nitrite oxidation of *Nitrospira spp*.). In contrast to the 16S rRNA results, *amoA* recorded the lowest copy numbers in all the 3 reactors compared with *nxrA* and *nxrB* (Fig. 4.6). The *amoA* ranged from 7.58×10^{1} - 4.45×10^{3} copies/L in reactor 1, 7.58×10^{1} - 4.30×10^{3} copies/L in reactor 2, and 2.38×10^{2} -2.66×10^{4} copies/L in reactor 3. The lowest *amoA* abundance was recorded during cold temperatures ranging from 17.5 -19.3 ºC (Jun 2020 to Aug 2020), which was found to be significantly correlated with temperature in the reactors (reactor 1: $r = 0.44$; reactor 2: $r = 0.62$ and reactor 3: $r = 0.56$; $p = 0.05$). A positive correlation was found between AOB gene copy numbers and ammonia removal efficiency in the reactors (reactor 1: $r = 0.67$; reactor 2: $r = 0.37$ and reactor 3: $r = 0.69$; $p = 0.05$). However, there was no correlation observed between *amoA* and DO concentration. COD/N ratio was observed to have no effect on *amoA.*

Unlike the quantification of 16S rRNA genes, with *Nitrobacter spp.* population being higher in reactors with high DO concentrations, an inverse relationship was observed with *nxrB* in reactors with high DO concentrations. There was no clear relation between DO concentration and the *nxrB.* However, there was a trend toward a higher population of *nxrB* at higher DO concentrations. Interestingly *nxrA* was not negatively impacted by high DO concentration. The *nxrB* was higher than the *nxrA* in all reactors. The *nxrA* and *nxrB* abundance in reactor 1 were within the range of 3.02×10^{2} -1.24×10^{4} and 1.14×10^{3} – 2.59×10^{4} copies/L respectively, while in reactor 2 it ranged from 3.02×10^{2} -2.79×10^{4} and 1.20×10^{3} – 1.07×10^{4} copies/L respectively and in reactor 3 the abundance was within the range of 1.34×10^{3} – 5.08×10^{4} and 1.36×10^{3} – 1.75×10^{5} copies/L, respectively.

The *nxrB* was the dominant NOB while the relative abundance of *nxrA* genes was generally low and consistent throughout this study in all three reactors (Fig. 4.6). The high relative abundance of *nxrB* may have been caused by (i) relatively high temperature, and nitrite concentration in this study and (ii) the existence of multiple copies of the *nxrB* gene in *Nitrospira* genomes such as COMMAMOX *Nitrospira*. Statistically, *nxrB* was observed to have a positive correction with temperature and nitrite concentration in all 3 reactors (reactor 1: rs= 0.53, and 0.36; reactor 2: rs = 0.64 and 0.54; reactor 3: rs = 0.55 and 0.47; p = 0.05), while *nxrA* showed no significant relationship to temperature and nitrite concentration. The *nxrB* was observed to be decreasing when the COD/N ratio was high, while *nxrA* remained consistent in all reactors when the COD/N ratio was high. A negative correlation was found between n*xrB* and COD/N ratio in all reactors (reactor 1: rs= -0.32; reactor 2: rs = -0.43; reactor 3: rs = -0.50; p = 0.05). However, a positive correlation was found between *nxrA* and COD/N ratio in all reactors (reactor 1: r = 0.49; reactor 2: r = 0.58 and reactor 3: r = 0.58; p = 0.05). The changes in AOB (*amoA*), and NOB (*nxrA* and *nxrB*) abundance across the study period is shown in Fig. 4.6.

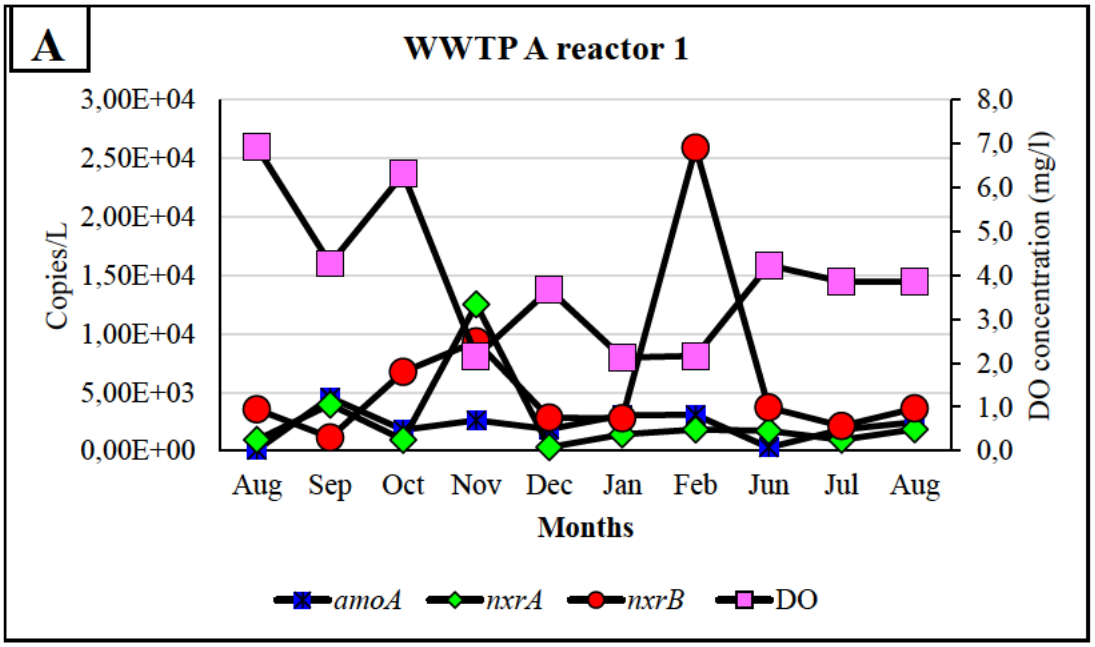

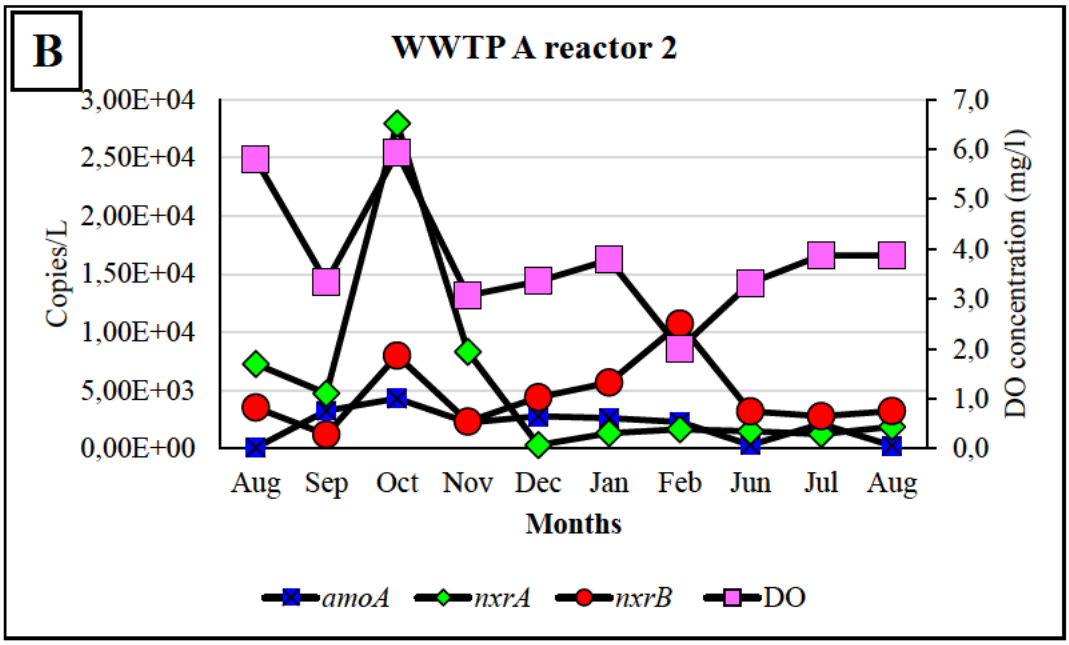

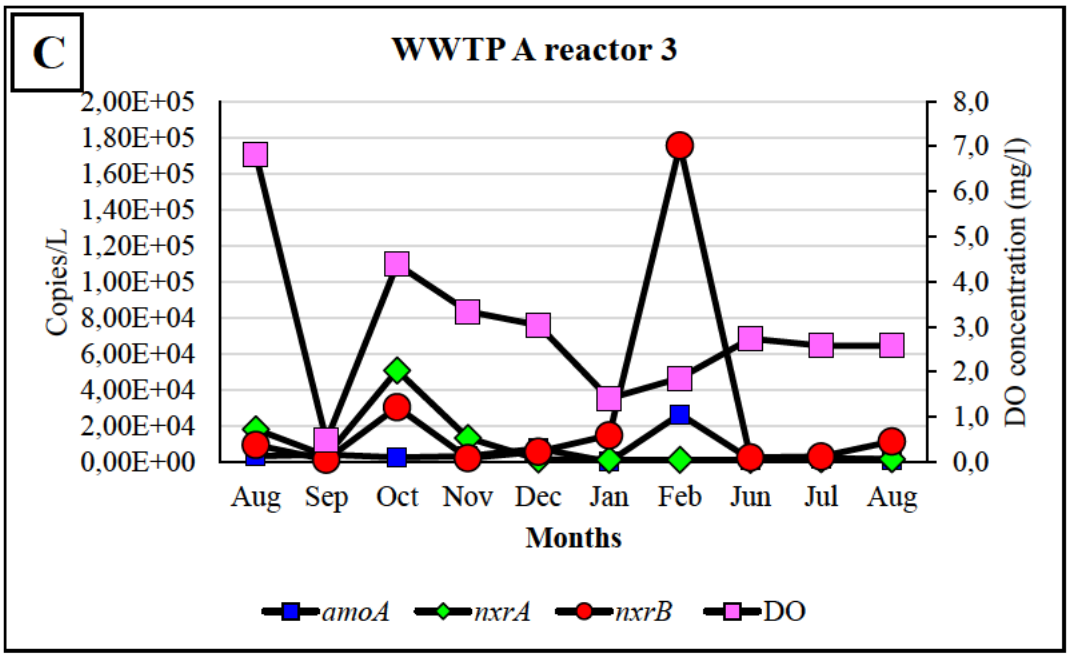

Figure 4.6: qPCR temporal changes in *amoA, nxrA, and nxrB*, (a) reactor 1, (b) reactor 2, and (c) reactor 3 during this study and ammonia removal rate of the plant.

4.3.3.2 Influence of DO concentration on dominant nitrifying bacterial communities and their functional genes in WWTP B

The *Nitrobacter spp*. copy numbers were observed to be the highest in the reactor when compared with AOB 16S rRNA (CTO) and *Nitrospira spp.* copy numbers. *Nitrobacter spp.* was the dominant NOB throughout the study. The AOB 16S rRNA (CTO) abundance ranged from $1.37\times 10^3 - 4.20\times 10^4$ copies/L while the *Nitrospira* and *Nitrobacter spp*. abundance ranged from $3.88\times 10^2 - 5.44\times 10^3$ copies/L and $1.30\times 10^1 - 1.79\times 10^5$ copies/L, respectively (Fig. 4.7). A high abundance of the AOB16S rRNA was observed when the temperature and COD/N were high in the reactor. The AOB16S rRNA population showed a strong positive correlation with temperature, and COD/N in the reactor (r = 0.78 and 0.41, p = 0.05) while the AOB16S rRNA population showed no clear correlation with DO concentration, ammonia removal efficiency, and nitrification rate. However, the DO concentration was observed to be positively correlated with the *Nitrospira* (r = 0.71, p = 0.05) and *Nitrobacter spp*. (r = 0.33). The changes in AOB 16S rRNA (CTO), *Nitrospira spp*., and *Nitrobacter spp*. abundance across the study period is shown in Fig. 4.7.

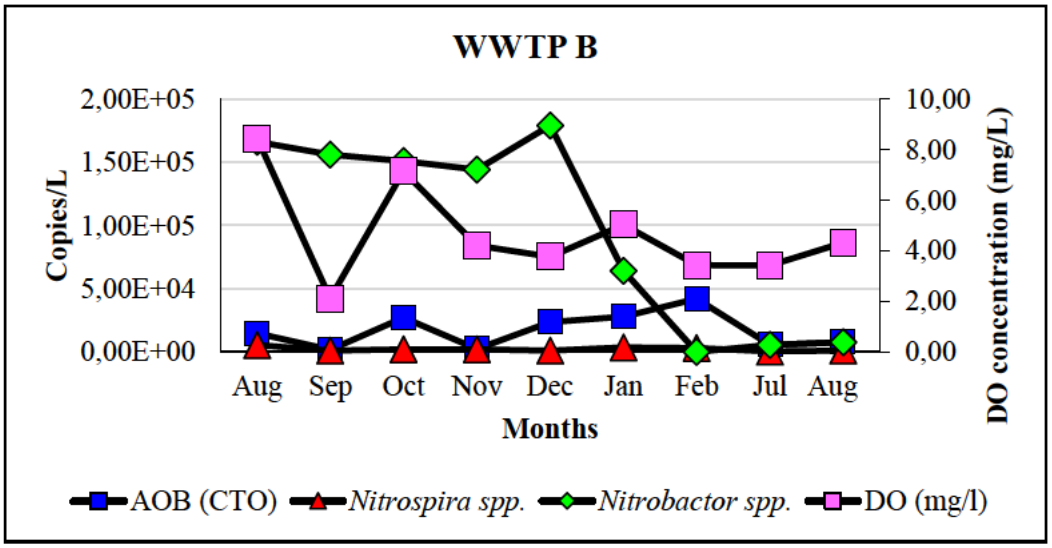

Figure 4.7: qPCR temporal changes in AOB (CTO), *Nitrospira spp*., and *Nitrobacter spp*. in the reactor during this study and ammonia removal rate of WWTP B.

On the other hand, with regard to the functional gene analysis, the *nxrB* copy numbers were observed to be higher in the reactor at WWTP B when compared with *amoA* and *nxrA*. The *amoA* abundance was found to be within the range 1.83×10^3 – 1.15×10^5 copies/L while the *nxrA* and *nxrB* abundance were within the range of $1.33\times 10^3 – 3.39\times 10^4$ and $6.18\times 10^2 – 1.70\times 10^5$ copies/L, respectively. The *nxrB* was the dominant NOB throughout this study. The highest *nxrB* was recorded during high temperatures (above 23°C) and high nitrite concentration (above 1 mg/L). The *nxrB* copy numbers were found to have a strong positive correlation with temperature and nitrite concentration in the reactor (rs= 0.64 and 0.71, p = 0.05) while a negative correlation was observed between *nxrA* and temperature (r -0.51, p = 0.05). However, the DO concentration showed no influence on the functional genes (*amoA, nxrA*, and *nxrB*). The changes in AOB (*amoA*), and NOB (*nxrA* and *nxrB*) abundance across the study period is shown in Fig. 4.8.

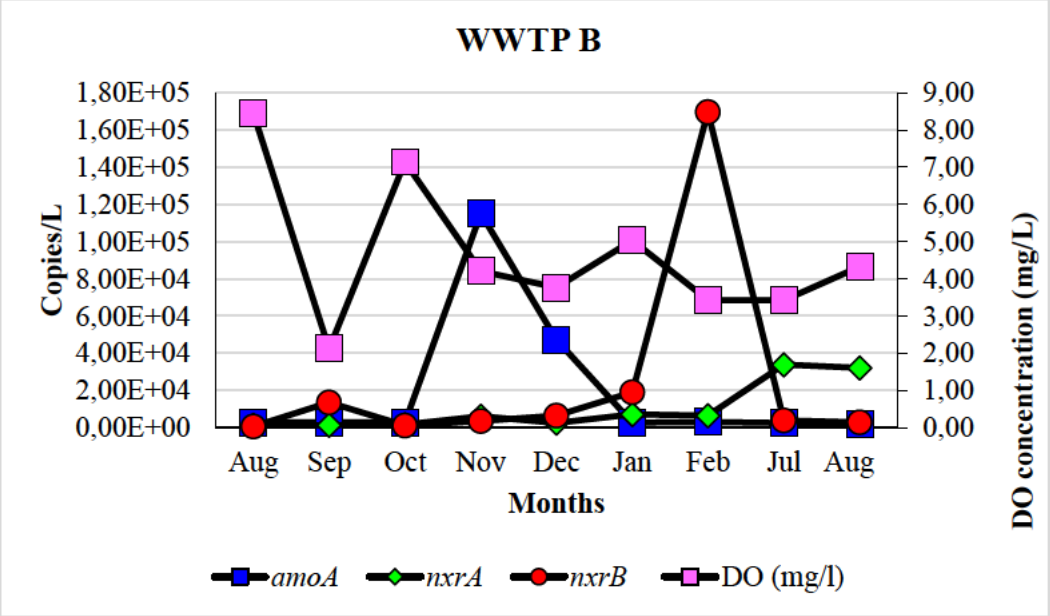

Figure 4.8: qPCR temporal changes in functional genes during this study and ammonia removal rate of the plant.

4.3.4 Functional gene expression

4.3.3.3 Effect of DO concentration on nitrifiers' functional gene expression profile in WWTP A

In terms of functional gene expression, a rapid increase in *nxrB* expression was observed in all reactors and corresponded well with the observed severe nitrite accumulation. In contrast, the expression levels of *nxrA* were relatively more consistent throughout the study period in all reactors. The highest *amoA* expression levels were recorded when DO concentrations were high (> 3.5 mg/L) in all 3 reactors. Reactor 1 was observed to have the highest gene expression level (*amoA*, *nxrA*, and *nxrB*) when compared with reactor 2 and reactor 3. Statistically, a positive correlation was found between AOB gene expression (*amoA*) and DO concentration in all reactors (reactor 1: r = 0.49; reactor 2: r = 0.78 and reactor 3: r = 0.32; p = 0.05). However, no clear correlation was found between NOB gene expression (*nxrA* and *nxrB*) and DO concentration.

A positive correlation was found between the *nxrB* expression and nitrite concentration in all the reactors (reactor 1: r = 0.48; reactor 2: r = 0.71 and reactor 3: r = 0.47; p = 0.05). In contrast, a negative correlation was found between *nxrA* expression and nitrite concentration in all reactors (reactor 1: r = -0.38; reactor 2: r = - 0.38 and reactor 3: r = -0.33; p = 0.05). The *amoA* expression was found to have a negative correlation with *nxrA* expression (reactor 1: r = - 0.41; reactor 2: r = - 0.43 and reactor 3: r = -0.36; p = 0.05) and *nxrB* expression (reactor 1: r = - 0.69; reactor 2: r = - 0.50 and reactor 3: r = -0.57; p = 0.05) while no clear correlation was found between *nxrA* and *nxrB*. The changes in gene expression levels of *amoA*, *nxrA*, and *nxrB* are shown Fig. 4.9.

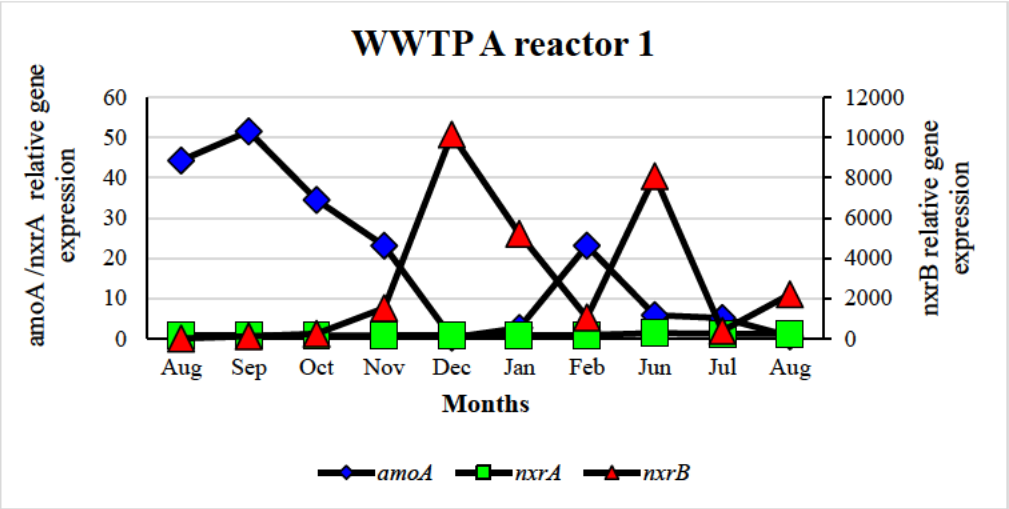

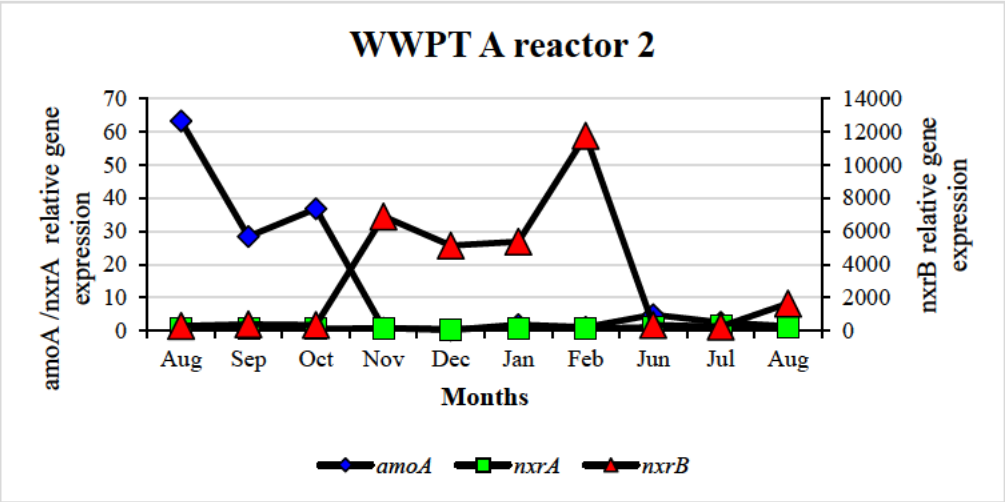

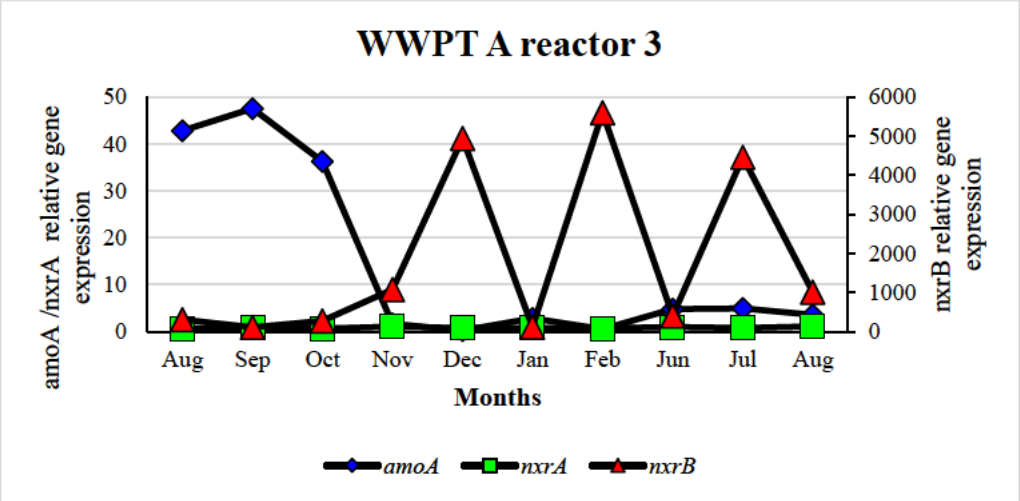

Figure 4.9: Relative expression profile of *amoA, nxrA*, and *nxrB* in (a) reactor 1, (b) reactor 2 and (c) reactor 3 WWTP A.

4.3.4.2 Effect of DO concentration on nitrifiers' functional gene expression profile in WWTP B

In terms of functional gene expression, a rapid decrease in *amoA* was observed in the reactor while a rapid increase was observed in the expression level of the *nxrB* during high temperature. In contrast, *nxrA* was relatively more consistent throughout the study period (Fig. 4.10). A negative correlation was observed between *nxrA* expression levels and DO concentration (r = - 0.34, p = 0.05). However, DO concentration showed no clear correlation with *amoA* and *nxrB* expression levels. A positive correlation was found between the *nxrB* expression and nitrite concentration in the reactor (r = 0.42). A negative correlation was found between *amoA* expression and temperature (r = -0.41) and nitrite concentration (r = -0.46) while *nxrB* expression was found to have a positive correlation with temperature (r = 0.38) and nitrite concentration (r = 0.42). However, no clear correlation was found between *nxrA*, temperature, and nitrite concentration. The *amoA* expression was found to have a negative correlation with *nxrA* and *nxrB* expression in the reactor (r = - 0.49 and - 0.63, respectively) while no clear correlation was found between *nxrA* and *nxrB* expression levels. The fold changes in expression levels of *amoA, nxrA*, and *nxrB* are shown in Fig. 4.10.

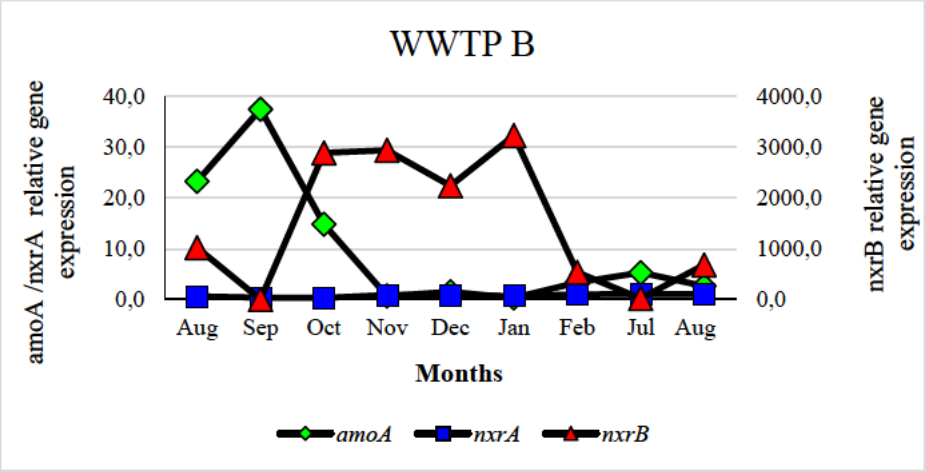

Figure 4.10: Relative expression profile of *amoA, nxrA,* and *nxrB* in the reactor at WWTP B

4.4 DISCUSSION

The qPCR and RT-q-PCR quantification methods applied in this study determined the abundance of nitrifying community structures and their functional gene expression in two fine-bubble diffused aerated WWTPs during varying operational and environmental conditions. The DO concentrations in this study (Figs.3.5 & 3.9) were found to be significantly higher than the recommended DO concentration (2 mg/L) for complete nitrification in all reactors (Uri-Carreño *et al.*, 2021, Behnisch *et al.*, 2018). In this study, a higher copy number of the AOB 16S rRNA was detected from WWTP A (Fig. 4.5) with a high COD/N ratio, while a low copy number from WWTP B (Fig. 4.8) with a low COD/N ratio. The qPCR results of AOB 16S rRNA in this study were similar to that of Kayee *et al.* (2016), who found an abundance of AOB 16S rRNA in municipal full-scale anoxic and aerobic tanks at Bangkok WWTP with a high COD/N ratio. Gao *et al.* (2013) found that a high ratio of COD/N (10:7) in full-scale WWTP led to an increase in the AOB 16S rRNA copy number.

Furthermore, the growth rate of NOB was observed to be slower than the AOB at WWTP A with a NOB/AOB ratio of 0.55 in reactor 1, 0.65 in reactor 2, and 2.35 in reactor 3 (Fig. 4.5) while in WWTP B, the NOB had an advantage over AOB with NOB/AOB ratio of 4.02 (Fig. 4.8). This may be due to NOB having a smaller endogenous decay coefficient than AOB. The difference in copy numbers between the two plants with fine bubble diffused aeration mode may be due to different configuration processes used. Bo and Xin (2012) reported that community structures of AOB and NOB were different among different water treatment processes and the AOB and NOB diversity can be influenced by both influent quality and the treatment processes. In addition, Wang *et al.* (2012b) reported that different environmental conditions may result in the selection of different microbial populations. In contrast, Liu and Wang (2013) found that the copy numbers of NOB were higher than the AOB copy numbers

under long-term low DO conditions in WWTP with surface aeration. The high copy number of AOB observed in this study may be due to the fine-bubble diffused aeration mode (operated relatively at high DO concentration) used in this study. Awolusi *et al.* (2015c) also found that the *Nitrobacter spp*. copy numbers were highest during their study, with 2 orders of magnitude above the AOB throughout the study.

Nitrobacter spp. and *Nitrospira spp.* were suggested to be r-strategists (having a high growth rate and a low substrate affinity) and K-strategists (having a low growth rate and a high substrate affinity), respectively (How *et al.*, 2021). In this study, a low copy number of *Nitrospira spp.* (NSR genes) were observed in WWTP A (Fig. 4.5) with a high COD/N ratio while higher *Nitrospira spp.* in WWTP B (Fig. 4.8) with a low COD/N ratio, which would benefit the competition of K-strategists. However, in both plants, no significant difference was found between *Nitrobacter*–specific 16S rRNA (Nitro 1198f /Nitro 1423r) and the COD/N ratio. Similarly, Phanwilai *et al.* (2020) found high copy numbers of *Nitrospira spp*. in the reactor with a low COD/N ratio (SF1) and low copy numbers of *Nitrospira spp*. in the reactor with a high COD/N ratio (SF2) while *Nitrobacter spp.* showed no difference in both reactors (SF1 and SF2).

The dominance of *Nitrobacter spp.* (r–strategist) over *Nitrospira spp.* (K-strategist) was observed at both WWTP A and WWTP B with high DO concentration and nitrite concentration. Awolusi *et al.* (2015a) and Coppens *et al.* (2016) reported similar results, whereby the dominance of *Nitrobacter spp*. over *Nitrospira spp*. was observed in WWTP after a spike of nitrite concentration and even after subsequent reduction of nitrite concentration was recorded. Phanwilai *et al.* (2020) studied the distribution of the NOB population in a full-scale WWTP by controlling DO concentration and found that *Nitrobacter spp*. was dominant when

DO concentration was high >2 mg/L. Consequently, high DO concentration and nitrite concentration would be a major operating condition that contributed to high *Nitrobacter spp*. in both plants, while *Nitrospira spp*. remained low. These findings suggested that the *Nitrospira spp.* has a competitive advantage over *Nitrobacter spp*. in an oxygen-limited environment. Similarly, Liu and Wang (2013), reported a high amount of *Nitrobacter spp.* when DO concentration was unlimited and nitrite concentration was above 5 mg/L while *Nitrospira spp.* were consistent.

The highest *amo*A copy number was observed in both the plants when the temperatures were high (>25.3 ºC), implying that increasing temperatures benefited AOB growth. Moreover, the *amo*A abundance showed an evident decrease when temperatures dropped to 17.5 ºC (Jun 2020 to Aug 2020) (Figs. 4.6 & 4.8), indicating that the AOB population was inhibited in low temperature and high DO concentration. The AOB communities are considered to be much more environmentally sensitive than the NOB (Wang *et al.*, 2021). The most widely used molecular marker for *nxrB* and *nxrA* detection is *nxr* which encodes nitrite oxidoreductase (NXR) (Pester *et al.*, 2014). Contrary to 16S rRNA quantification, the quantification of *nxrB* copy number was observed to be higher than that of *nxr*A in both plants (Figs. 4.6 & 4.8) operating at relatively high DO concentration while *nxrA* was not negatively impacted by high DO concentration. However, no significant correlation could be established between the *nxrB* and DO concentration, which may be due to the cross-correlational approach used.

Similarly, Zhang *et al.* (2021) reported a much higher *nxrB* copy number encoding *Nitrospira*-like NOB compared with *nxrA* encoding *Nitrobacter*-like NOB detected in the Self Powered Neutron Detector (SPND)-SBR reactor by qPCR. It was noted that a relatively high temperature and nitrite concentration in this study as well as the existence of multiple copies

of the *nxrB* in *Nitrospira* genomes such as COMAMMOX *Nitrospira* could be the contributing factors to the abundance of the *nxrB* in both plants. Daims *et al.* (2016), reported that the *nxr* sequences, derived from the *Nitrospira* NOB, show significant similarity to COMAMMOX *Nitrospira.* According to Lawson and Lücker (2018), all the known COMAMMOX bacteria belong to sublineage II of the genus *Nitrospira*. The phylogenetic analysis showed that the *nxrB* sequences (Fig. 4.3) in this study were related to uncultured *Nitrospira spp*., nitrite oxidoreductase subunit B which has been implicated in complete nitrification (COMAMMOX) (Daims *et al.*, 2015, Wang *et al.*, 2017c). The resulting *nxrB* phylogenetic tree confirms that the *nxrB* cannot be reliably used to distinguish COMAMMOX *Nitropira* from canonical *Nitrospira spp.* Roots *et al.* (2019) found that 15% of the *Nitrospira nxrB* sequences clustered with the *nxrB* in the COMAMMOX genomes.

In terms of functional gene expression, a rapid decrease in expression levels of *amoA* was observed in both plants (Figs. 4.7 & 4.10) while the expression levels of *nxrB* were observed to increase rapidly in both plants (Figs. 4.7 & 4.10), as the temperature increases. The high relative expression of *nxrB* may have been caused by (i) the high abundance of *Nitrospira*-like *nxrB* revealed by qPCR and (ii) the existence of COMAMMOX *Nitrospira* of the *nxrB* in *Nitrospira* genomes. In contrast, expression levels of the *nxrA* were relatively more consistent throughout the study period in both plants. Similarly, Kim *et al.* (2016) reported a rapid decrease in *amoA* expression levels while the expression levels of the *nxrA* were relatively lower and stable throughout the study. With regard to AOB gene, a positive correlation was found between AOB gene expression (*amoA*) and DO concentration in all reactors (reactor 1: $r = 0.49$; reactor 2: $r = 0.78$ and reactor 3: $r = 0.32$; $p = 0.05$) of WWTP A, but no clear correlation was found between NOB gene expression (*nxrA* and *nxrB*) and DO concentration in this plant. However, in WWTP B, a negative correlation was observed between *nxrA*

expression levels and DO concentration (r = - 0.34, p = 0.05) but no clear correlation was observed between *amoA* and *nxrB* expression levels in this plant. Environmental changes such as high DO concentration have been reported to inhibit the AOB activity while they do not have any influence on the NOB activity which may explain the decrease in *amoA* relative expression levels compared with the NOBs in this study as reported by Kim *et al.* (2016). Similarly, Kapoor *et al.* (2016) also reported a low AOB relative gene expression compared to the NOBs while investigating the effect of Cu (II) exposure on gene expression.

4.5 CONCLUSION

Among the 16S rRNA, AOB 16S rRNA (CTO) population represented the dominant bacterial group in WWTP A throughout the study period while *Nitrobacter spp*. was observed to be dominant in WWTP B. For the NOB population, both *Nitrobacter spp*. and *Nitrospira spp*. were found in significant numbers in both plants. Contrary to 16S rRNA, the dominance of the *nxrB* copy number over the *nxr*A copy number was observed in both plants operating at relatively high DO concentrations while *nxrA* was not negatively impacted by high DO concentration. The NOB population was observed to be more expressed than the *amoA* in both plants. The *nxrB* relative expression was high in both plants throughout the study period while the *nxrA* was observed to be constant in all reactors. The phylogenetic analysis of *nxrB* populations in both plants revealed similarities that are closely related to uncultured *Nitrospira spp*., nitrite oxidoreductase subunit B which has been implicated in complete nitrification (COMAMMOX).

CHAPTER 5: GENERAL SUMMARY, CONCLUSIONS, AND RECOMMENDATIONS

5.1 GENERAL SUMMARY AND CONCLUSIONS

In biological nitrogen removal processes, aeration plays a major role in sustaining a fully functional nitrifying population. An optimum dissolved oxygen concentration of (1.8 -2 mg/L) can support good nitrification. However, each nitrifier group has its specific affinity towards oxygen, and therefore a slight change in their level combined with other factors such as temperature, pH, and substrate concentration could hinder their specific function. Fine bubble diffused aeration technology is gaining ground as a preferred method of supplying oxygen in BNR plants, due to its advantages over surface aeration which include improved oxygen mass transfer leading to enhanced microbial performance.

Previous studies have focused mainly on the point of energy consumption and overall process efficiency. However, there have been limited studies conducted thus far to understand the functional microbial profile of the BNR plants operated using diffused aeration technology. The findings of this study, therefore, contribute to the existing literature in several ways; which include, 1) Evaluation of the process performance of diffused aerated full-scale WWTPs operated using two different configurations 2) distribution and dominance of key nitrifying bacteria in diffused aerated WWTPs, and 3) the functional activity of different nitrifying bacteria under varying operational conditions. The major conclusions drawn from this study are listed below.

- Despite the seasonal variations, both the studied plants (WWTP A and WWTP B), recorded high DO concentrations (≥3 mg/L) in all the reactors which are above the typical threshold level (1-2 mg/L) in conventional surface-aerated systems.
- A significant variation in COD removal was observed across the sampling period in both plants. It ranged from 75.09 - 94.95% at WWTP A, and 62.10 – 96.42% at WWTP B, however, no significant correlation was observed between DO concentration and COD removal.
- High and efficient ammonia removal was noticed in both the plants with an average of 95±5.6% in WWTP A and 98.02% in WWTP B. Ammonia removal showed a positive correlation with DO concentration at WWTP A while at WWTP B, no significant correlation was found between DO and ammonia removal.
- A decrease in DO concentration (≤3 mg/L) combined with an increase in temperature (≥22°C) led to an increase in nitrite accumulation in the effluent, demonstrating that the nitrite oxidation process is more sensitive to the change in DO concentration and temperature shifts.
- The microscopic analysis of the floc structure indicated the formation of good and compact flocs during most of the study period with occasional filamentous branching. The proliferation of filamentous bacteria in the flocs was also correlated with foaming incidents in WWTP A as well as an increase in MLSS and MLVSS concentration. However, this did not cause serious settling problems in the selected plants as indicated by lower SVI values (≤150mL/g) throughout the study period. However, no significant correlation was established between the DO concentration and SVI in this study suggesting that the DO level was within the optimum range and supported a well-balanced functional microbial community.

- Based on qPCR results, the AOB 16S rRNA gene abundance was high in all the three reactors in WWTP A compared to the NOB, while in WWTP B, the average 16S rRNA gene copies for NOB was higher than AOB, despite having similar DO concentrations. This difference in microbial dominance could therefore be a result of the difference in the process configuration of the two plants investigated. In relation to DO, a negative correlation was observed between AOB16S rRNA gene copies and DO concentration in reactor 1 ($r = -0.40$), while a positive correlation in reactor 3 ($r = 0.47$). However, no clear correlation was observed in reactor 2 as well as in WWTP B, indicating that DO was within the optimum for AOB growth.
- Among the NOBs, *Nitrobacter spp*. dominated in both the plants, however, no clear correlation was observed between the observed DO concentration and the *Nitrobacter spp* gene copies. However, there was a trend toward a higher population of *Nitrobacter spp*. at a higher DO concentration and nitrite concentration in both the plants. The *Nitrospira spp.* however, remained low in both the plants throughout the study period based on 16S rRNA gene copies despite the change in operational conditions.
- Using functional gene based primers, a positive correlation was found between AOB gene copies (amoA) and DO concentration in all reactors (reactor 1: $r = 0.49$; reactor 2: $r = 0.78$ and reactor 3: $r = 0.32$; $p = 0.05$) in WWTP A. In contrast, there was no clear correlation between amoA gene copies and the DO levels in WWTPB. In addition, the highest *amo*A gene copy numbers were observed when the temperature was high, implying that increasing temperatures benefited AOB growth in both plants. While for NOB, the *nxrB* (the functional and phylogenetic marker for *Nitrospira*) copy number was observed to be higher than that of *nxrA* (the functional and phylogenetic marker for *Nitrobacter*) in both plants. No significant correlation was observed between *nxrA* gene copies and DO level in WWTP A. However, in WWTP B, a negative correlation

was observed between *nxrA* gene copies levels and DO concentration (r = - 0.34, p = 0.05). However, no clear correlation was observed between *nxrB* gene copy number and DO levels.

- In terms of functional gene expression, a positive correlation was found between AOB gene expression (amoA) and DO concentration in all reactors (reactor 1: r = 0.49; reactor 2: r = 0.78 and reactor 3: r = 0.32; p = 0.05) at WWTP A, however, no clear correlation was found between NOB gene expression (*nxrA* and *nxrB*) and DO concentration. In WWTPB, a negative correlation was observed between *nxrA* gene expression levels and DO concentration (r = - 0.34, p = 0.05) however, no clear correlation was observed between amoA and nxrB gene expression levels.
- In addition, in contrast to the 16SrRNA gene copies an increase in the relative expression of *nxrB* was noticed in both the plants while the expression levels of the *nxrA* gene (*Nitrobacter spp*) were relatively more consistent throughout the study period in both plants.
- An increase in the relative expression of *nxrB* in these plants may be due to the high abundance of *Nitrospira*-like *nxrB* as revealed by qPCR and the existence of COMAMMOX *Nitrospira* of the *nxrB* in *Nitrospira* genomes. The phylogenetic analysis of *the nxrB* PCR product further confirmed close similarity with the uncultured *Nitrospira spp*., nitrite oxidoreductase subunit B, which was implicated in complete nitrification (COMAMMOX).
- In summary, the observations from this study, therefore, indicate that the observed DO concentration (≥3 mg/L) was well within the optimum range required for nitrification. When combined with other factors such as process configuration, temperature shifts, and substrate concentrations, it resulted in suppressing or in the dominance and activity of a specific group within the nitrifying bacteria. However, it did not significantly affect

the overall nitrification removal process due to the existence of a well-balanced nitrifying bacterial population. The study also confirmed the existence of a diverse group of nitrifying bacteria including the recently discovered COMAMMOX demonstrating that both the plants investigated in this study provided a conducive environment for the development of well-balanced nitrifying bacteria which are key for the overall nitrogen removal.

5.2 RECOMMENDATIONS

- There is a need for more research effort towards using next-generation sequencing or OMICS approach to identify the diverse and novel nitrifying bacterial population and their metabolic traits which are unattainable using conventional molecular techniques.
- Future work on nitrification dynamics in diffused aerated WWTP should emphasize correlating the plant operational and environmental condition to microbial community structure using a nonlinear modelling approach. This would help plant operators to make informed decisions.

REFERENCES

Aalto, S. L., Saarenheimo, J., Mikkonen, A., Rissanen, A. J. & Tiirola, M. 2018. Resistant ammonia-oxidizing archaea endure, but adapting ammonia-oxidizing bacteria thrive in boreal lake sediments receiving nutrient-rich effluents. *Environmental Microbiology,* **20,** 3616-3628.

Abdollahbeigi, M. & Asgari Bajgirani, M. 2020. Investigation of Nitrogen Removal in Municipal Wastewater Treatment Plants. *Journal of Chemical Reviews,* **2,** 257-273.

Adonadaga, M.-G. 2015. Effect of dissolved oxygen concentration on morphology and settleability of activated sludge flocs. *Journal of Applied & Environmental Microbiology,* **3,** 31-37.

Ahmad, H. A., Ni, S.-Q., Ahmad, S., Zhang, J., Ali, M., Ngo, H. H., Guo, W., Tan, Z. & Wang, Q. 2020. Gel immobilization: a strategy to improve the performance of anaerobic ammonium oxidation (anammox) bacteria for nitrogen-rich wastewater treatment. *Bioresource Technology,* **313,** 123642.

Al-Ahmady, K. K. 2006. Analysis of oxygen transfer performance on sub-surface aeration systems. *International Journal of Environmental Research and Public Health,* **3,** 301-308.

Åmand, L., Olsson, G. & Carlsson, B. 2013. Aeration control–a review. *Water Science and Technology,* **67,** 2374-2398.

Amoo, A. E. & Babalola, O. O. 2017. Ammonia-oxidizing microorganisms: key players in the promotion of plant growth. *Journal of Soil science and Plant Nutrition,* **17,** 935-947.

Annavajhala, M. K., Kapoor, V., Santo-Domingo, J. & Chandran, K. 2018. Comammox functionality is identified in diverse engineered biological wastewater treatment systems. *Environmental Science & Technology Letters,* **5,** 110-116.

Apha 2012. Standard methods for the examination of water and wastewater, 22nd edition edited by E. W. Rice, R. B. Baird, A. D. Eaton, and L. S. Clesceri. American Public Health Association (APHA), Washington, D.C., USA. *American Water Works Association (AWWA) and Water Environment Federation (WEF).*

Apha, A. 1998. Standard methods for the examination of water and wastewater. American Public Health Association. *Incorporated, Washington, DC.*

Asensi, E., Alemany, E., Duque-Sarango, P. & Aguado, D. 2019a. Assessment and modelling of the effect of precipitated ferric chloride addition on the activated sludge settling properties. *Chemical Engineering Research and Design,* **150,** 14-25.

Asensi, E., Alemany, E., Seco, A. & Ferrer, J. 2019b. Characterization of activated sludge settling properties with a sludge collapse-acceleration stage. *Separation and Purification Technology,* **209,** 32-41.

Avrahami, S., Jia, Z., Neufeld, J. D., Murrell, J. C., Conrad, R. & Küsel, K. 2011. Active autotrophic ammonia-oxidizing bacteria in biofilm enrichments from simulated creek ecosystems at two ammonium concentrations respond to temperature manipulation. *Applied Environmental Microbiology,* **77,** 7329-7338.

Awolusi, O., Kumari, S. & Bux, F. 2015a. Ecophysiology of nitrifying communities in membrane bioreactors. *International Journal of Environmental Science and Technology,* **12,** 747-762.

Awolusi, O., Nasr, M., Kumari, S. & Bux, F. 2018. Principal component analysis for the interaction of nitrifiers and wastewater environments at a full-scale activated sludge plant. *International Journal of Environmental Science and Technology,* **15,** 1477-1490.

Awolusi, O. O., Enitan, A. M., Kumari, S. & Bux, F. 2015b. Nitrification efficiency and community structure of municipal activated sewage sludge. *World Academy of Science, Engineering, and Technology, International Journal of Environmental, Chemical, Ecological, Geological and Geophysical Engineering,* **9,** 970-977.

Awolusi, O. O., Enitan, A. M., Kumari, S. & Bux, F. 2015c. Nitrification efficiency and community structure of municipal activated sewage sludge. *International Journal of Environmental, Chemical, Ecological, Geological and Geophysical Engineering,* **9,** 996-1003.

Bae, H., Chung, Y.-C., Yang, H., Lee, C., Aryapratama, R., Yoo, Y. J. & Lee, S. 2015. Assessment of bacterial community structure in nitrifying biofilm under inorganic carbon-sufficient and-limited conditions. *Journal of Environmental Science and Health, Part A,* **50,** 201-212.

Baek, S. H. & Kim, H. J. 2013. A mathematical model for simultaneous nitrification and denitrification (SND) in membrane bioreactor (MBR) under Low Dissolved Oxygen (DO) concentrations. *Biotechnology and Bioprocess Engineering,* **18,** 104-110.

Bani, A., Parati, K., Pozzi, A., Previtali, C., Bongioni, G., Pizzera, A., Ficara, E. & Bellucci, M. 2020. Comparison of the performance and microbial community structure of two outdoor pilot-scale photobioreactors treating digestate. *Microorganisms,* **8,** 1754.

Barnard, J. L., Dunlap, P. & Steichen, M. 2017. Rethinking the mechanisms of biological phosphorus removal: Barnard et al. *Water Environment Research,* **89,** 2043-2054.

Bartelme, R. P., Mclellan, S. L. & Newton, R. J. 2017. Freshwater recirculating aquaculture system operations drive biofilter bacterial community shifts around a stable nitrifying consortium of ammonia-oxidizing archaea and comammox Nitrospira. *Frontiers in Microbiology,* **8,** 101.

Bassin, J., Kleerebezem, R., Rosado, A., Van Loosdrecht, M. M. & Dezotti, M. 2012. Effect of different operational conditions on biofilm development, nitrification, and nitrifying microbial population in moving-bed biofilm reactors. *Environmental Science & Technology,* **46,** 1546-1555.

Behnisch, J., Ganzauge, A., Sander, S., Herrling, M. & Wagner, M. 2018. Improving aeration systems in saline water: measurement of local bubble size and volumetric mass transfer coefficient of conventional membrane diffusers. *Water Science and Technology,* **78,** 860-867.

Biechele, P., Busse, C., Solle, D., Scheper, T. & Reardon, K. 2015. Sensor systems for bioprocess monitoring. *Engineering in Life Sciences,* **15,** 469-488.

Bo, W. & Xin, W. 2012. Microbiological Diversity of the Biofilm Growth in Wastewater Treatment Ponds. *Fresenius Environmental Bulletin,* **21,** 2027-2037.

Braker, G., Zhou, J., Wu, L., Devol, A. H. & Tiedje, J. M. 2000. Nitrite reductase genes (nirK and nirS) as functional markers to investigate the diversity of denitrifying bacteria in Pacific Northwest marine sediment communities. *Applied and Environmental Microbiology,* **66,** 2096-2104.

Brotto, A. C. 2016. Microbial Structure and Function of Engineered Biological Nitrogen Transformation Processes: Impacts of Aeration and Organic Carbon on Process Performance and Emissions of Nitrogenous Greenhouse Gas, *Columbia University*.

Campbell, K., Wang, J. & Daniels, M. 2019. Assessing activated sludge morphology and oxygen transfer performance using image analysis. *Chemosphere,* **223,** 694-703.

Campbell, K., Wang, J., Tucker, R. & Struemph, C. 2021. Implementation of long solids retention time activated sludge process for the rural residential community. *Water Environment Research,* **93,** 174-185.

Cao, Y., Van Loosdrecht, M. & Daigger, G. 2020. The bottlenecks and causes, and potential solutions for municipal sewage treatment in China. *Water Practice and Technology,* **15,** 160-169.

Carvajal-Arroyo, J. M., Puyol, D., Li, G., Swartwout, A., Sierra-Álvarez, R. & Field, J. A. 2014. Starved anammox cells are less resistant to NO2− inhibition. *Water Research,* **65,** 170-176.

Chao, Y., Mao, Y., Yu, K. & Zhang, T. 2016. Novel nitrifiers and comammox in a full-scale hybrid biofilm and activated sludge reactor were revealed by a metagenomic approach. *Applied Microbiology and Biotechnology,* **100,** 8225-8237.

Cho, K. H., Kim, J.-O., Kang, S., Park, H., Kim, S. & Kim, Y. M. 2014. Achieving enhanced nitrification in communities of nitrifying bacteria in full-scale wastewater treatment plants via optimal temperature and pH. *Separation and Purification Technology,* **132,** 697-703.

Collings, E. J., Bunce, J. T., Jong, M.-C. & Graham, D. W. 2020. Impact of cold temperatures on nitrogen removal in denitrifying down-flow hanging sponge (DDHS) reactors. *Water,* **12,** 2029.

Coppens, J., Lindeboom, R., Muys, M., Coessens, W., Alloul, A., Meerbergen, K., Lievens, B., Clauwaert, P., Boon, N. & Vlaeminck, S. E. 2016. Nitrification and microalgae cultivation for two-stage biological nutrient valorization from source-separated urine. *Bioresource Technology*, **211,** 41-50.

Cydzik-Kwiatkowska, A. & Zielińska, M. 2016. Bacterial communities in full-scale wastewater treatment systems. *World Journal of Microbiology and Biotechnology,* **32,** 1-8.

Daims, H., Lebedeva, E. V., Pjevac, P., Han, P., Herbold, C., Albertsen, M., Jehmlich, N., Palatinszky, M., Vierheilig, J. & Bulaev, A. 2015. Complete nitrification by Nitrospira bacteria. *Nature,* **528,** 504.

Daims, H., Lücker, S. & Wagner, M. 2016. A new perspective on microbes formerly known as nitrite-oxidizing bacteria. *Trends in Microbiology,* **24,** 699-712.

Dan, N. H., Phe, T. T. M., Thanh, B. X., Hoinkis, J. & Le Luu, T. 2021. The application of intermittent cycle extended aeration systems (ICEAS) in wastewater treatment. *Journal of Water Process Engineering,* **40,** 101909.

De Lille, M. V., Berkhout, V., Fröba, L., Groß, F. & Delgado, A. 2015. Ammonium estimation in an ANAMMOX SBR treating anaerobically digested domestic wastewater. *Chemical Engineering Science,* **130,** 109-119.

De Temmerman, L., Maere, T., Temmink, H., Zwijnenburg, A. & Nopens, I. 2015. The effect of fine bubble aeration intensity on membrane bioreactor sludge characteristics and fouling. *Water Research,* **76,** 99-109.

De Vrieze, J., Pinto, A. J., Sloan, W. T. & Ijaz, U. Z. 2018. The active microbial community more accurately reflects the anaerobic digestion process: 16S rRNA (gene) sequencing as a predictive tool. *Microbiome,* **6,** 1-13.

Drewnowski, J., Remiszewska-Skwarek, A., Duda, S. & Łagód, G. 2019. Aeration process in bioreactors as the main energy consumer in a wastewater treatment plant. Review of solutions and methods of process optimization. *Processes,* **7,** 311.

Du, C., Cui, C.-W., Qiu, S., Shi, S.-N., Li, A. & Ma, F. 2017. Nitrogen removal and microbial community shift in an aerobic denitrification reactor bioaugmented with a Pseudomonas strain for coal-based ethylene glycol industry wastewater treatment. *Environmental Science and Pollution Research,* **24,** 11435-11445.

Duan, H., Ye, L., Wang, Q., Zheng, M., Lu, X., Wang, Z. & Yuan, Z. 2019. Nitrite oxidizing bacteria (NOB) contained in influent deteriorate mainstream NOB suppression by sidestream inactivation. *Water Research,* **162,** 331-338.

Duan, L., Song, Y., Xia, S. & Hermanowicz, S. W. 2013. Characterization of nitrifying microbial community in a submerged membrane bioreactor at short solids retention times. *Bioresource Technology,* **149,** 200-207.

Eikelboom, D. H. 2000. Process control of activated sludge plants by microscopic investigation, *International Water Association (IWA) publishing*.

Ferrera, I. & Sanchez, O. 2016. Insights into microbial diversity in wastewater treatment systems: How far have we come? *Biotechnology Advances,* **34,** 790-802.

Fowler, S. J., Palomo, A., Dechesne, A., Mines, P. D. & Smets, B. F. 2018. Comammox Nitrospira is abundant ammonia oxidizers in diverse groundwater-fed rapid sand filter communities. *Environmental Microbiology,* **20,** 1002-1015.

Fukushima, T. & Bond, P. L. 2010. Polymerase chain reaction (PCR) technology.

Gao, J.-F., Luo, X., Wu, G.-X., Li, T. & Peng, Y.-Z. 2013. Quantitative analyses of the composition and abundance of ammonia-oxidizing archaea and ammonia-oxidizing bacteria in eight full-scale biological wastewater treatment plants. *Bioresource Technology,* **138,** 285-296.

Ge, S.-J., Peng, Y.-Z., Cao, X., Wang, S.-Y. & Yang, A.-M. 2011. Optimization of a modified UCT step feed process treating municipal wastewater. *Huan Jing ke Xue= Huanjing Kexue,* **32,** 2006-2012.

Ge, S., Wang, S., Yang, X., Qiu, S., Li, B. & Peng, Y. 2015. Detection of nitrifiers and evaluation of partial nitrification for wastewater treatment: a review. *Chemosphere,* **140,** 85-98.

Geng, M., You, S., Guo, H., Ma, F., Xiao, X. & Zhang, J. 2021. Impact of fungal pellets dosage on the long-term stability of aerobic granular sludge. *Bioresource Technology,* **332,** 125106.

Giokas, D. L., Daigger, G. T., Von Sperling, M., Kim, Y. & Paraskevas, P. A. 2003. Comparison and evaluation of empirical zone settling velocity parameters based on sludge volume index using a unified settling characteristics database. *Water Research,* **37,** 3821-3836.

Graham, D. W., Knapp, C. W., Van Vleck, E. S., Bloor, K., Lane, T. B. & Graham, C. E. 2007. Experimental demonstration of chaotic instability in biological nitrification. *The International Society for Microbial Ecology (ISME) Journal,* **1,** 385.

Guillén, J. a. S. 2017. Autotrophic Nitrogen Removal from Low Concentrated Effluents: Study of system configurations and operational features for post-treatment of anaerobic effluents, *Chemical Rubber Company (CRC) Press*.

Guo, J., Peng, Y., Wang, S., Yang, X., Wang, Z. & Zhu, A. 2012. Stable limited filamentous bulking through keeping the competition between floc-formers and filaments in balance. *Bioresource Technology,* **103,** 7-15.

Han, N., Zhang, J., Hoang, M., Gray, S. & Xie, Z. 2021. A review of the process and wastewater reuse in the recycled paper industry. *Environmental Technology & Innovation,* **24,** 101860.

Hasan, H. A., Abdullah, S. R. S., Kamarudin, S. K., Kofli, N. T. & Anuar, N. 2013. Simultaneous NH4+-N and Mn2+ removal from drinking water using a biological aerated filter system: Effects of different aeration rates. *Separation and Purification Technology,* **118,** 547-556.

He, W., Xue, L., Gorczyca, B., Nan, J. & Shi, Z. 2018. Experimental and CFD studies of floc growth dependence on baffle width in square stirred-tank reactors for flocculation. *Separation and Purification Technology,* **190,** 228-242.

Hermansson, A. & Lindgren, P.-E. 2001. Quantification of ammonia-oxidizing bacteria in arable soil by real-time PCR. *Applied Environmental Microbiology,* **67,** 972-976.

Holmes, D. E., Dang, Y. & Smith, J. A. 2019. Nitrogen cycling during wastewater treatment. *Advances in Applied Microbiology,* **106,** 113-192.

How, S. W., Lim, S., Lim, P., Aris, A., Ngoh, G. C., Curtis, T. P. & Chua, A. S. M. 2018. Low-dissolved-oxygen nitrification in tropical sewage: an investigation on potential, performance and functional microbial community. *Water Science and Technology,* **77,** 2274-2283.

How, S. W., Shoji, T., Tan, C. K., Curtis, T. P. & Chua, A. S. M. 2021. Kinetic characterization of a low-dissolved-oxygen oxic-anoxic process treating low COD/N tropical wastewater revealed a selection of nitrifiers with high substrate affinity. *Journal of Water Process Engineering,* **43,** 102235.

Hu, B., Wang, T., Ye, J., Zhao, J., Yang, L., Wu, P., Duan, J. & Ye, G. 2019. Effects of carbon sources and operation modes on the performances of aerobic denitrification process and its microbial community shifts. *Journal of Environmental Management,* **239,** 299-305.

Huang, W., Liu, D., Huang, W., Cai, W., Zhang, Z. & Lei, Z. 2020. Achieving partial nitrification and high lipid production in an algal-bacterial granule system when treating low COD/NH4–N wastewater. *Chemosphere,* **248,** 126106.

Jenkins, D., Richard, M. G. & Daigger, G. T. 1993. Manual on the causes and control of activated sludge bulking and foaming. 2. *edited. Lewis*.

Jiang, C., Xu, S., Wang, R., Zhou, S., Wu, S., Zeng, X., Bai, Z., Zhuang, G. & Zhuang, X. 2018. Comprehensive assessment of free nitrous acid-based technology to establish partial nitrification. *Environmental Science: Water Research & Technology,* **4,** 2113-2124.

Jin, T., Zhang, T., Ye, L., Lee, O. O., Wong, Y. H. & Qian, P. Y. 2011. Diversity and quantity of ammonia-oxidizing Archaea and Bacteria in the sediment of the Pearl River Estuary, China. *Applied Microbiology and Biotechnology,* **90,** 1137-1145.

Johnston, J., Lapara, T. & Behrens, S. 2019. Composition and dynamics of the activated sludge microbiome during seasonal nitrification failure. *Scientific Reports,* **9,** 1-15.

Kapoor, V., Li, X., Chandran, K., Impellitteri, C. A. & Domingo, J. W. S. 2016. Use of functional gene expression and respirometry to study wastewater nitrification activity after exposure to low doses of copper. *Environmental Science and Pollution Research,* **23,** 6443-6450.

Kartal, B., Van Niftrik, L., Keltjens, J. T., Den Camp, H. J. O. & Jetten, M. S. 2012. Anammox—growth physiology, cell biology, and metabolism. *Advances in Microbial Physiology,* **60,** 211-262.

Kayee, P., Sonthiphand, P., Rongsayamanont, C. & Limpiyakorn, T. 2016. Archaeal" amoA" Genes Outnumber Bacterial" amoA" Genes in Municipal Wastewater Treatment Plants in Bangkok. *Microbial Ecology,* **72,** 262-262.

Kent, T. R., Sun, Y., An, Z., Bott, C. B. & Wang, Z.-W. 2019. Mechanistic understanding of the NOB suppression by free ammonia inhibition in continuous flow aerobic granulation bioreactors. *Environment International,* **131,** 105005.

Khatri, N., Khatri, K. K. & Sharma, A. 2020. Enhanced energy saving in wastewater treatment plant using dissolved oxygen control and hydrocyclone. *Environmental Technology & Innovation,* **18,** 100678.

Kim, J., Lim, J. & Lee, C. 2013. Quantitative real-time PCR approaches for microbial community studies in wastewater treatment systems: applications and considerations. *Biotechnology Advances,* **31,** 1358-1373.

Kim, Y. M., Park, H. & Chandran, K. 2016. Nitrification inhibition by hexavalent chromium Cr (VI)–Microbial ecology, gene expression, and off-gas emissions. *Water Research,* **92,** 254-261.

Koch, H., Van Kessel, M. A. & Lücker, S. 2019. Complete nitrification: insights into the ecophysiology of comammox Nitrospira. *Applied Microbiology and Biotechnology,* **103,** 177-189.

Kulkarni, P. 2012. Isolation, identification, and removal of the filamentous organism from SND-based SBR degrading nitrophenols. *Biodegradation,* **23,** 455-463.

Kumar, M., Shrivastava, N., Teotia, P., Goyal, P., Varma, A., Sharma, S., Tuteja, N. & Kumar, V. 2017. Omics: Tools for assessing environmental microbial diversity and composition. Modern Tools and Techniques to Understand Microbes. *Springer.*

Kumwimba, M. N. & Meng, F. 2019. Roles of ammonia-oxidizing bacteria in improving metabolism and cometabolism of trace organic chemicals in biological wastewater treatment processes: a review. *Science of the Total Environment,* **659,** 419-441.

Lares, M., Ncibi, M. C., Sillanpää, M. & Sillanpää, M. 2018. Occurrence, identification, and removal of microplastic particles and fibers in conventional activated sludge process and advanced MBR technology. *Water Research,* **133,** 236-246.

Lawson, C. E. & Lücker, S. 2018. Complete ammonia oxidation: an important control on nitrification in engineered ecosystems? *Current opinion in biotechnology,* **50,** 158-165.

Li, B. & Wu, G. 2014. Effects of sludge retention times on nutrient removal and nitrous oxide emission in biological nutrient removal processes. *International Journal of Environmental Research and Public Health,* **11,** 3553-3569.

Li, H., Zhang, Y., Yang, M. & Kamagata, Y. 2013. Effects of hydraulic retention time on nitrification activities and population dynamics of a conventional activated sludge system. *Frontiers of Environmental Science & Engineering,* **7,** 43-48.

Li, X., Zhang, M., Liu, F., Chen, L., Li, Y., Li, Y., Xiao, R. & Wu, J. 2018. Seasonality distribution of the abundance and activity of nitrification and denitrification microorganisms in sediments of surface flow constructed wetlands planted with Myriophyllum elatinoides during swine wastewater treatment. *Bioresource Technology,* **248,** 89-97.

Li, Z.-H., Guo, Y., Hang, Z.-Y., Zhang, T.-Y. & Yu, H.-Q. 2020. Simultaneous evaluation of bioactivity and settleability of activated sludge using fractal dimension as an intermediate variable. *Water Research,* **178,** 115834.

Liai, C., Hongxun, H., Weibiao, F. & Eryan, Z. Comparative Research to Surface Aeration and Blasting Aeration System Based on LCC Theory. IOP Conference Series: Earth and Environmental Science, 2017. *Institute of Physics (IOP) Publishing*, 012029.

Liu, G. 2012. Nitrification performance of activated sludge under low dissolved oxygen conditions, *Missouri University of Science and Technology*.

Liu, G. & Wang, J. 2013. Long-term low DO enriches and shifts the nitrifier community into activated sludge. *Environmental Science & Technology,* **47,** 5109-5117.

Liu, G. & Wang, J. 2017. Enhanced removal of total nitrogen and total phosphorus by applying intermittent aeration to the Modified Ludzack-Ettinger (MLE) process. *Journal of Cleaner Production,* **166,** 163-171.

Liu, T., Ma, B., Chen, X., Ni, B.-J., Peng, Y. & Guo, J. 2017. Evaluation of mainstream nitrogen removal by simultaneous partial nitrification, anammox, and denitrification (SNAD) process in a granule-based reactor. *Chemical Engineering Journal,* **327,** 973-981.

Liu, Y., Ngo, H. H., Guo, W., Peng, L., Wang, D. & Ni, B. 2019. The roles of free ammonia (FA) in biological wastewater treatment processes: A review. *Environment International*, **123,** 10-19.

Lukumbuzya, M., Kristensen, J. M., Kitzinger, K., Pommerening-Röser, A., Nielsen, P. H., Wagner, M., Daims, H. & Pjevac, P. 2020. A refined set of rRNA-targeted oligonucleotide probes for in situ detection and quantification of ammonia-oxidizing bacteria. *Water Research*, **186,** 116372.

Ma, B., Qian, W., Yuan, C., Yuan, Z. & Peng, Y. 2017a. Achieving mainstream nitrogen removal through coupling anammox with denitratation. *Environmental Science & Technology*, **51,** 8405-8413.

Ma, Y., Domingo-Felez, C., Plósz, B. G. & Smets, B. F. 2017b. Intermittent aeration suppresses nitrite-oxidizing bacteria in membrane-aerated biofilms: a model-based explanation. *Environmental Science & Technology*, **51,** 6146-6155.

Mbakwe, I., De Jager, P. C., Annandale, J. G. & Matema, T. 2013. Nitrogen mineralization from sludge in an alkaline, saline coal gasification ash environment.

Metcalf, Eddy, Abu-Orf, M., Bowden, G., Burton, F. L., Pfrang, W., Stensel, H. D., Tchobanoglous, G., Tsuchihashi, R. & Aecom 2014. *Wastewater Engineering: Treatment and Resource Recovery*, McGraw Hill Education.

Metch, J. W., Burrows, N. D., Murphy, C. J., Pruden, A. & Vikesland, P. J. 2018. Metagenomic analysis of microbial communities yields insight into the impacts of nanoparticle design. *Nature Nanotechnology*, **13,** 253-259.

Mohammed, R., Abu-Alhail, S. & Xi-Wu, L. 2014. Long-term operation of a novel pilot-scale six tanks alternately operating activated sludge process in treating domestic wastewater. *Environmental Technology*, **35,** 1874-1885.

Mulder, A., Van De Graaf, A. A., Robertson, L. & Kuenen, J. 1995. Anaerobic ammonium oxidation was discovered in a denitrifying fluidized bed reactor. *Federation of European Microbiological Societies* (*FEMS) Microbiology Ecology,* **16,** 177-183.

Nethaji, M., Ahilan, B., Ravaneswaran, K., Tamilarasu, A., Mahadevi, N. & Somu Sunder Lingam, R. 2021. Biofloc: Floc Types and Their Importance in Aquaculture. *Biotica Research Today,* **3,** 581-583.

Ngugi, D. K., Blom, J., Stepanauskas, R. & Stingl, U. 2016. Diversification and niche adaptations of Nitrospina-like bacteria in the polyextreme interfaces of Red Sea brines. *The International Society for Microbial Ecology (ISME) Journal,* **10,** 1383-1399.

Nowka, B., Off, S., Daims, H. & Spieck, E. 2015. Improved isolation strategies allowed the phenotypic differentiation of two Nitrospira strains from widespread phylogenetic lineages. *Federation of European Microbiological Societies* (*FEMS) Microbiology Ecology,* **91,** fiu031.

Odize, V. O. 2018. Diffuser fouling mitigation, wastewater characteristics, and treatment technology impact aeration efficiency. *Virginia Tech.*

Palomo, A., Jane Fowler, S., Gülay, A., Rasmussen, S., Sicheritz-Ponten, T. & Smets, B. F. 2016. Metagenomic analysis of rapid gravity sand filter microbial communities suggests novel physiology of Nitrospira *spp*. *The International Society for Microbial Ecology (ISME) Journal,* **10,** 2569-2581.

Pan, K.-L., Gao, J.-F., Fan, X.-Y., Li, D.-C. & Dai, H.-H. 2018. The more important role of archaea than bacteria in nitrification of wastewater treatment plants in a cold season despite their numerical relationships. *Water Research,* **145,** 552-561.

Pechaud, Y., Pageot, S., Goubet, A., Quintero, C. D., Gillot, S. & Fayolle, Y. 2021. Size of biological flocs in activated sludge systems: Influence of hydrodynamic parameters at different scales. *Journal of Environmental Chemical Engineering,* **9,** 105427.

Pelaz, L., Gómez, A., Letona, A., Garralón, G. & Fdz-Polanco, M. 2018. Nitrogen removal in domestic wastewater. Effect of nitrate recycling and COD/N ratio. *Chemosphere,* **212,** 8-14.

Pester, M., Maixner, F., Berry, D., Rattei, T., Koch, H., Lücker, S., Nowka, B., Richter, A., Spieck, E. & Lebedeva, E. 2014. NxrB encoding the beta subunit of nitrite oxidoreductase as a functional and phylogenetic marker for nitrite-oxidizing Nitrospira. *Environmental Microbiology,* **16,** 3055-3071.

Phanwilai, S., Noophan, P., Li, C.-W. & Choo, K.-H. 2020. Effect of COD: N ratio on biological nitrogen removal using full-scale step-feed in municipal wastewater treatment plants. *Sustainable Environment Research,* **30,** 1-9.

Philippot, L., Piutti, S., Martin-Laurent, F., Hallet, S. & Germon, J. C. 2002. Molecular analysis of the nitrate-reducing community from unplanted and maize-planted soils. *Applied and Environmental Microbiology,* **68,** 6121-6128.

Pigue, M. K. 2013. Changes in Dissolved Oxygen, Ammonia, and Nitrate Levels in an Extended Aeration Wastewater Treatment Facility When Converting From Counter Current to Disc Diffuser Aeration. *A Research paper was presented for the Master of Science in Agriculture and Natural Resources Degree. The University of Tennessee at Martin*.

Pinto, A. J., Marcus, D. N., Ijaz, U. Z., Bautista-De Lose Santos, Q. M., Dick, G. J. & Raskin, L. 2016. Metagenomic evidence for the presence of comammox Nitrospira-like bacteria in a drinking water system. *Msphere,* **1,** e00054-15.

Pittoors, E., Guo, Y. & Wh Van Hulle, S. 2014. Modeling dissolved oxygen concentration for optimizing aeration systems and reducing oxygen consumption in activated sludge processes: a review. *Chemical Engineering Communications,* **201,** 983-1002.

Pjevac, P., Schauberger, C., Poghosyan, L., Herbold, C. W., Van Kessel, M. A., Daebeler, A., Steinberger, M., Jetten, M. S., Lücker, S. & Wagner, M. 2017. AmoA-targeted polymerase chain reaction primers for the specific detection and quantification of comammox Nitrospira in the environment. *Frontiers in Microbiology,* **8,** 1508.

Poly, F., Wertz, S., Brothier, E. & Degrange, V. 2008. First exploration of Nitrobacter diversity in soils by a PCR cloning-sequencing approach targeting functional gene nxrA. *Federation of European Microbiological Societies* (*FEMS) microbiology ecology,* **63,** 132-140.

Puyol, D., Carvajal-Arroyo, J., Sierra-Alvarez, R. & Field, J. A. 2014. Nitrite (not free nitrous acid) is the main inhibitor of the anammox process at common pH conditions. *Biotechnology Letters,* **36,** 547-551.

Qian, W., Peng, Y., Li, X., Zhang, Q. & Ma, B. 2017. The inhibitory effects of free ammonia on ammonia-oxidizing bacteria and nitrite-oxidizing bacteria under anaerobic conditions. *Bioresource Technology,* **243,** 1247-1250.

Qin, N. 2018. Influence of C/N Ratios on Nitrification Performance in Membrane Aerated Biofilm Reactors.

Qiu, S., Li, Z., Hu, Y., Shi, L., Liu, R., Shi, L., Chen, L. & Zhan, X. 2021. What's the best way to achieve successful mainstream partial nitritation-anammox application? *Critical Reviews in Environmental Science and Technology,* **51,** 1045-1077.

Rakocy, J., Masser, M. P. & Losordo, T. 2016. Recirculating aquaculture tank production systems: aquaponics-integrating fish and plant culture.

Ramdhani, N. 2013. Detection and quantification of nitrifying bacteria from South African biological nutrient removal plants.

Reboleiro-Rivas, P., Martín-Pascual, J., Juárez-Jiménez, B., Poyatos, J., Vílchez-Vargas, R., Vlaeminck, S., Rodelas, B. & González-López, J. 2015. Nitrogen removal in a

moving bed membrane bioreactor for municipal sewage treatment: Community differentiation in attached biofilm and suspended biomass. *Chemical Engineering Journal,* **277,** 209-218.

Roman, M.-D. & Mureşan, M.-V. 2014. Analysis of oxygen requirements and transfer efficiency in a wastewater treatment plant. *International Journal of Latest Research in Science and Technology,* **3,** 30-33.

Ronan, E., Aqeel, H., Wolfaardt, G. M. & Liss, S. N. 2021. Recent advancements in the biological treatment of high-strength ammonia wastewater. *World Journal of Microbiology and Biotechnology,* **37,** 1-17.

Roots, P., Wang, Y., Rosenthal, A. F., Griffin, J. S., Sabba, F., Petrovich, M., Yang, F., Kozak, J. A., Zhang, H. & Wells, G. F. 2019. Comammox Nitrospira are the dominant ammonia oxidizers in a mainstream low dissolved oxygen nitrification reactor. *Water Research,* **157,** 396-405.

Rosso, D., Stenstrom, M. K. & Garrido-Baserba, M. 2020. Aeration and mixing.

Sanz, J. L. & Köchling, T. 2019. Next-generation sequencing and waste/wastewater treatment: a comprehensive overview. *Reviews in Environmental Science and Bio/Technology,* **18,** 635-680.

Shao, Y., Tao, X., Fan, H., Zhou, X.-H., Wang, H., Liu, G.-H., Xu, X. & Zhang, J. 2021. Determination of critical dissolved oxygen for effective mass transfer of activated sludge flocs based on microelectrode detection technology. *International Journal of Environmental Science and Technology***,** 1-11.

Smarzewska, S. & Morawska, K. 2021. Wastewater treatment technologies. Handbook of Advanced Approaches Towards Pollution Prevention and Control. *Elsevier*.

Smeulders, M. J., Peeters, S. H., Van Alen, T., De Bruijckere, D., Nuijten, G. H., Jetten, M. S. & Van Niftrik, L. 2020. Nutrient limitation causes differential expression of

transport-and metabolism genes in the compartmentalized anammox bacterium Kuenenia stuttgartiensis. *Frontiers in Microbiology***,** 1959.

Sobotka, D., Kowal, P., Zubrowska-Sudoł, M. & Mąkinia, J. 2018. COMAMMOX-a new pathway in the nitrogen cycle in wastewater treatment plants. *Journal of Civil Engineering and Environmental Sciences,* **4,** 031-033.

Soliman, M. & Eldyasti, A. 2018. ammonia-oxidizing Bacteria (AOB): opportunities and applications—a review. *Reviews in Environmental Science and Bio/Technology,* **17,** 285-321.

Song, X., Zhao, L., Liu, D. & Zhao, J. Step-feeding SBR for nitrogen removal from expressway service area sewage. AIP Conference Proceedings, 2017. *American Institute of Physics (AIP) Publishing LLC*, 040021.

Sorokin, D. Y., Lücker, S., Vejmelkova, D., Kostrikina, N. A., Kleerebezem, R., Rijpstra, W. I. C., Damsté, J. S. S., Le Paslier, D., Muyzer, G. & Wagner, M. 2012. Nitrification expanded: discovery, physiology, and genomics of a nitrite-oxidizing bacterium from the phylum Chloroflexi. *The International Society for Microbial Ecology (ISME) Journal,* **6,** 2245-2256.

Speirs, L., Rice, D. T., Petrovski, S. & Seviour, R. J. 2019. The phylogeny, biodiversity, and ecology of the Chloroflexi in activated sludge. *Frontiers in Microbiology***,** 2015.

Stein, L. Y. & Klotz, M. G. 2016. The nitrogen cycle. *Current Biology,* **26,** R94-R98.

Suryavanshi, M., Jaipuria, J., Mehta, A., Kumar, D., Panigrahi, M. K., Verma, H., Saifi, M., Sharma, S., Tandon, S. & Doval, D. C. 2019. Droplet digital polymerase chain reaction offers an improvisation over conventional immunohistochemistry and fluorescent in situ hybridization for ascertaining Her2 status of breast cancer. *South Asian Journal of Cancer,* **8,** 203.

Tamura, K., Peterson, D., Peterson, N., Stecher, G., Nei, M. & Kumar, S. 2011. MEGA5: molecular evolutionary genetics analysis using maximum likelihood, evolutionary distance, and maximum parsimony methods. *Molecular Biology and Evolution,* **28,** 2731-2739.

Tamura, K., Stecher, G., Peterson, D., Filipski, A. & Kumar, S. 2013. MEGA6: molecular evolutionary genetics analysis version 6.0. *Molecular Biology and Evolution,* **30,** 2725-2729.

Taylor, S. C., Laperriere, G. & Germain, H. 2017a. Droplet Digital PCR versus qPCR for gene expression analysis with low abundant targets: from variable nonsense to publication quality data. *Scientific Reports,* **7,** 2409.

Taylor, S. C., Laperriere, G. & Germain, H. 2017b. Droplet Digital PCR versus qPCR for gene expression analysis with low abundant targets: from variable nonsense to publication quality data. *Scientific Reports,* **7,** 1-8.

Tchobanoglous, G. 2014. Wastewater Engineering: Treatment and Resource Recov*ery-Vol. 2, McGraw-Hill*.

Thakur, I. S. & Medhi, K. 2019. Nitrification and denitrification processes for mitigation of nitrous oxide from wastewater treatment plants for biovalorization: Challenges and opportunities. *Bioresource Technology,* **282,** 502-513.

Tsotetsi, T. N., Collins, N. E., Oosthuizen, M. C. & Sibeko-Matjila, K. P. 2018. Selection and evaluation of housekeeping genes as endogenous controls for quantification of mRNA transcripts in Theileria parva using quantitative real-time polymerase chain reaction (qPCR). *PloS one,* **13,** e0196715.

Turunen, V., Sorvari, J. & Mikola, A. 2018. A decision support tool for selecting the optimal sewage sludge treatment. *Chemosphere,* **193,** 521-529.

Uri-Carreño, N., Nielsen, P. H., Gernaey, K. V. & Flores-Alsina, X. 2021. Long-term operation assessment of a full-scale membrane-aerated biofilm reactor under Nordic conditions. *Science of the Total Environment,* **779,** 146366.

Ushiki, N., Fujitani, H., Aoi, Y. & Tsuneda, S. 2013. Isolation of Nitrospira belonging to sublineage II from a wastewater treatment plant. *Microbes and Environments***,** ME13042.

Ushiki, N., Jinno, M., Fujitani, H., Suenaga, T., Terada, A. & Tsuneda, S. 2017. Nitrite oxidation kinetics of two Nitrospira strains: the quest for competition and ecological niche differentiation. *Journal of Bioscience and Bioengineering,* **123,** 581-589.

Van Den Broeck, R., Van Dierdonck, J., Nijskens, P., Dotremont, C., Krzeminski, P., Van Der Graaf, J., Van Lier, J., Van Impe, J. & Smets, I. 2012. The influence of solids retention time on activated sludge bioflocculation and membrane fouling in a membrane bioreactor (MBR). *Journal of Membrane Science,* **401,** 48-55.

Van Hullebusch, E. D., Yekta, S. S., Calli, B. & Fermoso, F. G. 2019. Biogeochemistry of major elements in anaerobic digesters: carbon, nitrogen, phosphorus, sulfur, and iron. *Trace Elements in Anaerobic Biotechnologies***,** 1.

Van Kessel, M. A., Speth, D. R., Albertsen, M., Nielsen, P. H., Op Den Camp, H. J., Kartal, B., Jetten, M. S. & Lücker, S. 2015. Complete nitrification by a single microorganism. *Nature,* **528,** 555-559.

Vu, M.-H., Sakar, M. & Do, T.-O. 2018. Insights into the recent progress and advanced materials for photocatalytic nitrogen fixation for ammonia (NH3) production. *Catalysts,* **8,** 621.

Wagner, M., Stenstrom, M. K., Jenkins, D. & Wanner, J. 2014. Aeration and mixing, *International Water Association (IWA) Publishing*, London.

Wang, J., Cahyadi, A., Wu, B., Pee, W., Fane, A. G. & Chew, J. W. 2020. The roles of particles in enhancing membrane filtration: A review. *Journal of Membrane Science,* **595,** 117570.

Wang, J., Li, L., Liu, Y. & Li, W. 2021. A review of partial nitrification in biological nitrogen removal processes: from development to application. *Biodegradation,* **32,** 229-249.

Wang, J., Rong, H. & Zhang, C. 2018. Evaluation of the impact of dissolved oxygen concentration on biofilm microbial community in sequencing batch biofilm reactor. *Journal of Bioscience and Bioengineering,* **125,** 532-542.

Wang, L., Lim, C. K., Dang, H., Hanson, T. E. & Klotz, M. G. 2016a. D1FHS, the type strain of the ammonia-oxidizing bacterium Nitrosococcus wardiae spec. nov.: enrichment, isolation, phylogenetic, and growth physiological characterization. *Frontiers in Microbiology,* **7,** 512.

Wang, L., Zheng, Z., Luo, X. & Zhang, J. 2011. Performance and mechanisms of a microbial-earthworm ecofilter for removing organic matter and nitrogen from synthetic domestic wastewater. *Journal of Hazardous Materials,* **195,** 245-253.

Wang, P., Yu, Z., Qi, R. & Zhang, H. 2016b. Detailed comparison of bacterial communities during seasonal sludge bulking in a municipal wastewater treatment plant. *Water Research,* **105,** 157-166.

Wang, T., Zhang, H., Gao, D., Yang, F. & Zhang, G. 2012a. Comparison between MBR and SBR on Anammox start-up process from the conventional activated sludge. *Bioresource Technology,* **122,** 78-82.

Wang, X., Hu, M., Xia, Y., Wen, X. & Ding, K. 2012b. Pyrosequencing analysis of bacterial diversity in 14 wastewater treatment systems in China. *Applied and Environmental Microbiology,* **78,** 7042-7047.

Wang, X., Li, J., Liu, R., Hai, R., Zou, D., Zhu, X. & Luo, N. 2017a. Responses of bacterial communities to CuO nanoparticles in activated sludge system. *Environmental Science & Technology,* **51,** 5368-5376.

Wang, Y., Chen, J., Zhou, S., Wang, X., Chen, Y., Lin, X., Yan, Y., Ma, X., Wu, M. & Han, H. 2017b. 16S rRNA gene high-throughput sequencing reveals a shift in nitrogen conversion related microorganisms in a CANON system in response to salt stress. *Chemical Engineering Journal,* **317,** 512-521.

Wang, Y., Ma, L., Mao, Y., Jiang, X., Xia, Y., Yu, K., Li, B. & Zhang, T. 2017c. Comammox in drinking water systems. *Water Research,* **116,** 332-341.

Wanner, J. & Torregrossa, M. 2017. Aeration tank and secondary clarifier as one system. *Activated Sludge Separation Problems: Theory, Control Measures, Practical Experiences,* 67.

Wen, R., Jin, Y. & Zhang, W. 2020. Application of the anammox in China—a review. *International Journal of Environmental Research and Public Health,* **17,** 1090.

Wu, L., Shen, M., Li, J., Huang, S., Li, Z., Yan, Z. & Peng, Y. 2019. Cooperation between partial-nitrification, complete ammonia oxidation (comammox), and anaerobic ammonia oxidation (anammox) in sludge digestion liquid for nitrogen removal. *Environmental Pollution,* **254,** 112965.

Yin, Z., Bi, X. & Xu, C. 2018. Ammonia-oxidizing archaea (AOA) play with ammonia-oxidizing bacteria (AOB) in nitrogen removal from wastewater. *Archaea,* **2018**.

Yu, C., Hou, L., Zheng, Y., Liu, M., Yin, G., Gao, J., Liu, C., Chang, Y. & Han, P. 2018. Evidence for complete nitrification in enrichment culture of tidal sediments and diversity analysis of clade a comammox Nitrospira in natural environments. *Applied Microbiology and Biotechnology,* **102,** 9363-9377.

Zeng, Y., De Guardia, A., Ziebal, C., De Macedo, F. J. & Dabert, P. 2012. Nitrification and microbiological evolution during aerobic treatment of municipal solid wastes. *Bioresource Technology,* **110,** 144-152.

Zhang, C., Qian, Y., Yuan, L., He, S., Wang, Y. & Wang, L. 2018. Nutrients removal performance of a denitrifying phosphorus removal process in alternate anaerobic/anoxic–aerobic double membrane bioreactors (A2N-DMBR). *Water Science and Technology,* **78,** 1741-1752.

Zhang, G., Huang, J., Jia, M., Liu, F., Yang, Y., Wang, Z. & Han, G. 2019. ammonia-oxidizing Bacteria and Archaea: Response to Simulated Climate Warming and Nitrogen Supplementation. *Soil Science Society of America Journal,* **83,** 1683-1695.

Zhang, X., Wu, P., Ma, L., Chen, J., Wang, C., Liu, W. & Xu, L. 2021. A Novel Simultaneous Partial Nitrification and Denitratation (SPND) Process in Single Micro-aerobic Sequencing Batch Reactor for Stable Nitrite Accumulation under Ambient Temperature. *Chemical Engineering Journal***,** 130646.

Zhang, Y. & Liu, W.-T. 2019. The application of molecular tools to study the drinking water microbiome–Current understanding and future needs. *Critical Reviews in Environmental Science and Technology,* **49,** 1188-1235.

Zhao, Z., Huang, G., He, S., Zhou, N., Wang, M., Dang, C., Wang, J. & Zheng, M. 2019. Abundance and community composition of comammox bacteria in different ecosystems by a universal primer set. *Science of The Total Environment,* **691,** 146-155.

Zorz, J. K., Kozlowski, J. A., Stein, L. Y., Strous, M. & Kleiner, M. 2018. Comparative proteomics of three species of ammonia-oxidizing bacteria. *Frontiers in Microbiology*, **9,** 938.

Zou, S., Yan, N., Zhang, C., Zhou, Y., Wu, X., Wang, J., Liu, Y., Zhang, Y. & Rittmann, B. E. 2019. Acclimation of nitrifying biomass to phenol leads to persistent resistance to inhibition. *Science of The Total Environment,* **693,** 133622.

APPENDIX

APPENDIX 1: The temperature variation within the reactor during the study at WWTP A and WWTP B

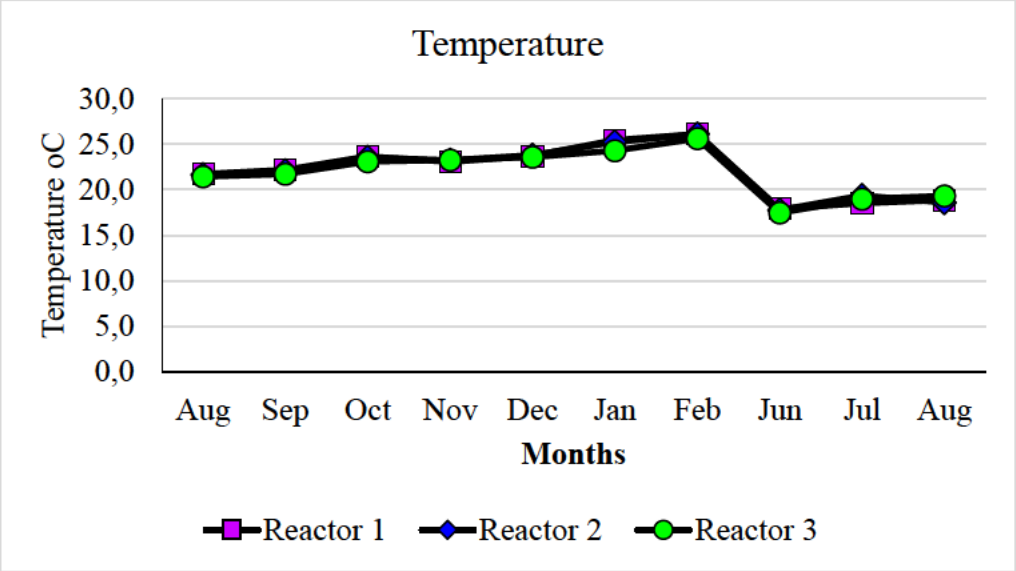

Figure S1.1: The temperature variation within the reactor during the study at WWTP A.

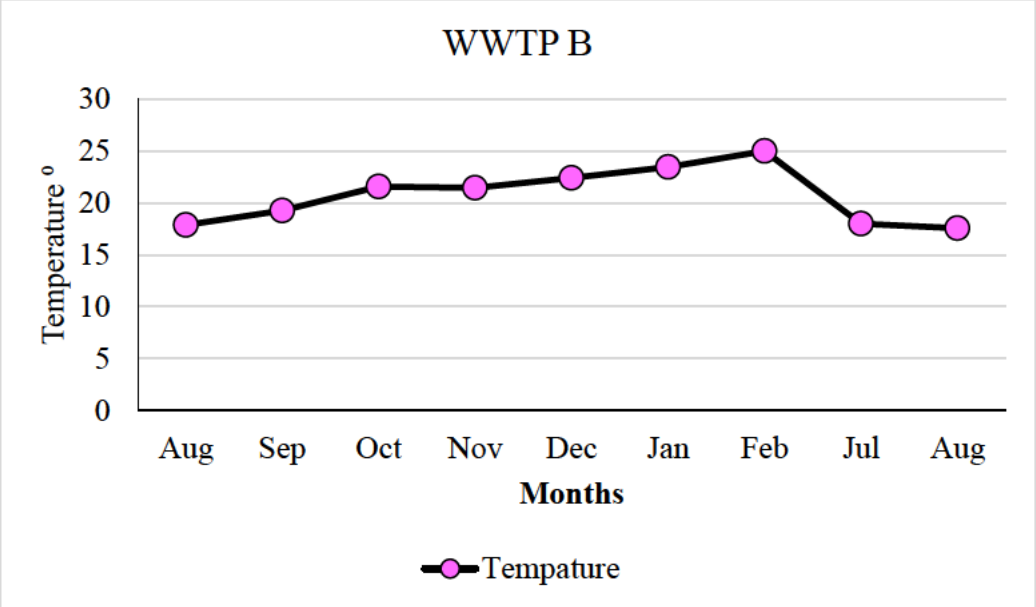

Figure S1.2: The temperature within the reactor during the study at WWTP B.

APPENDIX 2: Sludge foaming at WWTP A

Figure S2.1: Foaming in reactor 1 (A), reactor 2 (B), and reactor 3 (C) at WWTP A

APPENDIX 3: Preparation of Gallery Auto-analyser reagents

Ammonia

Reagent 1:

- 65 g Sodium salicylate + 65 g Trisodium citrate into 400 mL of ddH2O.
- Lower the pH to < 8.0 with 0.4 % HNO3
- Add 0.49 g Na-nitroprusside
- Make up to a final volume of 500 mL with ddH2O

Reagent 2:

- 16 g NaOH in 250 mL ddH2O
- Add 1 g Na-dichloroisocyanurate
- Make up to 500 mL with ddH2O

Total Oxidised Nitrogen Test

Reagent 1:

- 0.8 g NaOH in 100 ml ddH2O

Reagent 2:

- Dissolve 65 mg Hydrazine sulfate in 80 mL ddH2O.
- Add 0.15 mL Copper sulfate solution (390 mg CuSO4.5H2O in 100 mL H2O)
- Add 1 mL Zinc sulfate solution (450 mg ZnSO4.H2O in 100mL)
- Make up to 100 mL

Reagent 3:

- Dissolve 5 mL Phosphoric acid, 0.5 g Sulphanilamide, and 25 mg N-naphthylethylenediamine-HCl
- Dilute to 100 mL with ddH2O.

- Stored in a dark bottle.

Total Oxidised Nitrogen Standard

- 72.17 mg KNO_3 in 100 mL of ddH_2O

Nitrite-N Test

Reagent:

- Dissolve 5 mL Phosphoric acid, 0.5 g Sulphanilamide, and 25 mg N-naphthylethylenediamine-HCl
- Dilute to 100 mL with ddH_2O.
- Stored in a dark bottle.

Nitrite Standard

- Dissolve 49.25 mg in 100 mL

APPENDIX 4: Preparation of chemical oxygen demand (COD) reagents

Digestion solution

- 1.0216 g K_2CrO_7(dried) in 50mL dH_2O then
- Add 16.7mL concentrated H_2SO_4, add 3.33g $HgSO_4$
- Dissolve, cool, and dilute to 100mL with dH_2O

Sulfuric acid - silver sulfate reagent

- 5.5 Ag_2SO_4→ 1 kg H_2SO_4

Fresh Potassium hydrogen phthalate (KHP) standard

- Crush, and dry (KHP), in an oven at 120 ^{0}C for 1 hour
- Dissolve 425 mg KHP in dH_2O, dilute to 500 mL dH_2O
- Now, the concentration is 1000 mg O_2/L

APPENDIX 5: Preparation of gram reagents

Gram Crystal Violet Solution:

- 20 g of crystal violet

-95 % dye content, in 100 mL of ethanol

- 1 g of ammonium oxalate in 100 mL of water

Stock solution:

- 1 mL of the crystal violet

- 10 mL of water

- 40 mL of the oxalate stock solution.

Gram Iodine Solution:

- 1 g of iodine

- 2 g of potassium iodide

- 3 g of sodium bicarbonate in 300 mL of water.

Gram Decolorizer Solution:

- equal volumes of 95 % ethanol and acetone.

Gram Safranin Solution:

- 2.5 g of safranin O in 100 mL of 95 % ethanol to make a.

Stock solution:

- One part of the stock solution with five parts of water.